# ROLE OF FUNGAL-BACTERIAL INTERACTIONS FOR IMPROVED HEXACHLOROCYCLOHEXANE (HCH) BIODEGRADATION IN SOIL

**PH.D. THESIS**

**KHAN NELSON (MSc)**

**H80/51557/2017**

**A THESIS SUBMITTED IN FULFILMENT OF THE REQUIREMENT FOR AWARD OF THE DEGREE OF DOCTOR OF PHILOSOPHY IN BIOCHEMISTRY OF THE UNIVERSITY OF NAIROBI**

**MARCH 2023**

## DECLARATION

This thesis is my original work and has not been presented for a degree in any other University.

Signature……. Date……30. 03.2023……

Khan Nelson

H80/51557/2017

This thesis has been submitted for examination with our approval as the university and academic supervisors.

Signature……. Date……03.04.2023……

Prof. Edward K. Muge

Department of Biochemistry

University of Nairobi

Signature…. ……. Date……03.04.2023……

Dr. Benson M. Wamalwa

Department of Chemistry

University of Nairobi

Signat…… Date……03.04.2023……

Prof. Francis J. Mulaa

Department of Biochemistry

University of Nairobi

Signature Digital unterschrieben von Lukas Johannes Ivo Wick Gessler DN: c=DE, o=Helmholtz-Zentrum fuer Umweltforschung GmbH - UFZ, sn=Wick Gessler, givenName=Lukas Johannes Ivo, cn=Lukas Johannes Ivo Wick Gessler Datum: 2023.04.02 12:43:11 +02'00' Date 02.04.2023

Dr. Lukas Y. Wick

Department Umweltmikrobiologie

Helmholtz-Zentrum fur Umweltforshung-UFZ, Germany

## DEDICATION

I dedicate this research work to the almighty God for his faithfulness throughout the research period and for enabling me to obtain funding and scholarship opportunities and to overcome numerous challenges that I faced during the research study. I also dedicate this work to my loving mother Valleria Ayuma Oddiaga, and my wonderful aunt Evelyne Oresi Oddiaga for their prayers and encouragement as the journey was quite tough and challenging. Likewise, I dedicate this work to my sister Nahrien Khan my brother Steve Khan, and the entire extended family for their support. God bless you all.

## ACKNOWLEDGEMENT

I extend my sincere gratitude to the following individuals for their immense support of this research work. My supervisors Dr. Edward Muge, Dr. Benson Wamalwa, Prof. Francis J. Mulaa, and Prof. Lukas Wick for the guidance and advice throughout the research work from proposal writing, to seeking funds and a scholarship opportunity, conducting laboratory experiments, manuscripts drafting, and compiling this thesis. In addition, I am especially grateful to DAAD, Lukas Wick and Hauke Harms for an opportunity for a research stay at UFZ in Germany. I also wish to thank the International Foundation for Science (IFS) for funding part of the research work and the department of Biochemistry, University of Nairobi for providing me with an opportunity and appropriate work environment to pursue my work. My gratitude also goes to Dr. Nico Jehmlich for his guidance and input in proteomic work and Dr. Ulisses Nunes da Rocha, Dr. Rene Kallies, and Rodolfo Brizola Toscan for their assistance in whole-genome sequence analysis work. I appreciate the nice work atmosphere created by all members of the bioavailability group and the laboratory technicians Birgit Würz, Jana Reichenbach, and Rita Remer for their skilled experimental assistance. Their help was priceless. Last but not least, I thank all my officemates, Tom Berthold, Yongping Shan, and Zishu Liu for their help and advice in day-to-day life matters and for making my Ph.D. time at UFZ both enriching and enjoyable.

## TABLE OF CONTENTS

## LIST OF TABLES

## LIST OF FIGURES

## LIST OF ABBREVIATIONS AND ACRONYMS

| | |
|---|---|
| ALT | Alanine aminotransferase |
| ALP | Alkaline phosphatase |
| ASP | Africa Stockpiles Programme |
| AST | Aspartate aminotransferase |
| 4-CBA | 4-Chlorobenzoic acid |
| BLAST | Basic local alignment search tool |
| DBP | Dichlorobenzophenone |
| 2,5-DCHQ | 2,5-dichlorohydroquinone |
| DDD | dichlorodiphenyldichloroethane |
| DDE | Dichlorodiphenyldichloroethylene |
| DDT | Dichlorodiphenyltrichloroethane |
| HCB | Hexachlorobenzene |
| HCH | Hexachlorocyclohexane |
| IDT | Integrated DNA Technologies |
| LDH | Lactate dehydrogenase |
| MA | Maleylacetate |
| MCMC | Markov Chain Monte Carlo |
| MSM | Mineral Salt Media |
| NIST | National institute of standard and technology |
| PB | Phosphate buffer |
| γ-PCCH | Pentachlorocyclohexene |
| POPs | Persistent Organic Pollutants |
| PDA | Potato dextrose agar |
| SC | Stockholm Convention |
| SIP | Stable Isotope Probing |
| TCCH | Tetrachlorocyclohexene |
| TCCOL | Tetrachlorocyclohexanol |
| WRF | White rot fungi |

## PUBLISHED ARTICLES

### Publications

Part of this work has been published in peer reviewed journals, presented in chapter 3 and chapter 4 of this thesis and as a preprint presented in chapter 5.

i. Nelson Khan, Rodolfo Brizola Toscan, Accadius Lunayo, Benson Wamalwa, Edward Muge, Francis J. Mulaa, René Kallies, Hauke Harms, Lukas Y. Wick, Ulisses Nunes da Rochad (2021). Draft Genome Sequence of Fusarium equiseti K3, a Fungal Species Isolated from Hexachlorocyclohexane-Contaminated Soil. Microbiology Resourse Announcements, 10 (47), e.00885-21, https://doi.org/10.1128/MRA.00885-21.

ii. Nelson Khan, Rodolfo Brizola Toscan, Accadius Lunayo, Benson Wamalwa, Edward Muge, Francis J. Mulaa, René Kallies, Hauke Harms, Lukas Y. Wick, Ulisses Nunes da Rochad (2022). Draft Genome Sequences of Two *Sphingobium* Species Associated with Hexachlorocyclohexane (HCH) Degradation Isolated from an HCH-Contaminated Soil. Microbiology Resourse Announcements, 11(3), mra.00886-21, https://doi.org/10.1128/mra.00886-21.

iii. Nelson Khan, Edward Muge, Francis J. Mulaa, Benson Wamalwa, Martin von Bergen, Nico Jehmlich, Lukas Y. Wick (2023). Mycelial nutrient transfer promotes bacterial co-metabolic organochlorine pesticide degradation in nutrient-deprived environments. ISME Journal, https://doi.org/10.1038/s41396-023-01371-7.

### Posters

i. $N^2$ Science Communication Conference. Berlin, Germany, 6 – 8 November 2017.
Nelson Khan, Edward Muge, Benson Wamalwa, Francis J. Mulaa, Lukas Y. Wick. Role of fungal-bacterial interactions in the degradation of organochlorine pesticides.

ii. ISME 17 Conference. Leipzig, Germany, 12 – 17 August 2018.
Nelson Khan, Edward Muge, Francis J. Mulaa, Nico Jehmlich, Lukas Y. Wick. Mycelial nutrient transfer facilitates bacterial co-metabolic degradation of an organochlorine pesticide in nutrient deprived environment.

iii. 3rd International Conference in Microbial Ecotoxicology, EcotoxicoMic 2022. Montpellier, France, 15 – 18 November 2022.
Nelson Khan, Edward Muge, Francis J. Mulaa, Benson Wamalwa, Martin von Bergen, Nico Jehmlich, Lukas Y. Wick. Mycelial nutrient transfer promotes bacterial co-metabolic organochlorine pesticide degradation in nutrient-deprived environments.

## ABSTRACT

Organochlorine pesticides (OCPs), such as hexachlorocyclohexane (HCH) were extensively used across the globe for agricultural and public health purposes due to their effectiveness, relatively low cost, and ease of use. Their use was however restricted or banned in most countries across the world owing to their toxicity to non-target organisms, persistence in the environment, and ability to bio-accumulate in the food chain. Despite the restricted use or complete ban, HCH continues to pose serious environmental and health risks. However, the use of naturally existing microorganisms for the bioremediation of hazardous compounds and their detoxification has been proposed as a viable strategy to maintain environmental health. Therefore, the present study was aimed to (i) isolate fungal-bacterial couple from HCH-contaminated soil, (ii) test whether fungal mycelia can act as effective transport networks for HCH isomers, and (iii) test the effect of mycelial-mediated nutrient transfer to HCH degrading bacteria on the biodegradation of HCH isomers. Culture-dependent approaches were applied to isolate and characterize two HCH-degrading bacterial species and a fungal species from HCH-contaminated soil collected from a former obsolete pesticide store in Kitengela, Kenya (GPS: 01.49 S, 37.048E). Using a combination of the 16S gene, ITS gene, and whole genome sequencing the two bacteria were identified as, *Sphingobium* sp. strain S6 and S8 respectively, while the fungus was identified as *F. equiseti* strain K3. Both bacterial isolates were shown to effectively degrade all four HCH isomers. The degradation rates of γ-HCH were higher than those of α- and δ-HCH ($p < 0.041$) while no significant difference ($p > 0.12$) in the degradation rates of α- and δ-HCH was observed in both *Sphingobium* strains, while β-HCH had the lowest removal rate. Therefore, the removal rates of HCH isomers in both bacteria were in the order $\gamma > \alpha \approx \delta > \beta$. Subsequently, *lin* genes responsible for HCH degradation, identical to those found in other HCH degrading sphingomonads were identified by gene sequencing and from their 4.1 Mb draft genomes consisting of 4,015 and 4,039 protein-coding sequences (CDS) for *Sphingobium* sp. strain S6 and *Sphingobium* sp. strain S8 respectively. The fungal isolate, on the other hand, poorly degraded HCH isomers in the order $\beta > \alpha > \delta > \gamma$. ANOVA revealed statistically significant differences in the degradation of the HCH isomers ($p < 0.0039$). To test the effectiveness of mycelia as transport vectors for HCH isomers, a laboratory-based microcosm system designed to mimic air-water interfaces in soil was used while the *F. equiseti* species was used as a model organism. The fungus transported 0.09 – 0.6 µg of different HCH isomers in the order $\gamma > \alpha > \delta \approx \beta$ over a 3cm distance and the isomer-specific translocation was likely influenced by their octanol-air partition coefficients (log $K_{OA}$). To test the effect of

mycelial-mediated nutrient transfer to HCH-degrading bacteria on HCH biotransformation in a nutrient-deprived environment, the poorly HCH-degrading fungus (*Fusarium equiseti* strain K3) and the HCH-degrading bacterium (*Sphingobium* sp. strain S8) were used in a spatially structured laboratory-based model ecosystem. Subsequently, a combination of $^{13}$C-labelled fungal biomass and protein-based stable isotope probing (protein-SIP) was used to trace the incorporation of $^{13}$C fungal metabolites into bacterial proteins while simultaneously determining the biotransformation of the HCH isomers. Relative isotope abundance (RIA, 7.1 – 14.2%), labeling ratio (LR, 0.13 – 0.35), and the shape of isotopic mass distribution profiles of bacterial peptides indicated the transfer of $^{13}$C-labeled fungal metabolites into bacterial proteins. The distinct $^{13}$C incorporation into the haloalkane dehalogenase (linB) and 2,5-dichloro-2,5-cyclohexadiene-1,4-diol dehydrogenase (LinC), key enzymes in metabolic HCH degradation, underpinned the role of mycelial nutrient transfer in co-metabolic bacterial HCH degradation in heterogeneous habitats. Bacterial nutrient uptake from mycelia increased HCH removal by twofold as compared to bacterial monocultures. The findings from this study forms an important basis for the development of efficient bioremediation strategies in which either natural or artificial HCH degrading fungal-bacterial couple can be introduced into contaminated sites by bio-augmentation to improve biotransformation of micropollutants such as HCH.

# CHAPTER ONE

# 1.0 INTRODUCTION

## 1.1. Background of the study

The organochlorine pesticide hexaclorocyclohexane (HCH) is a polychlorinated, saturated cyclic hydrocarbon consisting of a cyclohexane ring to which hydrogen and chlorine atoms are connected to every carbon (Kumari et al., 2002; Lal et al., 2006; Nayyar & Lal, 2016; Prakash et al., 2004). HCH was extensively produced and used from the early 1950s to the late1980s against agricultural pests and for public health programs under the commercial name "Lindane" (Nayyar & Lal, 2016; Vijgen et al., 2019). For agricultural purposes, Lindane was used as an insecticide for crop and seed treatment, timber, and lumber treatment, and against ectoparasites in cattle and other farm animals (Girish & Kunhi, 2013). In public health programs, Lindane was used in the control of insect-borne disease programs and as a prescription drug for the treatment of scabies and human infections of head lice (Girish & Kunhi, 2013; Humphreys et al., 2008).

Lindane was named after the Dutch scientist, Dr. Teunis van der Lindan who discovered its insecticidal properties in 1912 (Girish & Kunhi, 2013). The commercial production of HCH was started in 1945 (Girish & Kunhi, 2013; Kumar & Pannu, 2018) in a process that involves the chlorination of Benzene in presence of ultra-violet (UV) light resulting in a mixture of five stable isomeric forms in different proportions as follows: α-HCH (60-70%), β-HCH (5-12%), γ-HCH (10-12%), δ-HCH (6-10%) and ε-HCH (3- 4%) (**Figure 2.1**) (Lal et al., 2010; Nayyar et al., 2014). The HCH isomeric forms differ from each other by the spatial arrangement of the chlorine atom on the cyclohexane ring, which determines their stability and hence persistence in the environment (Girish & Kunhi, 2013; Lal et al., 2006; Nayyar et al., 2014). Among the HCH isomers, however, only the γ- isomer (also referred to as Lindane) has insecticidal activity (Kumar & Pannu, 2018; Lal et al., 2010; Nayyar et al., 2014; Slade, 1945). HCH isomeric mixture is therefore subjected to fractional crystallization and concentration to purify γ-HCH isomer to at least 99% purity while the other isomers are discarded as HCH muck (Kumar & Pannu, 2018; Nayyar et al., 2014). Lindane production is, therefore, an inefficient process such that for each ton of γ-HCH isomer (lindane) produced approximately 8 to 12 tons of HCH muck (containing α-, β-, γ-, δ- and ε- isomers) are obtained (Girish & Kunhi, 2013; Kumar & Pannu, 2018; Nayyar et al., 2014; Vijgen, 2006).

Hexachlorocyclohexane was marketed in two formulations namely; technical HCH (t-HCH, which consists of all the five stable isomers) and lindane (which consists of >99% pure γ-HCH) (Alvarez et al., 2012). Though only γ-HCH exhibits insecticidal properties (Lal et al., 2010; Slade, 1945), technical HCH was mostly used as an inexpensive but effective insecticide in developing countries, while lindane was commonly used in the developed countries (Lal et al., 2010). The large-scale manufacture of lindane in the developed countries coupled with the indiscriminate use of technical HCH in the developing countries over the past 60 years has created a severe environmental contamination problem on a global scale (Lal et al., 2010; Nayyar et al., 2014). Previous studies estimate the global use of lindane for agricultural purposes at around 450,000 tons and the total global use at about 600,000 tons for the period between 1950 and 2000 (Girish & Kunhi, 2013; Vijgen, 2006). Due to its production inefficiencies, possible HCH residuals (assuming a factor of 8 for each ton of lindane produced) are estimated at 4.8 million tons worldwide, creating a severe environmental problem (Vijgen et al., 2019; Vijgen, 2006). The other major concern has been the open stockpiles of HCH waste, the lack of proper management and disposal of HCH waste, and the continuous shifting of HCH muck from the dumpsites (Nayyar & Lal, 2016; Vijgen et al., 2019).

The use of HCH was however restricted or banned in the 1970s and 1990s in developed countries due to its persistence in the environment, its potential to elicit toxic effects in higher animals, and ability to bioaccumulate in the food chain (Alvarez et al., 2012; Camacho-Pérez et al., 2012; Girish & Kunhi, 2013; Mansour, 2009). The persistence of HCH in soil, coupled with other natural processes such as evaporation into the atmosphere and surface runoffs caused by rain resulted in their ubiquitous distribution in the environment (Mansour, 2009). These factors have made HCH isomers to be classified among persistent organic pollutants (POPs) under the Stockholm Convention (SC) on POPs (Camacho-Pérez et al., 2012; Lal & Saxena, 1982; Mansour, 2009). Despite the restricted use or complete ban in most countries, HCH continues to pose a serious environmental risk and health concerns, particularly in highly contaminated former production or dumping sites, especially in developing countries (Boltner et al., 2005; Lal et al., 2010). The problem is further compounded by the biotransformation and bioaccumulation of HCH residues through the food chain and food web including humans (Nayyar & Lal, 2016).

Microbial biodegradation of hazardous compounds and their detoxification has therefore been proposed as one promising strategy to remediate contaminated sites and maintain environmental health (Alvarez et al., 2012; Kumar & Pannu, 2018; Pant et al., 2013).

Biodegradation of HCH has been reported for both fungi (Fuentes, Benimeli, Cuozzo, Sáez, et al., 2010; Guillén-Jiménez et al., 2012; Phillips et al., 2005; Singh & Kuhad, 1999, 2000) and bacteria (Boltner et al., 2005; Lal et al., 2006, 2010; Nayyar & Lal, 2016) under aerobic and anaerobic conditions (Kumar & Pannu, 2018; Saez et al., 2017). *Clostridium* species (including *C. rectum* and *C. sphenoides*) (Haider, 1979; Heritage & Rae, 1977; Ohisa et al., 1980) and some representatives of *Enterobacteriaceae* and *Bacillaceae* (Francis et al., 1975; Haider, 1979) have been demonstrated to degrade γ-HCH under anaerobic conditions. On the other hand, aerobic degradation of HCH isomers has been reported in bacteria belonging to the family *Sphingomonadaceae* (Boltner et al., 2005; Lal et al., 2006, 2010) and some white-rot fungi, including *Phanerochaete chrysosporium*, *Phanerochaete sordida*, *Cyathus bulleri* and *Trametes hirsutus* (Singh & Kuhad, 1999, 2000).

Despite the diverse number of known HCH degraders, members of the family *Sphingomonadaceae* have been shown to completely mineralize HCH and therefore play a crucial role in aerobic HCH degradation (Lal et al., 2006). Close to thirty HCH-degrading sphingomonads have been reported from different parts of the world, including; Spain (Mohn et al., 2006), Germany (Boltner et al., 2005), France (Cérémonie et al., 2006), India (Bala et al., 2010; Nayyar & Lal, 2016; Sahu et al., 1990), Japan (Ito et al., 2007; Senoo & Wada, 1989) Czech Republic (Niharika et al., 2013) and China (Mohn et al., 2006). Among the numerous HCH-degrading sphingomonads reported, three distinct species, namely, *Sphingobium japonicum* UT26 (Japan) (Senoo & Wada, 1989), *Sphingobium indicum* B90A (India) (Sahu et al., 1990) and *Sphingobium francense* Sp+ (France) (Cérémonie et al., 2006) have extensively been studied. In addition, the HCH degradation pathway and the catabolic genes (referred to as *lin* genes), necessary for aerobic degradation of HCH that were initially identified and characterized for *S. japonicum* UT26 (Nagata et al., 1999) have been identified for all the other HCH-degrading sphingomonads reported from different geographical locations across the world (Boltner et al., 2005; Lal et al., 2006; Mohn et al., 2006). These bacteria may therefore play a key role in the development of HCH bioremediation technologies.

Though a large number of bacteria with HCH degrading capacity have been isolated and characterized (Zhang et al., 2020), their application in bioremediation is limited by several physical, environmental and biological factors such as temperature, pH, the concentration of biomass, initial HCH concentration and its bioavailability (Saez et al., 2017; Zhang et al., 2020). This is compounded by the tendency of many organic contaminants to adsorb to surfaces and accumulate in organic matter, leading to a decline in their bioavailability (Furuno et al.,

2010, 2012; Harms et al., 2011). Such accumulation normally occurs in inhospitable, toxic environments that lack water and nutrients needed to support the growth of potential bacterial degraders (Harms et al., 2011). Previous reports suggest that ideal bioremediation machinery should possess special properties including (i) the ability to cope with harsh environmental conditions and track contamination even in pores and organic matter, (ii) a catabolic capacity that does not rely on the availability of the pollutant as a substrate for growth, and (iii) the ability to transport nutrients, water, and metabolically active organisms to contaminated spots (Harms et al., 2011).

Unlike most bacteria, mycelial fungi have been demonstrated to possess higher resistance to nutrient and water limitations (Worrich et al., 2017) due to their ability to extend mycelial structures that can efficiently translocate nutrients and water between sources to sink regions (Harms et al., 2011; Worrich et al., 2017). In addition, mycelial structures have been shown to act as transport vectors for pollutants and pollutant-degrading bacteria, and therefore influence the biodegradation of organic pollutants in soil (Wick et al., 2010). These fungal properties, coupled to the non-specific transformation of hydrophobic organic contaminants by fungal catabolic exo-enzymes may render xenobiotic compounds more water-soluble increasing their accessibility to the catabolic interacting bacteria (Harms et al., 2011; Wick et al., 2010). Fungal-bacterial co-cultures have been shown to display most of the features of ideal bioremediation machinery (Espinosa-Ortiz et al., 2021; Harms et al., 2011). To this end, improved biodegradation of certain pollutants has been reported when combined fungal-bacterial treatments were used compared to pure cultures or communities of either of them (Espinosa-Ortiz et al., 2021). This study, therefore, focused on the isolation and characterization of fungal-bacterial couple from HCH-contaminated Kenyan soil, assessed the extent of fungal-mediated transport of HCH in porous media, and finally the effect of mycelial nutrient transfer on co-metabolic degradation of HCH by bacteria.

### 1.2. Problem statement

The use of technical HCH, lindane, and other organochlorine pesticides (OCPs) was severely restricted or completely banned between the 1970s and 1990s in most countries due to their persistence in the environment, their ability to bioaccumulate in the food chain, and their toxicity effects to non-target higher organisms (Girish & Kunhi, 2013; Mansour, 2009; Nayyar et al., 2014). Despite the restricted use or complete ban, HCH continues to pose a serious environmental risk and health concerns partly due to high levels of contamination at former production sites, (Vijgen et al., 2019; Vijgen, 2006) unsustainable disposal methods (Nayyar

& Lal, 2016; Vijgen, 2006) and accumulation of stockpiles following the ban particularly in the developing countries (Boltner et al., 2005; Lal et al., 2010; Mansour, 2009).

According to Africa Stockpiles Programme (ASP), Africa is estimated to have accumulated at least 50,000 tons of obsolete pesticides in addition to thousands of tons of contaminated soil over several decades of use (Mansour, 2009). Some African countries including; Ethiopia, Mali, Morocco, Botswana, South Africa, and Tanzania were estimated to have more than 1000 tons of obsolete pesticide stocks (Elfvendahl et al., 2004; Mansour, 2009). Groundwater and soil contaminated by pesticides near pesticide dump sites and obsolete pesticide stores have also been reported in several developing countries (Mansour, 2009).

In Kenya for instance, the use of dichlorodiphenyl trichloroethane (DDT) was banned in 1985 while that of aldrin, dieldrin, and lindane were banned in 1992 (Wandiga, 2001). However, HCH residues have recently been detected in air and soil samples in Nairobi (Aucha et al., 2017), water and sediments from Rusinga island in lake Victoria (Osoro, 2016), and in agricultural soil in Meru county (Marete et al., 2019), showing the extent of contamination in Kenya. Traditional methods that have been used for the removal of these pollutants and remediation of contaminated sites include transport of the contaminants to specialized landfills, excavation, incineration, chemical or microwave-induced oxidation, and in situ vitrification (Alvarez et al., 2012; Kumar & Pannu, 2018). The use of these conventional remediation methods is however considered unsustainable and has therefore raised environmental concerns due to the release of toxic intermediates and the spread of contamination to new sites (Kumar & Pannu, 2018; Mansour, 2009). There is therefore a strong need to develop minimally hazardous and environmentally friendly approaches that can be used for the remediation of HCH-contaminated sites.

### 1.3. Justification

Microbial biodegradation of hazardous compounds and their detoxification has been proposed as one of the promising strategies to remediate contaminated sites and maintain environmental health (Alvarez et al., 2012; Kumar & Pannu, 2018; Pant et al., 2013). Microbial degradation of xenobiotic compounds is considered to be effective, minimally hazardous, and environmentally friendly (Kumar & Pannu, 2018; Pant et al., 2013). Though lindane and other HCH isomers were only released to the environment in the 1940s, certain microorganisms including both bacteria and fungi have acquired the capacity to biodegrade and mineralize these compounds (Saez et al., 2017). In that regard, HCH-degrading microorganisms may therefore

be used as models to decipher their evolution and adaptation to HCH degradation and as a biotechnological tool for the bioremediation of contaminated environments (Saez et al., 2017).

Though a large number of HCH-degrading bacteria have been reported, sphingomonads stand out as the group of choice for further research on strain development for bioremediation purposes, due to the extensive availability of information regarding their HCH-degrading metabolic pathways (Alvarez et al., 2012). Most research in the context of microbial HCH degradation has been achieved with pure cultures which have allowed for detailed studies by which the pesticide is metabolized to be elucidated, genes involved in the pesticide degradation pathway to be characterized, and the degradation products to be isolated and identified (Aislabie & Lloyd-Jones, 1995; Camacho-Pérez et al., 2012; Lal et al., 2006, 2010). Further studies on the characterization of HCH catabolic enzymes (lin enzymes) are however needed to develop more robust bioremediation technologies (Alvarez et al., 2012; Nayyar et al., 2014). The availability of a genome inventory for HCH-degrading sphingomonads has also opened a window for comparative genomics analysis of the architecture and content of their genomes (Nayyar & Lal, 2016).

In the natural environment, however, microorganisms do not exist in anexic conditions, but rather as part of complex microbial communities (Espinosa-Ortiz et al., 2021). Therefore, the use of single cultures for bioremediation has numerous metabolic limitations which can easily be alleviated by the use of mixed cultures or microbial co-cultures including fungi and bacteria (Espinosa-Ortiz et al., 2021; Saez et al., 2017; Zhang et al., 2020). In microbial co-culture systems, bacteria and fungi would potentially combine the catalytic specialties from both species/strains to efficiently metabolize pesticide contaminants and increase resistance to constantly fluctuating environmental conditions (Espinosa-Ortiz et al., 2021; Saez et al., 2017). Improved biodegradation of certain pollutants has been reported, when combined fungal-bacterial treatments were used compared to pure cultures or communities of either of them (Espinosa-Ortiz et al., 2021), hence the growing interest in engineering artificial fungal-bacterial consortia for the development of more robust bioremediation technologies.

### 1.4. General objective

To isolate and characterize hexachlorocyclohexane (HCH) degrading fungal-bacterial couple from contaminated soil and to assess the role of fungal mycelia as transport networks for HCH and as a source of carbon substrates to HCH degrading bacteria for improved HCH degradation respectively.

#### 1.4.1. Specific objectives

i. To isolate HCH degrading fungal-bacterial couple from Kenyan contaminated soil, assess their HCH degrading capacities, and characterize the genes involved in HCH degradation.
ii. To assess and quantify the effectiveness of fungal mycelium as a HCH transport network as a means to increase their bioavailability and bioaccessibility.
iii. To assess the effectiveness of fungal-bacterial co-cultures in the biodegradation of HCH by quantifying nutrient transfer from fungal mycelia to co-metabolic HCH degrading bacteria.

### 1.5. Research hypothesis

i. **Hypothesis 1:** HCH catabolic genes (*lin* genes) among different HCH degrading bacteria vary in sequence homology.
ii. **Hypothesis 2:** Fungal mycelia improve HCH biodegradation efficiency by increasing its accessibility and bioavailability to HCH-degrading bacteria through hyphal HCH transport.
iii. **Hypothesis 3:** Fungal mycelia increase HCH biodegradation by providing carbon-substrates to co-metabolically HCH-degrading bacteria.

### 1.6. Research questions

i. Do HCH catabolic genes (*lin* genes) among different HCH degrading bacteria vary in sequence their homology?
ii. Can fungal mycelia act as effective transport networks for HCH isomers?
iii. Can fungal mycelia increase HCH biodegradation by providing C-substrates to co-metabolically HCH-degrading bacteria?

# CHAPTER TWO

# 2.0 LITERATURE REVIEW

## 2.1. Organochlorine pesticides (OCPs)

Organochlorine pesticides (OCPs) are among the halogenated organic compounds that were extensively used across the globe for agricultural activities and public health purposes due to their effectiveness, ease of use, and relatively low production cost (Girish & Kunhi, 2013; Pant et al., 2013; Porto et al., 2011). OCPs were first introduced in the 1940s and 1950s and were frequently used to curb human and animal diseases that are transmitted by insects and mites, and against insect pests that damage crops (Lal & Saxena, 1982; Muchiri et al., 2002; Pant et al., 2013). This class of pesticides includes halogenated hydrocarbons such as (i) chlorinated hydrocarbons (which include: chlordecone, dodecachlorine, and toxaphene); (ii) chlorinated derivatives of diphenyl ethane (which include: dichlorodiphenyl trichloroethane-DDT and its respective metabolites, dichlorodiphenyldichloroethane-DDD, dichlorodiphenyldichloroethylene-DDE, and methoxychlor); (iii) cyclodiene (which include: aldrin, chlordane, dieldrin, endrin, heptachlor, heptachlor-epoxide and nonachlor); (iv) hexachlorobenzene (HCB) and (v) hexachlorocyclohexane (HCH) (which include: α-, β-, γ-, δ- and ε-HCH or lindane) (**Figure 2.1**) (Porto et al., 2011).

Organochlorine pesticides persist in the environment, a property that made them attractive pesticides because, a single application could be effective for months (Mansour, 2009). The use of OCPs was however banned or restricted in the 1970s and 1990s in most countries due to their persistence in the environment, toxicity to non-target higher animals, and ability to bioaccumulate in the food chain (Alvarez et al., 2012; Girish & Kunhi, 2013; Mansour, 2009). They were therefore classified among the persistent organic pollutants (POPs) under the Stockholm Convention (SC) on POPs (Mansour, 2009; Vijgen et al., 2011, 2018; Vijgen, 2006). In Kenya for instance, the use of DDT was banned in 1985 while that of aldrin, dieldrin, and lindane were banned in 1992 (Wandiga, 2001).

Despite the complete ban or restricted use in most countries, OCPs continue to pose a serious environmental risk, particularly in areas with high levels of contamination such as former production sites and dumping sites of stockpiles following the ban (Boltner et al., 2005; Lal et al., 2010; Mansour, 2009). According to Africa Stockpile Programme (ASP), Africa is estimated to have accumulated a stockpile of at least 50,000 tons of obsolete pesticides in addition to thousands of tons of contaminated soil (Mansour, 2009). African countries such as

Botswana, Ethiopia, Mali, Morocco, South Africa, and Tanzania were estimated to possess more than 1000 tons of obsolete OCP stockpiles. Contaminated groundwater and soil near dump sites and obsolete pesticide stores have also been reported in several developing countries (Elfvendahl et al., 2004; Mansour, 2009).

### 2.2. Hexachlorocyclohexane (HCH), production and properties

Commercial production of HCH was started in the 1940s (Girish & Kunhi, 2013; Kumar & Pannu, 2018), in a process that involves photochlorination of benzene in presence of UV light, resulting to a mixture of different proportions of five stable isomeric forms including, α-HCH (60-70%), β-HCH (5-12%), γ-HCH (10-12%), δ-HCH (6-10%) and ε-HCH (3- 4%) (Girish & Kunhi, 2013; Lal et al., 2010; Nayyar et al., 2014; Nayyar & Lal, 2016). The γ-HCH isomer (the only isomer that possesses insecticidal activity) was purified from the mixture, also called "technical HCH (t-HCH)" and marketed as lindane, while the rest of the isomers including, α-, β-, δ- and ε-isomers were discarded as 'HCH muck' (Lal et al., 2010; Nayyar et al., 2014; Nayyar & Lal, 2016). The HCH isomeric forms differ from each other by the spatial position and arrangement of chlorine atoms on the cyclohexane ring, which determine their stability, persistence, toxicity, and other physical properties (**Table 2.1**) (Lal et al., 2006, 2010; Nayyar et al., 2014; Phillips et al., 2005).

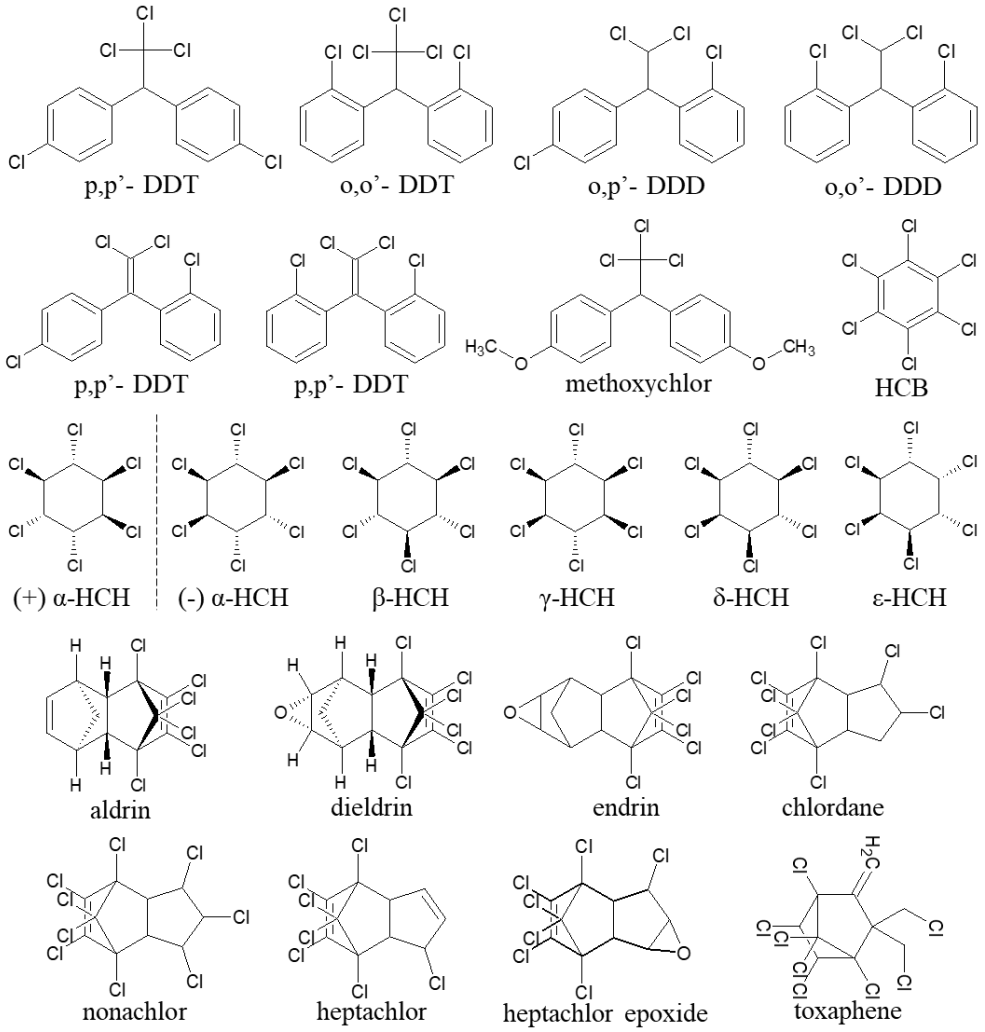


**Figure 2.1:** Structures of different organochlorine pesticides (adapted from Porto et al., 2011).

The γ-isomer has three axial and three equatorial (aaaeee) chlorine atoms, the α-isomer has two axial and four equatorial (aaeeee) chlorine atoms, while the δ-isomer has one axial and five equatorial (aeeeee) chlorine atoms (**Table 2.1**) (Nayyar et al., 2014; Phillips et al., 2005). It has previously been proposed that the presence of axial chlorine atoms provides suitable sites for enzymatic degradation (Okai et al., 2010; Phillips et al., 2005). Previous observations, therefore, indicate that α- and γ-HCH isomers are more easily biodegradable than the δ-isomer which has more chlorine atoms in the equatorial position (Phillips et al., 2005). In contrast, β-HCH isomer has all its chlorine atoms oriented in the equatorial position (eeeeee), making it the most structurally stable isomer and hence recalcitrant and resistant to microbial degradation (Nayyar et al., 2014; Phillips et al., 2005).

The properties of HCH isomers, therefore, influence their volatilization and transport in the atmosphere, distribution, and environmental fate (Nayyar & Lal, 2016; Phillips et al., 2005).

The main risks associated with HCH are, (i) the purification of the insecticidal γ-isomer from the technical mixture, which has led to the accumulation of stockpiles of HCH muck at former production sites (Lal et al., 2010; Nayyar & Lal, 2016) and (ii) the use of the technical mixture for agricultural and public health purposes, particularly in the developing countries that has led to the spread of environmental pollution (Nayyar et al., 2014; Nayyar & Lal, 2016).

**Table 2.1:** Physiochemical characteristics of the four stable HCH isomers (adapted from ATSDR, 2002; Phillips et al., 2005; Nayyar et al., 2014; and Shoeib & Harner, 2002).

| Property | α-HCH | β-HCH | γ-HCH | δ-HCH |
|---|---|---|---|---|
| Conformation | aaeeee | eeeeee | aaaeee | aeeeee |
| Molecular weight | 290.83 | 290.83 | 290.83 | 290.83 |
| Melting point (ºC) | 159 – 160 | 314 – 315 | 112.5 | 141 – 142 |
| Boiling point | 288ºC at 760 mmHg | 60ºC at 0.5 mmHg | 323.4ºC at 760 mmHg | 60ºC at 0.36 mmHg |
| Density ($g/cm^3$) | 1.87 at 20ºC | 1.89 at 19ºC | 1.89 at 19ºC | NDA |
| Solubility in water (ppm) | 10 | 5 | 17 | 10 |
| Solubility in organic solvents (g): | | | | |
| Ethanol (per 100g) | 1.8 | 1.1 | 6.4 | 24.4 |
| Ether (per 100g) | 6.2 | 1.8 | 20.8 | 35.4 |
| Benzene (per 100g) | NDA | 1.9 | 28.9 | 41.4 |
| Partition coefficients: | | | | |
| log $K_{OW}$ | 3.8 | 3.78 | 3.72 | 4.14 |
| log $K_{OC}$ | 3.57 | 3.57 | 3.57 | 3.8 |
| log $K_{OA}$ | 7.61 | 8.88 | 7.85 | 8.84 |
| Henry's law constant | $6.86 \times 10^{-6}$ | $4.5 \times 10^{-7}$ | $3.5 \times 10^{-6}$ | $2.1 \times 10^{-7}$ |
| Vapour pressure (mmHg) | $4.5 \times 10^{-5}$ at 25ºC | $3.6 \times 10^{-7}$ at 20ºC | $4.2 \times 10^{-5}$ at 20ºC | $3.5 \times 10^{-5}$ at 25ºC |

a = axial; e = equatorial; NDA = No data available

### 2.3. The use and global distribution of hexachlorocyclohexane

Lindane was mainly used for agricultural and public health purposes to control insect pests and insect-borne diseases (Girish & Kunhi, 2013; Humphreys et al., 2008). Previous reports estimate the global use of lindane for agricultural purposes at 450,000 tons, while its use on livestock, forestry applications, and pharmaceutical purposes is estimated at 150,000 tons resulting to a total global production estimate of 600,000 tons for the period between 1950 and 2010 (Nayyar & Lal, 2016; Vijgen et al., 2011; Vijgen, 2006). Since lindane production is a highly inefficient process, HCH muck (assuming a factor of 8-12 tons for each ton of lindane produced in the purification process) is estimated at between 4.8 to 7.2 million tons worldwide (Nayyar et al., 2014; Vijgen et al., 2011; Vijgen, 2006).

Hexachlorocyclohexane has emerged as a critical environmental contaminant in the past few decades. The indiscriminate and unregulated disposal of the HCH muck, has resulted to the accumulation of HCH stockpiles and dumpsites (Nayyar et al., 2014). Heavily contaminated dumpsites (over 50,000 tons of HCH stockpiles) have been reported in different countries across the world including: Brazil (Österreicher-Cunha et al., 2003), Canada (Phillips et al., 2006; Shen et al., 2004), China (Zhu et al., 2005), France (Cérémonie et al., 2006), Germany (Jürgens & Roth, 1989; Popp et al., 2000; Sievers & Friesel, 1989), Greece (Golfinopoulos et al., 2003), India (Prakash et al., 2004; Singh et al., 2007), Japan (Senoo & Wada, 1989), Spain (Concha-Graña et al., 2006; Rubinos et al., 2007) and United States (Phillips et al., 2006). Many other countries with unknown levels of contamination have also been reported (Vijgen et al., 2011) (**Figure 2.2**).

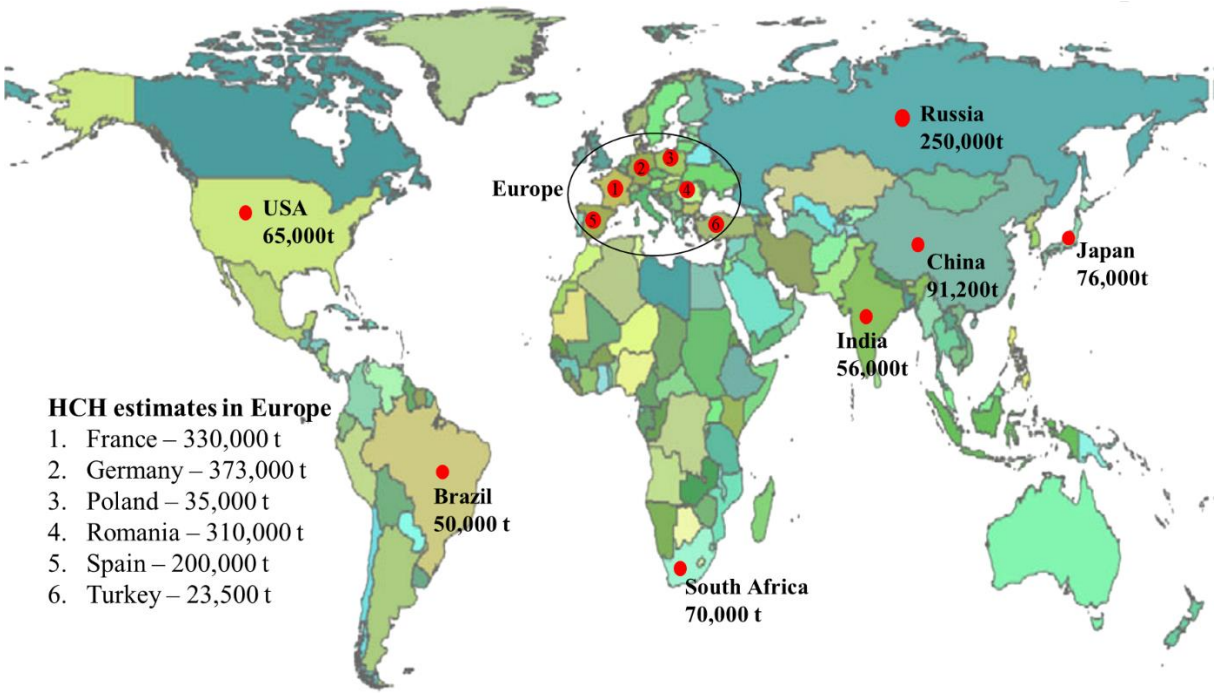


**Figure 2.2:** Reported estimates of the quantities (in tons) of HCH muck stockpiles in HCH dumpsites present in different selected countries around the world (adapted from Vijgen et al., 2011).

### 2.4. Levels of HCH contamination in Kenya

Organochlorine pesticides were extensively used for the control of maize and cotton pests in Kenya (Wandiga, 2001). Aldrin, dieldrin, endrin, heptachlor, and lindane were widely used as pesticides for seed dressing, resulting in the ubiquitous presence of these pesticides in the Kenyan environment (Aucha et al., 2017; Muchiri et al., 2002; Wandiga, 2001). Detectable levels of HCH isomers and other OCPs were recently reported in agricultural soil, water,

sediment samples, and selected organisms in Kenya (Aucha et al., 2017; Muchiri et al., 2002; Osoro, 2016). Osoro, (2016) recently reported significant levels of HCH isomers in water and sediment samples from Rusinga Island, Lake Victoria, including; α-HCH (7.02 ±0.01 µg/L in water and 22.62 ±3.23 µg/kg in sediments), β-HCH (2.96 ±0.97 µg/L in water and 21.94 ±4.21 µg/kg in sediments) and γ-HCH (0.52 ±0.01 µg/L in water and 6.23 ±1.95 µg/kg in sediments). Furthermore, the presence of α-, β-, and γ-HCH were reported in soil and air samples from Industrial area, Dandora and Kabete dumpsites within Nairobi (Aucha et al., 2017). In mount Kenya regions β-HCH was recorded as the most abundant while α-HCH the least abundant, in the analyzed samples (Aucha et al., 2017). HCH residues were also recorded in agricultural soil samples from Imenti North and South sub-counties in Meru county (Marete et al., 2019). Mean HCH isomer concentrations of up to; 60.6 ±8.2 µg/kg of α-HCH, 50.1 ±7.2 µg/kg of β-HCH, 40.7 ±1.9 µg/kg of γ-HCH and 0.6 ±0.1 µg/kg of δ-HCH were recorded in Imenti North subcounty, while upto; 2.4 ±0.4 µg/kg of α-HCH, 14.9 ±2.2 µg/kg of β-HCH, 2.8 ±0.1 µg/kg of γ-HCH and 0.5 ±0.04 µg/kg of δ-HCH were recorded in Imenti South sub county (Marete et al., 2019).

### 2.5. Environmental fate and transport of hexachlorocyclohexane

Following application or disposal in soil, the distribution and environmental fate of HCH is influenced by several factors, including; (i) loss by volatilization into the atmosphere, (ii) adsorption to soil particles and organic matter, (iii) loss through surface runoffs and leaching into ground water (iv) loss though uptake by plants and animals and (v) loss through chemical and microbial transformation (**Figure 2.3**) (Delcour et al., 2015; Girish & Kunhi, 2013; Shen et al., 2004; Zhang et al., 2020). The distribution and behavior of organic pollutants (such as HCH) in the atmosphere depend on; their physical and chemical properties, reactivity, location of the contaminant source, and dynamics of the atmosphere (Shen et al., 2004).

#### 2.5.1. Volatilization

Volatilization occurs when liquid or solid compounds transfer to gaseous phase (Delcour et al., 2015). This is one of the critical causes of the presence of organic contaminants in air and is normally influenced by elevated temperatures and the exposure of contaminants to direct sunlight (Delcour et al., 2015; Yeo et al., 2003). Pollutants with low volatility stay airborne for short periods, they tend to attach to atmospheric particles and quickly return to the ground. On the other hand, those with high volatility, low reactivity, and high Henry´s law constant (such as HCH) can stay airborne for prolonged periods before settling to the ground (Shen et al.,

2004). Following volatilization, contaminants can be dispersed by wind thousands of kilometers from their points of source to other pristine environments resulting in new contamination in form of aerial dry or wet deposition (Figure 3) (Delcour et al., 2015; Dubus et al., 2000; Shen et al., 2004; Yeo et al., 2003).

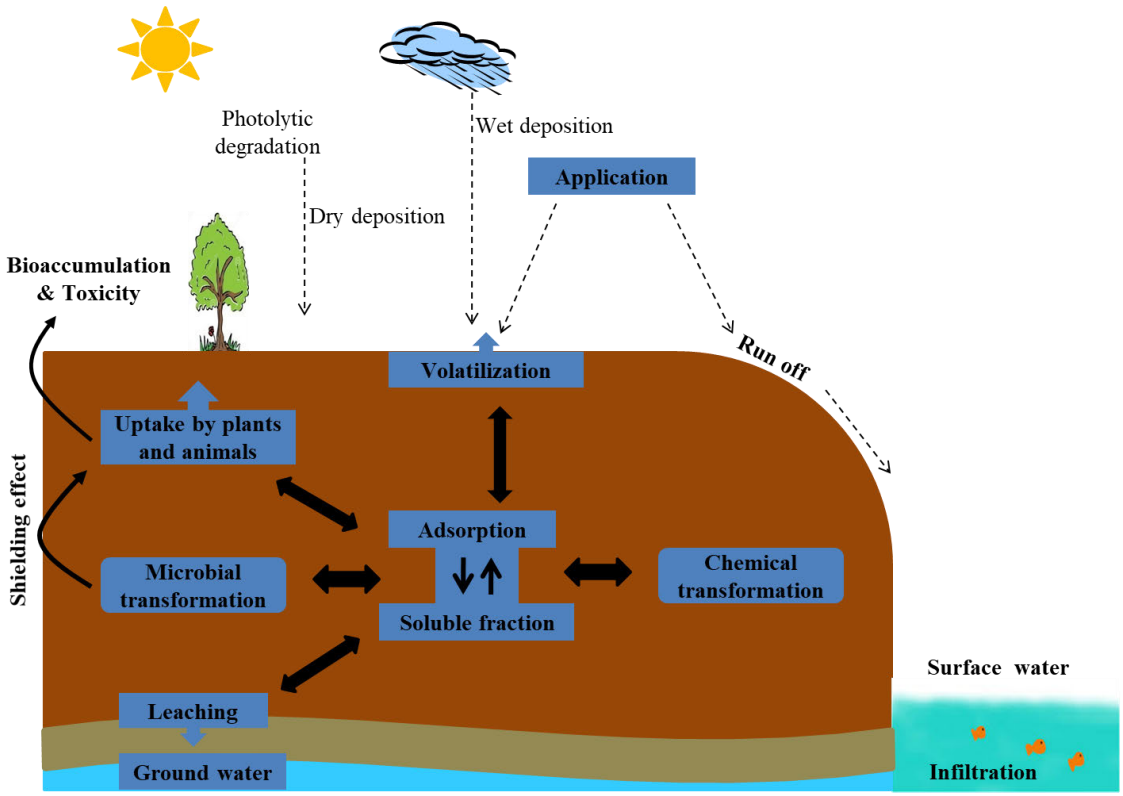


**Figure 2.3:** Processes that influence the distribution and environmental fate of HCH after application (adapted from Delcour et al., 2015).

### 2.5.2. Runoffs and leaching

Contamination of surface water by pesticide residues is often caused by waste water discharge and surface runoffs from points of the contamination source (Huber et al., 2000; Otieno et al., 2013). Surface runoffs have been implicated as the major source of aquatic contamination particularly in agricultural areas. Previous reports have linked increased applied pesticide loss to runoffs during heavy rains resulting in heavy contamination in aquatic systems (Otieno et al., 2013; Regnery & Püttmann, 2010). Once in aquatic systems, organic pesticide residues adsorb to suspended particles which eventually settle in sediments, that serve as essential habitats for aquatic organisms which would then bioaccumulate these pollutants (Phillips et al., 2003).

On the other hand, leaching is the percolation of organic chemicals through soil into the ground, eventually leading to contamination of ground water (Delcour et al., 2015). Generally, the leaching of organic contaminants in soil is influenced by their solubility in water and their affinity to bind soil particles (Dorsey et al., 2005; Pérez-Lucas et al., 2019). Leaching of pesticides through soil is facilitated by irrigation or rain water, therefore leaching has been reported to be high for; (i) persistent compounds with weak adsorption properties, (ii) climates with high precipitation, and, (iii) soil with sandy texture and low organic matter (Pérez-Lucas et al., 2019). HCH has generally been shown to have low mobility in soil, based on laboratory studies that used soil columns with soils of both high and low organic matter (Dorsey et al., 2005; Reinhart et al., 1991). Soils with high organic matter and clay are however thought to slow water movement and easily adsorb many pesticides, hence preventing the leaching of organic contaminants into the ground better than soils with sandy texture (Pérez-Lucas et al., 2019).

### 2.5.3. Adsorption

The adsorption of pesticides in soil determines their efficacy and the adverse environmental impact they might cause (Wadaskar et al., 2006). Soil organic matter is the most important factor that governs the sorption and desorption of HCH isomers, where increased sorption was observed with increased soil organic matter (Pérez-Lucas et al., 2019; Wahid & Sethunathan, 1979). Once applied to soil, HCH strongly adsorbs to soil organic matter rendering it relatively immobile (Girish & Kunhi, 2013). Pesticides that strongly adsorb to soil particles pose less risk to groundwater contamination through leaching. However, they may pose a serious contamination risk to surface water when soil is eroded into surface water bodies (Wadaskar et al., 2006).

### 2.5.4. Uptake by plants and animals

Plants growing in HCH-contaminated environments have been shown to accumulate HCH in their tissues (Girish & Kunhi, 2013). Two pathways through which organic contaminants enter plants have been proposed, (i) the soil-plant pathway, which involves adsorption of pollutants by the roots tissues from contaminated soil and translocation to the aerial parts of the plants through the xylem, and (ii) the air-plant pathway, which involves adsorption of contaminants to the aerial plant biomass from the surrounding air following volatilization from soil (Abhilash et al., 2008; Calvelo Pereira et al., 2008; Girish & Kunhi, 2013). The uptake and bioaccumulation of contaminants by plants is one of the crucial processes that determine

pollutant transfer within the food chain and food web (**Figure 2.3**) (Abhilash et al., 2008; Bacci et al., 1992; Calvelo Pereira et al., 2008).

### 2.5.5. Transformation and degradation

Hexachlorocyclohexane can undergo both chemical and biological transformation in the environment (Wacławek et al., 2019). Chemical transformation of HCH has been reported to include; oxidative elimination (which includes free radical addition), reductive elimination (including, hydrogenolysis and dihaloelimination), and β-elimination (which includes alkaline mediated transformation) (Wacławek et al., 2019). On the other hand, the biological (microbial) transformation of HCH (both oxic and anoxic) has been reported in several studies and reviews (Lal et al., 2006, 2010; Lal & Saxena, 1982; Phillips et al., 2005). The microbial transformation of HCH has a shielding effect on uptake by plants and animals and toxicity (**Figure 2.3**).

## 2.6. Toxicological profile of hexachlorocyclohexane

The production and extensive use of HCH over the decades resulted in detrimental effects on non-target biota of both soil and aquatic environment (Zhang et al., 2020). The persistence and lipophilic properties of HCH isomers enable them to bioaccumulate in the food chain, making HCH one of the most hazardous POPs (Tsygankov et al., 2019; Zhang et al., 2020). Lindane poses a threat to a range of organisms including, microorganisms, plants, invertebrates, fish, birds, and mammals (Sang & Petrovic, 1999; Zhang et al., 2020).

Martinez-Toledo et al. (1993) showed that lindane application at concentrations of 3.5-15kg/ha resulted in a significant decrease in the population of nitrifying bacteria (*Nitrosomonas* spp., *Nitrosolobus* spp., and *Nitrobacter* spp.) in agricultural soil (Girish & Kunhi, 2013; Martinez-Toledo et al., 1993). In addition, the presence of 10µg/ml lindane adversely affected the growth and denitrifying activity of *Xanthobacter autotrophicus* CECT 7064 in a liquid medium (Sáez et al., 2006). HCH has been shown to reduce plant seed germination vigor and is highly toxic to fish and aquatic invertebrates (Bidlan et al., 2004; Girish & Kunhi, 2013). In humans, HCH has adverse effects on the neurological system, liver, and kidneys and is also suspected to be carcinogenic (Girish & Kunhi, 2013; Sauviat & Pages, 2002; Zhang et al., 2020). Lindane is a neurotoxin that disrupts the activity of γ-aminobutyric acid (GABA) neurotransmitter by interacting with the $GABA_A$ receptor-chloride channel complex (Pomés et al., 1994). Previous studies have demonstrated increased activity of liver function test enzymes such as lactate dehydrogenase (LDH), alkaline phosphatase (ALP), alanine aminotransferase (ALT), and

aspartate aminotransferase (AST) in mice models as an indication of the harmful effects of HCH on the liver (Girish & Kunhi, 2013). Lindane has also been shown to be mildly estrogenic in female mice and to cause testes atrophy in male mice (Girish & Kunhi, 2013).

### 2.7. Microbial degradation of hexachlorocyclohexane

Microbial degradation of organic contaminants such as HCH has been proposed as the most auspicious strategy to maintain environmental health (Pant et al., 2013). Microorganisms are considered as effective, minimally hazardous, and environmentally friendly for pollutants removal from contaminated sites (Pant et al., 2013). Toxicity and persistence of xenobiotic compounds are determined by their degree of halogenation (Saez et al., 2017), therefore, dehalogenation (removal of the halogen atom) is considered as the most critical reaction in microbial degradation of halogenated organic pollutants (Camacho-Pérez et al., 2012; Saez et al., 2017). Dehalogenation is thought to reduce recalcitrance to biodegradation and the formation of toxic biodegradation intermediates in the subsequent steps (Camacho-Pérez et al., 2012). Microorganisms with HCH degradation capacity have attracted attention because they provide an opportunity to be utilized for in situ bioremediation and detoxification of contaminated environments (Girish & Kunhi, 2013). Microbial degradation of HCH has been reported in both fungi (Bumpus et al., 1985; Guillén-Jiménez et al., 2012; Phillips et al., 2005; Sagar & Singh, 2011) and bacteria (Boltner et al., 2005; Lal et al., 2006, 2010; Nayyar et al., 2014; Nayyar & Lal, 2016) under both aerobic and anaerobic conditions (Kumar & Pannu, 2018; Saez et al., 2017).

#### 2.7.1. Hexachlorocyclohexane degradation by fungi

Fungi have been reported to have the capacity to degrade a variety of xenobiotic pollutants such as pesticides, hydrocarbons, and azo dyes (Nagpal et al., 2008; Saez et al., 2017). Among different fungi, white-rot fungi (WRF) have been shown to have a high degradation efficiency for a variety of xenobiotics (Nagpal et al., 2008; Saez et al., 2017; Sagar & Singh, 2011). HCH degradation by different strains of WRF have previously been reported, including; *Bjerkandera adusta* (J. C. Quintero et al., 2007), *Phanerochaete chrysosporium* (Mougin et al., 1996), *Phanerochaete sordida*, *Cyathus bulleri* (Singh & Kuhad, 2000), *Trametes hirsutus* (B. K. Singh & Kuhad, 1999) and *Pleurotus ostreatus* (Rigas et al., 2009). Quintero et al. (2007) demonstrated bioremediation of the four major isomers of HCH using *B. adusta* in a slurry system. The capacity of WRF to degrade HCH is attributed to their ability to produce highly efficient, non-specific extracellular enzymes that catalyze a range of oxidation reactions

resulting in the breakdown of contaminants (Nagpal et al., 2008). Some of the non-specific enzymes secreted by WRF include lignin modifying enzymes such as; laccases, lignin and manganese peroxidases, and phenol oxidases (Hatakka, 1994; Nagpal et al., 2008).

Besides WRF, non-white rot fungi (non-WRF) have recently been demonstrated to degrade HCH (Saez et al., 2017). The non-WRF reported to degrade HCH include; *Fusarium poae* and *Fusarium solani* isolated from HCH contaminated soil (Sagar & Singh, 2011), *Fusarium verticillioides* AT-100 isolated from *Agave tequilana* leaves (Guillén-Jiménez et al., 2012) and *Conidiobolus* 03-1-56 isolated from litter (Nagpal et al., 2008). Some metabolites identified during fungal HCH degradation studies include; γ-pentachlorocyclohexene (γ-PCCH), tetrachlorocyclohexene (TCCH) tetrachlorocyclohexenol (TCCOL), Phenol and benzoic acid (**Figure 2.4**) (Guillén-Jiménez et al., 2012; Singh & Kuhad, 2000).

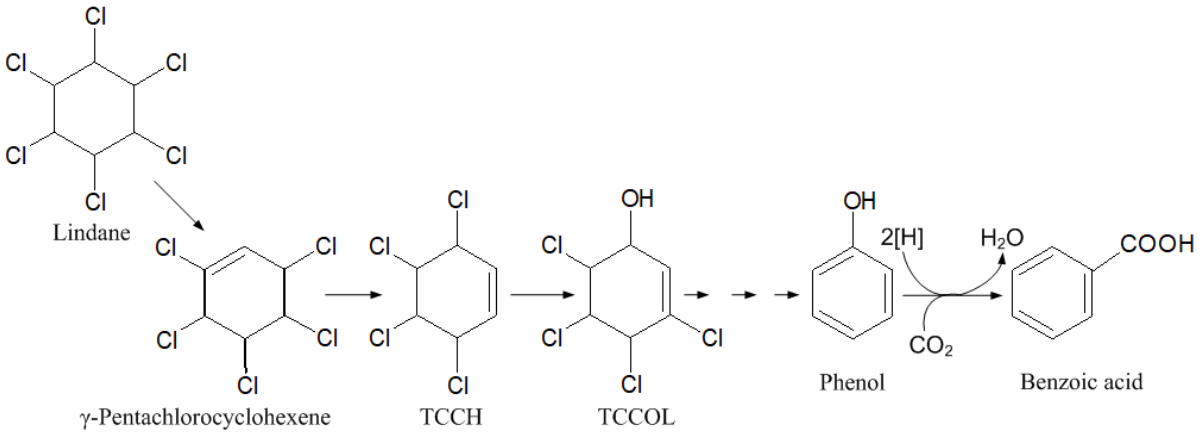


**Figure 2.4:** Proposed HCH degradation steps by fungi. Compounds: TCCH = tetrachlorocyclohexene, TCCOL = tetrachlorocyclohexenol (adapted from Guillén-Jiménez et al., 2012 and Singh & Kuhad, 2000).

### 2.7.2. Hexachlorocyclohexane degradation by bacteria

The HCH degradation capacity of bacteria has been reported under both oxic and anoxic conditions (Alvarez et al., 2012; Lal et al., 2010; Phillips et al., 2005), where some bacterial strains have been shown to utilize HCH as a sole carbon source (Phillips et al., 2005). Monochlorobenzene and benzene have been reported as the final products under anoxic HCH degradation (Beland et al., 1976; Boyle et al., 1999; Lal et al., 2010; Middeldorp et al., 1996), while complete mineralization has only been observed under oxic conditions (Lal et al., 2006, 2010; Nayyar & Lal, 2016).

#### 2.7.2.1. Anaerobic degradation

Hexachlorocyclohexane degradation in bacteria was initially believed to mainly occur under anaerobic conditions where various levels of anaerobic degradation of HCH isomers were reported (Lal et al., 2010; Phillips et al., 2005). A study by Ohisa et al. (1980) initially proposed an anaerobic degradation mechanism of γ-HCH that involve two dichloroelimination steps resulting in the formation of γ-3,4,5,6-tetrachlorocyclohexene (γ-TCCH) and 5,6-dichlorocyclohexadiene and a dehydrochlorination reaction to produce chlorobenzene **(Figure 2.5)**. Several subsequent studies confirmed the presence of γ-TCCH as an anaerobic degradation intermediate of γ-HCH (Beland et al., 1976; Heritage & MacRae, 1977; Jagnow et al., 1977; Lal et al., 2010; Ohisa et al., 1980). Traces of trichlorobenzene and benzene were also identified in the reaction mixture by (Jagnow et al., 1977). Other studies suggest that anaerobic degradation of other HCH isomers including α-, β-, and δ-HCH also proceeds through successive dichloroelimination steps followed by dehydrochlorination to produce chlorobenzene (**Figure 2.5**) (Heritage & MacRae, 1977; Lal et al., 2010; Middeldorp et al., 1996). More recently Quintero et al. (2005) suggested an alternative anaerobic HCH degradation pathway that generates chlorobenzene from all the four major HCH isomers. In their study of unidentified anaerobic microbial liquid and soil slurry systems Quintero et al. (2005) identified pentachlorocyclohexane, 1,2- and 1,3-dichlorobenzene (DCB) and chlorobenzene (CB).

#### 2.7.2.2. Aerobic degradation

Several aerobic HCH degraders have previously been reported (Alvarez et al., 2012; Gupta et al., 2000; Lal et al., 2010), however, most of the aerobic HCH degraders known belong to the *Sphingomonadaceae* family (Lal et al., 2006, 2010; Nayyar & Lal, 2016). The first aerobic HCH degrading bacterium was reported in 1989 in Japan (Senoo & Wada, 1989), several subsequent reports from other countries then followed (Boltner et al., 2005; Ito et al., 2007; Mohn et al., 2006; Sahu et al., 1990). Close to thirty HCH-degrading sphingomonads have been reported from different parts of the world, however, three species namely, *Sphingobium japonicum* UT26 (Japan) (Senoo & Wada, 1989), *Sphingobium indicum* B90A (India) (Sahu et al., 1990) and *Sphingobium francense* Sp+ (France) (Cérémonie et al., 2006) have extensively been studied.

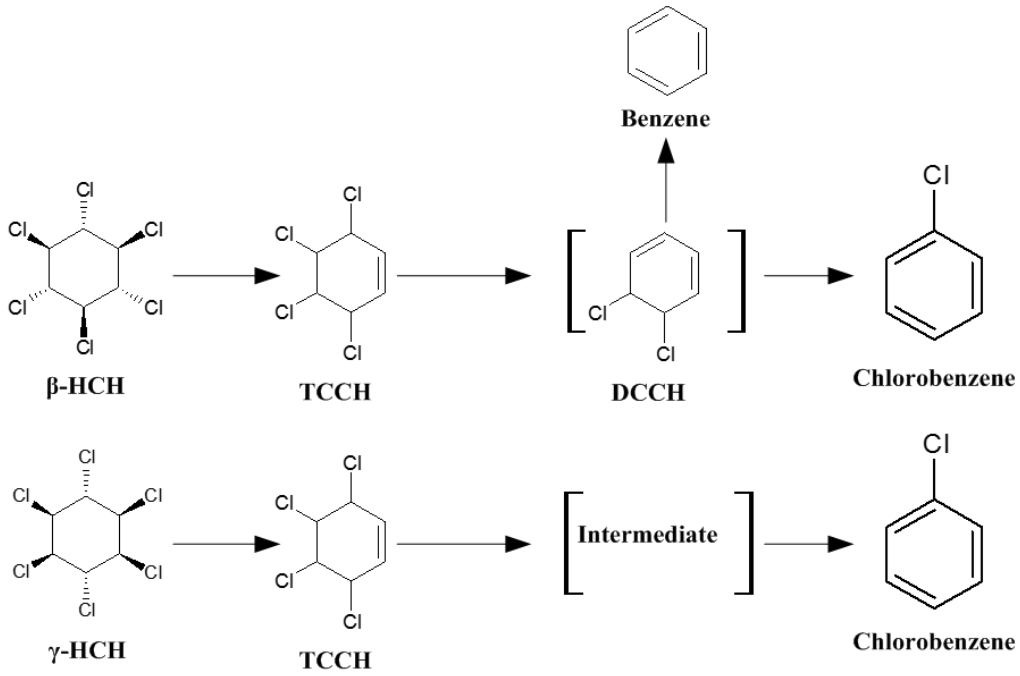


**Figure 2.5:** Proposed anaerobic HCH degradation pathway for γ-HCH and β-HCH. Shown in square brackets are compounds not yet empirically determined (adapted from Lal et al., 2010).

Since the first report of aerobic HCH degradation (Senoo & Wada, 1989), extensive research to decipher the aerobic degradation pathway has been conducted in various research groups (Lal et al., 2006, 2010; Nayyar & Lal, 2016). A detailed aerobic γ-HCH degradation pathway was first elucidated for *S. japonicum* UT26 (Nagata et al., 2007), where two degradation stages were reported, namely; upstream and downstream pathways (**Figure 2.6**). The upstream pathway involves dechlorination reactions where γ-HCH is metabolized to 2,5-DCHQ (2,5-dichlorohydroquinone) which is further metabolized to $CO_2$ and $H_2O$ in the downstream pathway (Endo et al., 2005; Lal et al., 2006, 2010; Nayyar & Lal, 2016). A similar pathway has been reported in all the other sphingomonads, however, isomer-specific differences have been reported in the early steps of the degradation pathway in different strains (**Figure 2.6**) (Lal et al., 2006, 2010; Nayyar & Lal, 2016).

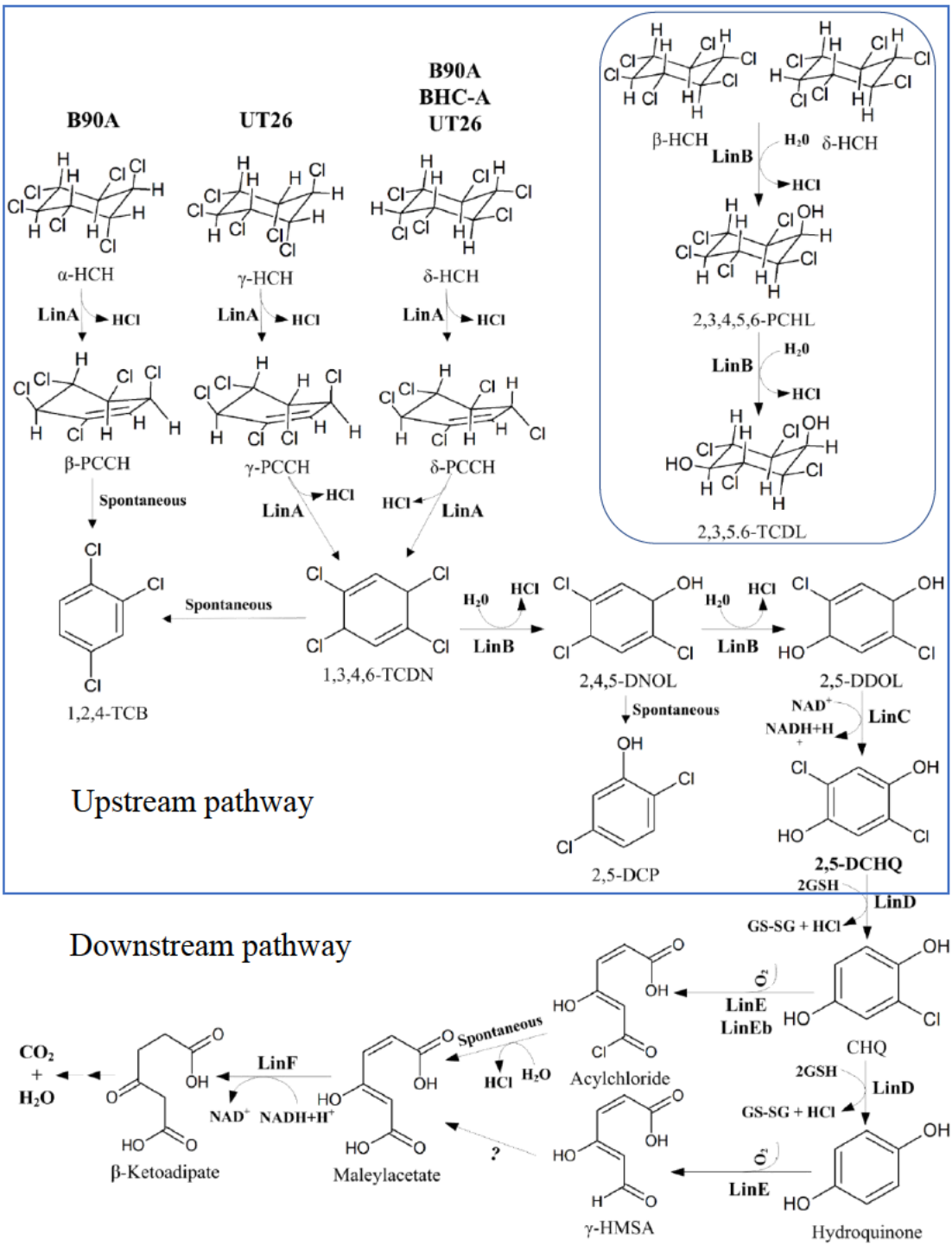


**Figure 2.6:** A scheme of the proposed degradation pathway of different HCH isomers by the upstream and downstream pathways of aerobic HCH degradation (adapted from Nayyar & Lal, 2016).

### 2.7.2.3. Genes involved in aerobic HCH degradation (*Lin* genes)

The catabolic genes associated with aerobic degradation of HCH (termed as *Lin* genes) were first elucidated for *S. japonicum* UT26 (Nagata et al., 1999) and subsequently in *S. indicum* B90A (Dogra et al., 2004) and all the other HCH-degrading sphingomonads that have currently

been reported (Boltner et al., 2005; Lal et al., 2006, 2010; Nayyar & Lal, 2016). The HCH degradation pathway consists of eight structural genes (*Lin A* to *Lin J*), a *Lin C*-like gene (*Lin X*) and a regulatory gene (*Lin R*) (**Table 2.2**) (Dogra et al., 2004; Lal et al., 2006). The aerobic bio-transformation of γ-HCH to 2,5-dichlorohydroquinone (2,5-DCHQ) in the upstream stage proceeds through; two steps of dehydrochlorination catalyzed by *Lin*A (γ-HCH dehydrochlorinase), two steps of hydrolytic dehalogenation catalyzed by *Lin*B (haloalkane dehalogenase), and one dehydrogenation step catalyzed *Lin*C (2,5-dichloro-2,5-cyclohexadiene-1,4-diol dehydrogenase) (Girish & Kunhi, 2013; Lal et al., 2010; Nayyar & Lal, 2016). 2,5-DCHQ is subsequently metabolized in the downstream pathway by *Lin*D (2,5-DCHQ dechlorinase), *Lin*E (CHQ 1,2-dioxygenase), *Lin*F (maleylacetate reductase), *Lin*GH (succinyl-CoA: 3-oxoadipate CoA transferase) and *Lin*J (β-ketoadipyl CoA thiolase) to succinyl-CoA and acetyl CoA which enters the tricarboxylic acid pathway (**Figure 2.6**) (Lal et al., 2010; Nayyar & Lal, 2016). *Lin*R is a Lys-type transcriptional regulator that is reported to regulate the expression of *Lin*D and *Lin*E (Boltner et al., 2005; Nagata et al., 1999). *Lin*X codes for a dehydrogenase that has similar activity to *Lin*C (Boltner et al., 2005; Dogra et al., 2004). Table 3 summarises the characteristics of reported Lin genes. Other noteworthy *Lin* genes include *Lin*KLMN which code for a putative ABC-type transporter that is thought to be important in the utilization of γ-HCH by *S. japonicum* UT26 (Nagata et al., 2007).

### 2.8. Factors affecting HCH degradation

The degradation of HCH is influenced by chemical, physical and biological factors such as; pH, temperature, availability of additional carbon sources, HCH concentration, and bioavailability among other factors (Kumar & Pannu, 2018; Saez et al., 2017).

#### 2.8.1. Effect of pH

Variations in pH affect the growth of HCH degraders during the degradation process, therefore pH has previously been reported as one of the key factors that affect HCH degradation (Kumar & Pannu, 2018; Saez et al., 2017). A study by Elcey & Kunhi (2010) found that an adapted consortium could degrade γ-HCH at pH levels ranging from 3 to 9, with the optimum being at a more neutral range of between pH 6 and 8. Murthy & Manonmani (2007), on the other hand, found that a defined consortium of 10 microorganisms did not degrade γ-HCH at pH 4. The chances of microbial survival in the consortium gradually improved as the pH levels were increased towards neutrality. In a study on the effects of initial pH on γ-HCH removal by *Streptomyces* sp. M7 in soil extract, Benimeli et al. (2007), reported the highest removal of the

pesticide at an initial pH of 7. In contrast, Okeke et al. (2002) an optimal pH of 9 for microbial growth and degradation of γ-HCH in soil slurries.

**Table 2.2:** Reported Lin genes from *S. japonicum* UT26, *S. indicum* B90A and *S. francense* Sp+ (adapted from Dogra et al., 2004; Lal et al., 2006; Nagata et al., 1999).

| | Nucleotides (amino acids) | | | G+C content (%) | | | Function | Expression in B90A, UT26, Sp+ |
|---|---|---|---|---|---|---|---|---|
| **Genes** | **B90A** | **UT26** | **Sp+** | **B90A** | **UT26** | **Sp+** | **B90A, UT26, Sp+** | |
| *Lin*A1 | 462 (154) | ** | ** | 52.7 | ** | ** | Dehydrochlorinase | Constitutive |
| *Lin*A2 /*Lin*A[a] | 468 (156) | 468 (156) | 468 (156) | 53.9 | 53.9 | 53.9 | Dehydrochlorinase | |
| *Lin*B | 888 (296) | 888 (296) | 888 (296) | 62.5 | 62.5 | 62.5 | Halidohydrolase | Constitutive |
| *Lin*C | 750 (250) | 750 (250) | 750 (250) | 64.5 | 64.3 | 64.5 | Dehydrogenase | Constitutive |
| *Lin*D | 1038 (346) | 1038 (346) | 1038 (346) | 61.8 | 61 | 61.8 | Reductive dechlorinase | Inducible |
| *Lin*E | 963 (321) | 963 (321) | 963 (321) | 60.1 | 60.1 | 60.1 | Ring-cleavage dioxygenase | Inducible |
| *Lin*R | 909 (303) | 909 (303) | 909 (303) | 60.3 | 61.3 | 60.3 | Transcriptional regulator | ? |
| *Lin*X1 | 750 (250) | 750 (250) | 750 (250) | 64.5 | 64.5 | 64.5 | Dehydrogenase | ? |
| *Lin*X2 | 750 (250) | ** | ** | 64.5 | ** | ** | Dehydrogenase | ? |
| *Lin*X3 | 750 (250) | ** | ** | 64.5 | ** | ** | Dehydrogenase | ? |
| *Lin*F | * | 1056 (352) | * | * | 68.1 | * | Reductase | ? |
| *tnp*A | 792 (264) | 792 (264) | 792 (264) | 61 | 61 | 61 | Transposase | ? |

*LinA*[a]: *LinA* gene from *S. japonicum* UT26 and *S. francense* Sp+. (**): not detected; (*): not determined; (?): not known.

### 2.8.2. Temperature

Temperature changes up to specified limits may affect HCH removal by influencing the biological activity of degraders or modifying the levels of bioavailability through reduced sorption (Kumar & Pannu, 2018; Phillips et al., 2005; Saez et al., 2017). Generally, the optimum temperature for HCH biodegradation in soil slurry, soil, and bacterial cultures has been reported to be in the range of 25 ºC to 30 ºC (Benimeli et al., 2007; Boltner et al., 2005; Elcey & Kunhi, 2010; Mohn et al., 2006). Elcey & Kunhi, (2010) studied γ-HCH degradation

across a wide temperature range and found that chloride ions were released at temperatures as low as 5 ºC and as high as 60 ºC at 8% and 18% respectively. Optimum chloride release however occurred at 30 – 35 ºC (Elcey & Kunhi, 2010). Similar results were observed by Benimeli et al. (2007), where maximum removal of γ-HCH by *Streptomyces* sp. M7 was observed at 30 ºC.

### 2.8.3. Inoculum size

The amount of microbial cells in the active growth phase (inoculum) has been reported to affect the degradation rate of xenobiotic compounds (Kumar & Pannu, 2018; Saez et al., 2017). Several studies have shown that larger inoculum sizes increase the degradation efficiency of HCH up to a certain extent beyond which further increase has no additional benefit on the pesticide removal (Guillén-Jiménez et al., 2012; Kumar & Pannu, 2018). Using an immobilized *Streptomyces* consortium (Saez et al. (2014) observed a higher γ-HCH removal at $10^7$ CFU/g of inoculum than smaller inoculum sizes. Higher cell densities, however, had no additional benefit (Saez et al., 2014). Similar results were observed by (Fuentes et al., 2010), that the inoculum size and the rate of γ-HCH clearance are not directly proportional.

### 2.8.4. Additional carbon source

It has previously been demonstrated that additional carbon sources besides the target pollutant can affect its (pollutant) degradation through co-metabolism (García-Rivero & Peralta-Pérez, 2008; Saez et al., 2017). Benimeli et al. (2007) demonstrated that *Streptomyces* sp. M7 simultaneously consumed glucose and γ-HCH. They also showed that high glucose concentrations stimulated biomass yields and γ-HCH removal (Benimeli et al., 2007). Guillén-Jiménez et al. (2012), observed that the addition of agave leaves to the degradation culture medium increased fungal γ-HCH degradation by biostimulation. Similar results were reported by Álvarez et al. (2012), where higher levels of γ-HCH removal by *Streptomyces* strains A5 and M7 were observed in presence of root exudates as additional carbon sources. However, degradation of xenobiotic compounds such as HCH has also been shown to be influenced by other factors such as the kind of microbial community present, pollutant concentration, and concentration of other nutrients, among other factors (Kumar & Pannu, 2018; Saez et al., 2017). Additional carbon sources alone, therefore, may not always promote contaminant degradation process, and in some cases even limit the degradation process (Kumar & Pannu, 2018; Pino et al., 2011; Saez et al., 2017).

### 2.8.5. Hexachlorocyclohexane concentration

Hexachlorocyclohexane concentration influences soil microbial communities, stimulating the growth of some microorganisms while inhibiting the growth of others (Phillips et al., 2005). The concentration of the contaminant is therefore one of the key factors that influence biomass growth and degradation. Very low pollutant concentration may not activate degradative enzymes, while excessive levels may be toxic to the microorganisms (Awasthi et al., 2000; Kumar & Pannu, 2018; Saez et al., 2017). While studying the ability of a Pandoreae sp. to remove γ-HCH in liquid and soil slurry systems, Okeke et al. (2002), observed that γ-HCH removal increased with concentration up to 150 mg/L but decreased at 200 mg/L. Effects of increased concentration on γ-HCH removal was also observed by Guillén-Jiménez et al. (2012).

### 2.8.6. Bioavailability

Factors that influence HCH solubility and sorption such as vapor pressure and soil organic and moisture content may affect its mobility in soil and hence the bioavailability and degradation (Saez et al., 2017). In addition, HCH can volatilize thereby altering its concentration in liquid and solid phases of soil as well as its bioavailability (Phillips et al., 2005; Saez et al., 2017). Previous studies have shown that increased soil water content decreases the adsorption of hydrophobic compounds, due to hydration of the adsorbent surfaces which lowers the accessibility of adsorption sites (Kumar & Pannu, 2018; Roy et al., 2000; Saez et al., 2017). Soil properties and composition have also been shown to influence HCH bioavailability and degradation (Kumar & Pannu, 2018). Soil with high silt content has greater moisture retention which may improve HCH bioavailability (Phillips et al., 2005). On the other hand soil with high organic content decreases the bioavailability of contaminants (Kumar & Pannu, 2018; Saez et al., 2017; Vlčková & Hofman, 2012).

## 2.9. Bioremediation of hexachlorocyclohexane

Bioremediation is the process of modifying or removing toxic pollutants from the environment using living organisms such as bacteria, fungi, and plants (Cutright & Erdem, 2012; Girish & Kunhi, 2013). Bioremediation technologies can potentially be used to clean up contaminated soils, contaminant stockpiles, liquid wastes, and commodities (Lal et al., 2010; Russell et al., 1998; Sutherland et al., 2004). Though HCH is no longer mainly used as an insecticide, bioremediation of previously contaminated soil and stockpiles is a top priority (Lal et al., 2010). In addition, contamination of liquid wastes such as agricultural runoff and commodities

remains an environmental concern due to diffusion from heavily contaminated soils and stockpiles (Lal et al., 2010).

Biostimulation and bioaugmentation are the two major approaches that have been applied for soil bioremediation. Biostimulation entails the provision of oxygen and/or inorganic nutrients to resident bacteria that can degrade the pollutant in question (Lal et al., 2010). On the other hand, bioaugmentation entails the introduction of additional microorganisms with the ability to degrade the contaminant, either naturally or through genetic manipulation (Lal et al., 2010). Both approaches have been used to clean up HCH-contaminated sites with varying degrees of effectiveness (Bidlan et al., 2004; Lal et al., 2010; Mertens et al., 2006; Phillips et al., 2006).

## 2.10. Fungal-bacterial co-cultures in contaminant degradation and bioremediation

Though microbial catalysts offer a promising strategy to maintain environmental health, their use is normally impeded by the tendency of many organic contaminants to adsorb and accumulate onto organic matter, decreasing their bioavailability (Furuno et al., 2010, 2012; Harms et al., 2011). The accumulation of organic contaminants mostly occurs in toxic and hostile environments devoid of nutrients and water required to promote the growth of potential degraders. Previous reports suggest that ideal bioremediation machinery should be able to cope with harsh environmental conditions and have the capacity to track contamination in soil pores and organic matter. In addition, appropriate decontamination machinery should have a catabolic capacity that does not rely on the availability of the pollutant as a substrate for growth and have the ability to transport water, required nutrients, and metabolically active organisms to contaminated spots (Harms et al., 2011).

Most of the characteristics ideal for bioremediation are displayed by fungi, either alone or in cooperation with bacteria and plants, and are therefore considered important components for the development of bioremediation technologies (Harms et al., 2011; Wick et al., 2010). The key characteristics of fungi that contribute to their suitability for bioremediation are their ability to degrade organic contaminants or influence their bioavailability, and their ability to grow mycelial structures (called hyphae) (Finlay, 2008; Harms et al., 2011). Other notable features of fungi as ideal organisms for bioremediation are, the low specificity of their catabolic enzymes and the non-reliance on pollutants as growth substrates (Harms et al., 2011). Furthermore, despite the minuscule nature of hyphae, which have diameters of 2-10 μm, fungi

are among the world's largest living organisms, with reported networks spanning hundreds of hectares (Furuno et al., 2012).

### 2.10.1. Mycelial-mediated dispersal of bacteria ("fungal highways")

Previous studies have demonstrated that mycelial structures provide an efficient dispersal network (fungal highways) that facilitates both random and targeted movement of otherwise immobilized bacteria (**Figure 2.7**) (Furuno et al., 2010; Wick et al., 2010). The dispersal of bacteria is achieved by the ability of fungal mycelia to grow along surfaces, via pores, and through air gaps that allow them to connect air-filled spaces found between water-filled pores (**Figure 2.7**) (Wick et al., 2010). Kohlmeier et al. (2005) observed fungus-mediated dispersal of bacteria of up to 1cm $d^{-1}$ in an artificial laboratory system. Fungal-mediated transport was however shown to be dependent on bacterial motility and surface characteristics of both partners (Kohlmeier et al., 2005). It was further observed that motile hydrocarbon-degrading bacteria were widely dispersed over the hydrophilic fungus *Fusarium oxysporum* while non-flagellated bacteria were not dispersed on established mycelia (Kohlmeier et al., 2005). Mycelial-mediated transport ("fungal highways" (Kohlmeier et al., 2005)) is thought to facilitate the dispersal of indigenous bacteria towards pollutants pockets suitable for degradation. This increases the bioavailability of contaminants by reducing the distances between bacterial degraders and their respective compounds (Kohlmeier et al., 2005; Wick et al., 2010).

### 2.10.2. Mycelial-mediated translocation of nutrients and contaminants ("fungal pipelines")

Translocation of cellular material through mycelial network is essential for fungi to flourish in heterogeneous environments (Jennings, 1987; Wick et al., 2010). Mycelial networks must therefore translocate nutrients across spatially dispersed sources and sink while maintaining their structural integrity from mycophagy or random damage (Bebber et al., 2007; Wick et al., 2010). Evidence of both passive (diffusion-driven) and active (metabolically-driven) translocation of contaminants by fungal mycelia (fungal pipelines) has been demonstrated (**Figure 2.7**) (Schamfuß et al., 2013, 2014; Wick et al., 2010). On the other hand, previous reports revealed the ability of underground fungal networks to connect plants by translocating nutrients between them or providing nutrients to associated bacteria within their hyphosphere, thus shaping the communities above and below the earth's surface (Whitfield, 2007; Wick et al., 2010). More recently, experimental evidence for stimulation of bacterial activity by

mycelial-mediated nutrient supply in a resource-scarce environment was demonstrated (Worrich et al., 2017).

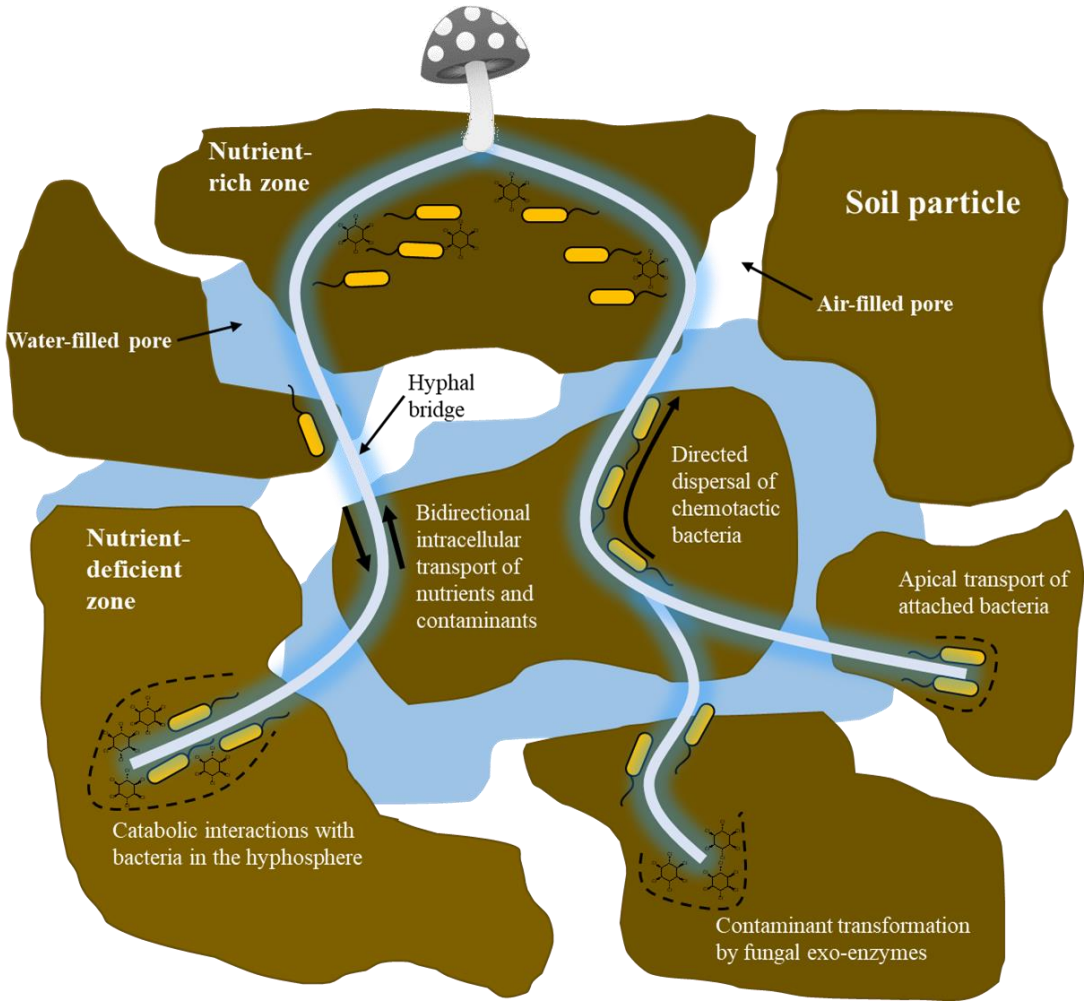


**Figure 2.7:** A schematic depiction of the impact of fungal-mediated transport pathways on pollutant biodegradation in soil (adapted from Wick et al., 2010).

## 2.11. Stable isotope probing

Stable isotope probing (SIP) is a well-established method in microbial ecology for identifying metabolically important players in microbial communities using stable isotope isotope-labeled substrates such as D,$^{13}$C, $^{15}$N,$^{18}$O and $^{34/36}$S (Jehmlich et al., 2008, 2010, 2016; Taubert et al., 2011). There are SIP variants that target distinct biomarker molecules resulting from metabolic tagging of biomass by stable isotopes (Neufeld, et al., 2007a). The target biomarkers include labeling of deoxyribonucleic acid (DNA-SIP) (Neufeld, et al., 2007b), ribonucleic acid (RNA-SIP), phospholipid fatty acids (PLFA-SIP) (Boschker et al., 1998; Richnow et al., 2002), amino acids (Richnow et al., 2002) and proteins (Jehmlich et al., 2010, 2016).

### 2.11.1. Protein SIP

The involvement of proteins in enzymatic catalysis makes them ideal for studying the structure and function of microbial communities because they provide both functional and phylogenetic information (Jehmlich et al., 2008). The incorporation of stable isotopes (typically $^{13}C$ or $^{15}N$) into proteins has become a powerful tool for quantitative and qualitative proteome research because the incorporation rates are a useful indicator for determining the overall metabolic activity and protein turnover rates (Jehmlich et al., 2016). Metabolic protein labeling can be achieved in two ways, (i) utilizing labeled substrates (such as $^{13}C$-glucose or $^{15}N$-ammonium) that are biochemically assimilated into amino acids (Jehmlich et al., 2010, 2016), or (ii) utilizing individually labeled amino acids that can be supplied in the medium (Chen et al., 2015).

The use of stable isotope-labeled substrates is appealing because mass spectrometry can be used to measure the mass shifts that would permit the quantitative assessments of isotope incorporation (Jehmlich et al., 2010, 2016). The rate of isotope incorporation is then used as an indirect indicator of metabolic activity relative to a specific substrate (Jehmlich et al., 2016). The mass spectrometry data are used to extract two important parameters, i.e (i) the relative isotope abundance (RIA), which refers to the number of labeled atoms in a peptide as an indicator of the fraction of labeled substrate that was assimilated, and (ii) the labeling ratio (LR), which provides the ratio of labeled to unlabeled peptides as an indicator of protein turnover rates following the addition of the labeled substrate (Jehmlich et al., 2008, 2010, 2016). Protein-SIP experimental workflow includes; protein extraction, separation by 1-D gel electrophoresis, in-gel digestion of proteins, mass spectrometry, and bioinformatics analysis (MetaProSIP) which calculates and exports SIP parameters (as *.csv files) for subsequent analysis and interpretation (**Figure 2.8**).

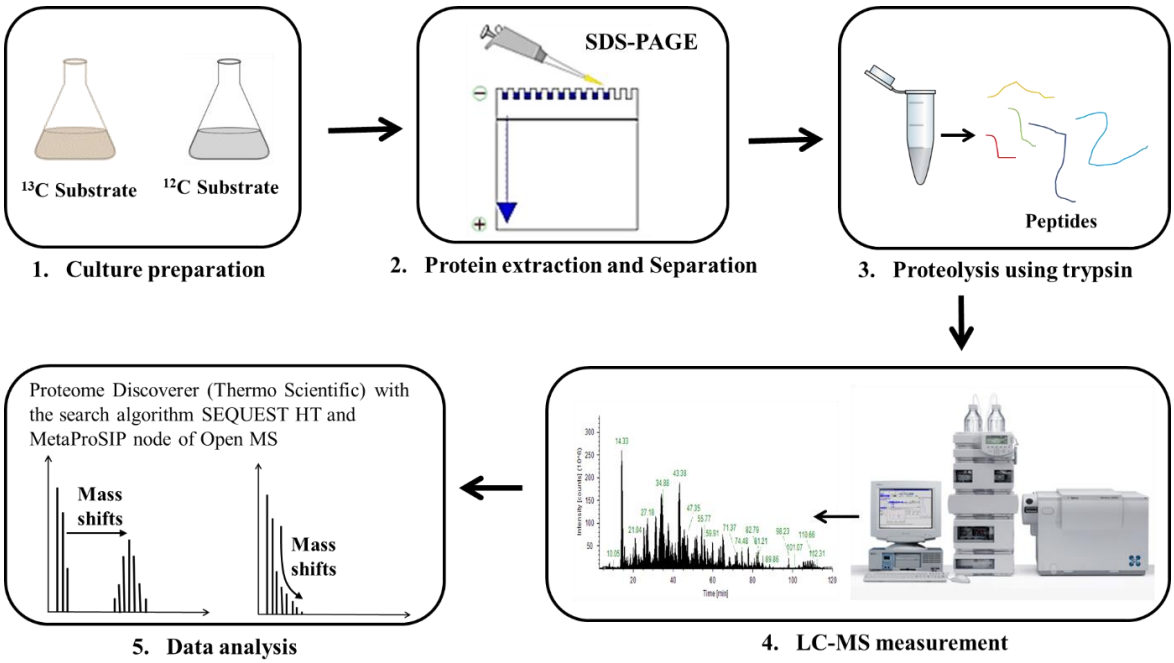


**Figure 2.8:** Experimental workflow of Protein-SIP (adapted from Jehmlich et al., 2016).

# CHAPTER THREE

## 3.0 Characterization of hexachlorocyclohexane (HCH)-degrading *Sphingobium* species isolated from HCH contaminated soil.

### 3.1. Abstract

Hexachlorocyclohexane remains a common pollutant despite the restricted or complete ban on its commercial use globally. HCH-degrading bacteria are however believed to have a potential for active bioremediation processes. In the present study, two HCH-degrading *Sphingobium* strains (S6 and S8) were isolated from HCH-contaminated soil collected from a former obsolete pesticide storage site in Kitengela, Kenya (GPS: 01.49 S, 37.048E). Based on 16S rDNA gene sequencing, the two strains were closely related to *S. quisquiliarum* P25, a known HCH-degrader with sequence identities greater than 98%, and were shown to effectively degrade all the four HCH isomers in the order γ-HCH > δ-HCH ≈ α-HCH > β-HCH. Subsequently, six *lin* genes responsible for HCH degradation including; five structural genes (*linA*, *linB*, *linC*, *linD* and *lin E*) and a regulatory gene *linR*, identical to those from other HCH degraders were identified. The respective Lin protein sequences had high similarity to those reported from *S. japonicum* UT26 except LinB which had five mutations that might be responsible for the moderate degradation of β-HCH observed in the two isolates. The draft genomes were 4,173,956bp and 4,170,555bp consisting of 4,015 and 4,039 protein-coding sequences (CDS) for *Sphingobium* sp. strain S6 and *Sphingobium* sp. strain S8 respectively. The *lin* genes responsible for HCH degradation were identified, and gene clusters for degradation of other xenobiotic compounds were predicted. This research, therefore, adds to the diversity of HCH degraders and that of LinB sequences which would aid in unraveling the molecular mechanism of degradation and bioremediation of HCH isomers, particularly β-HCH.

### 3.2. Introduction

Hexachlorocyclohexane is a cyclic organochloride insecticide that was widely used for agricultural pest management and in public health programs for the control of vector-borne diseases (Lal et al., 2006; Singh & Kuhad, 1999). HCH is commercially produced by chlorination of benzene in the presence of UV light, yielding a mixture of four stable isomeric forms (also referred to as technical HCH). The HCH isomers and their respective proportions during the production process are; α- (60-70%), β- (5-12%), γ- (10-12%), and δ- (6-10%). However, among the different HCH isomers, only γ-HCH isomer (commonly referred to as lindane) has insecticidal properties and is normally purified from the rest of the isomers

(referred to as `HCH muck`) which are normally disposed of (Lal et al., 2006; Manickam et al., 2008; Singh & Kuhad, 1999).

Lindane production and its use over the years have resulted in the accumulation of dangerous stockpiles of toxic HCH waste (Lal et al., 2006, 2010; Manickam et al., 2008; Okai et al., 2010). Due to mounting concerns about HCH toxicity to non-target organisms and persistence in the environment, its use has been restricted or completely banned in most parts of the world. (Boltner et al., 2005; Dogra et al., 2004; Lal et al., 2010; Walker et al., 1999). Despite the ban or restricted use, HCH continues to pose a serious environmental and health risk, particularly in areas where HCH was previously applied and at former production or dumping sites (Boltner et al., 2005). The widespread contamination necessitates the development of mechanisms to alleviate the environmental risks posed by HCH residues to plant, animal, and human health (Girish & Kunhi, 2013; Lal et al., 2010; Nayyar & Lal, 2016). Microbial degradation has therefore been proposed as a promising and eco-friendly strategy for biodegradation of organic contaminants such as HCH and bioremediation of contaminated sites (Girish & Kunhi, 2013; Pant et al., 2013).

Microbial degradation of HCH isomers has been reported for both fungi (Bumpus et al., 1985; Guillén-Jiménez et al., 2012; Phillips et al., 2005; Sagar & Singh, 2011) and bacteria (Boltner et al., 2005; Lal et al., 2006, 2010; Mohn et al., 2006; Nagata et al., 2007; Nayyar & Lal, 2016) under both aerobic and anaerobic conditions (Kumar & Pannu, 2018; Phillips et al., 2005; Saez et al., 2017). However, complete mineralization of HCH has only been observed to occur under aerobic conditions (Manickam et al., 2008; Mohn et al., 2006; Nagata et al., 2007). Despite the numerous numbers of known HCH degrading microbes, members of the family *Sphingomonadaceae* have been shown to play a central role in the aerobic biodegradation of HCH (Boltner et al., 2005; Lal et al., 2006, 2010).

Among the numerous HCH-degrading sphingomonads reported, three distinct species, namely, *Sphingobium japonicum* UT26 (Japan) (Senoo & Wada, 1989), *Sphingobium indicum* B90A (India) (Sahu et al., 1990) and *Sphingobium francense* Sp+ (France) (Cérémonie et al., 2006) have extensively been studied. The HCH degradation pathway and the catabolic genes (known as *lin* genes) required for aerobic degradation of γ-HCH were initially identified and described for *S. japonicum* UT26 (Nagata et al., 1999) and subsequently for *S.indicum* B90A (Dogra et al., 2004). Nearly identical *lin* genes have been identified in all the other HCH-degrading sphingomonads reported from different geographical locations across the world

(Boltner et al., 2005; Lal et al., 2006; Mohn et al., 2006; Pal et al., 2005). Two important stages (the upstream and downstream pathways) involved in the degradation of γ-HCH have been described. Dechlorination reactions that convert γ-HCH to 2,5-dichlorohydroquinone (2,5-DCHQ), form the upstream pathway, while those reactions that convert 2,5-DCHQ to tricarboxylic acid cycle (TCA) cycle intermediates, constitute the downstream pathway (Endo et al., 2005; Manickam et al., 2008).

Bioremediation by bioaugmentation has been demonstrated to offer a promising biotechnological strategy to clean up contaminated environments (Cao et al., 2013; Lal et al., 2010). Several studies have demonstrated the successful removal of HCH isomers from aquatic and soil environments using microbial degraders (Bidlan et al., 2004; Mertens et al., 2006; Raina et al., 2008). Such strategies would be greatly enhanced by screening and exploring more isolates, thereby increasing the pool of HCH degraders and *lin* genes variants (Lal et al., 2010). In the present study, two HCH-degrading *Sphingobium* strains were isolated from HCH-contaminated Kenyan soil collected from a former pesticide storage facility in Kitengela, Kenya. The isolates were phylogenetically identified and their relative HCH degradation capacities and associated *lin* genes were examined. To our knowledge, this is the first report on HCH-degrading *Sphingobium* species isolated from Kenya. This research, therefore, adds to the diversity of HCH degraders and that of LinB gene sequences which would aid in unraveling the molecular mechanism of degradation of HCH isomers, particularly β-HCH.

## 3.3. Materials and Methods

### 3.3.1. Chemicals and reagents

Hexane (LiChrosolv grade), Acetone (99.8%), and γ-HCH (97%) and HCH Mix (HCH analytical standard mixture of isomers, α: β: γ: δ = 1:1:1:1) were either purchased from Sigma (Munich, Germany) or Merck (Darmstadt, Germany) and were of analytical grade. PCR primers used were purchased from Integrated DNA Technologies (IDT, Iowa USA), while kits necessary for PCR amplification were purchased from Roche (Mannheim, Germany).

### 3.3.2. Isolation of HCH-degrading bacteria by enrichment cultures

The HCH degrading bacteria were isolated by enrichment culture technique. HCH-contaminated soil samples used in this study were collected from a former obsolete pesticide store in Kitengela, Kenya (GPS: 01.49 S, 37.048E) and transported to the lab wrapped in sterile aluminum foil and Ziplock bags. One gram of the soil sample was extracted with hexane/acetone (3:1, v/v) and subjected to GC/MS analysis to establish the level of

contamination. For bacterial isolation, 5g of the soil was added into a sterile 50ml minimum salt medium (MSM) spiked with 100 µg $mL^{-1}$ γ-HCH in a 100 mL Erlenmeyer flask without any additional carbon source. The MSM medium contained (in $gL^{-1}$): 1g $K_2HPO_4$, 1 g $KH_2PO_4$,1 g $NH_4NO_3$, 0.2 g $MgSO_4.7H_2O$, 5 mg $Fe(SO_4)$, 5 mg $Na_2MoO_4.2H_2O$, 5 mg $MnSO_4.4H_2O$ and pH 7 as described previously by Senoo & Wada, (1989). The cultures were incubated in a rotary shaker at 30 ºC and 150rpm for 14 days. Serial dilution of the enrichment cultures ($10^{-3}$ to $10^{-6}$ times) was prepared and spread on 1:10 diluted Luria-Bertani (LB) agar plates spiked with 100 µg $mL^{-1}$ γ-HCH (at this concentration γ-HCH formed visible precipitate in the agar medium). The plates were then incubated at 30 ºC for 4 days. HCH degrading bacteria were identified as colonies exhibiting a clear zone where HCH precipitate had disappeared. Two bacterial isolates, designated as strain-S6 and strain-S8 that displayed clear zones around their colonies were selected and repeatedly (~5 to 6 times) spread on the same medium to obtain pure cultures for use in subsequent studies.

### 3.3.3. Biochemical, and molecular characterization of the HCH-degrading bacterial isolates

The physiological and biochemical profiles of the two bacterial isolates (strain-S6 and strain-S8) were tested using biology GNIII microtiter plates (Biolog, USA) (Bochner, 1989) according to the manufacturer's instructions. The 16S rRNA gene sequencing was used for molecular identification of the bacterial isolates according to Nelson et al. (2021). The16S sequences were used for BLAST searches in the GenBank database at NCBI using the BLASTn algorithm with default settings, the database set at 16S ribosomal RNA sequences (Bacteria and Archaea), and optimized for highly similar sequences (Altschul et al., 1990). Seventeen homologous bacterial 16S rDNA sequences with identities above 98% and 100% coverage retrieved from the database, were aligned in MUSCLE, version 3.6 (Edgar, 2004). The Bayesian phylogenetic approach in MrBayes, version 3.1.2 (Huelsenbeck & Ronquist, 2001) was used to perform phylogenetic analysis based on the nucleotide sequences. A total of 1,000,000 trees were generated, from which a tree was sampled every 1000 generations. The Bayesian consensus trees were constructed using the 'sum p' and 'sum t' options in MrBayes and the branching confidence was calculated as posterior probabilities. The trees were visualized in Figtree, version 1.4.3 (http://tree.bio.ed.ac.uk/).

### 3.3.4. Dechlorinase assay for detection of haloalkane dehalogenase activity

To detect HCH degrading bacteria with haloalkane dehalogenase enzyme activity, a colorimetric assay was performed in a 96-well microtiter plate according to the method previously described by Phillips et al. (2001). The assay is based on the decrease in pH of a weakly buffered medium containing phenol red as an indicator. Visual color change from red to yellow indicated dichlorination of Lindane and subsequent decrease in pH in the reaction mixture as a result of chloride ion release. Wells without cell-free extract were used as controls.

### 3.3.5. Biodegradation of HCH isomers in liquid-culture

To examine HCH degradation by pure cultures, the isolates (S6 and S8) were pre-cultured in LB medium to an $OD_{600}$ of about 1 (~3 days) and harvested by centrifugation at 7000 rpm and 15 ºC for 10 min. The cells were washed twice with MSM without a carbon source and resuspended in the same medium to a final $OD_{600}$ of about 3 as previously described by (Boltner et al. (2005). Fifty µl of cell suspension was then used to inoculate 2.5 mL of MSM medium containing 1% glucose and 10 µg $mL^{-1}$ (34.4 µM) of each HCH isomer in a mixture in previously prepared 20 mL head space GC vials. The vials were incubated in a rotary shaker at 30ºC and 150rpm. At specific time intervals (0, 1, 2, 5, 7, 9, and 24 hrs) three vials were used for extraction and GC analysis of residual HCH in the reaction mixture. Uninoculated media was used as abiotic controls. All experiments were conducted in triplicate.

### 3.3.6. Analytical Methods (Gas chromatography "GC" analysis)

To monitor HCH degradation in liquid culture, Triplicate bottles were used at every time point and extracted with 5ml hexane containing 0.31 µg $L^{-1}$ DDT as the internal standard. The bottles were then frozen at -20 ºC overnight to separate the solvent and aqueous phase. The extract was transferred into clean glass vials and dried with Sodium sulfate. A hundred µL of the extract was then mixed with 10 µL of 4-chlorobenzotrichloride as injection standard and analyzed by GC (HP 7890 Series GC, Agilent) with 20m 0.18mm 18µm column (Agilent). Helium was used as a carrier gas with a flow rate of 1 mL $min^{-1}$.

### 3.3.7. PCR amplification and analysis of *lin* Genes

Total genomic DNA from the S6 and S8 bacterial isolates was harvested using Quick-DNA Fungal/Bacterial Kit (Zymo Research) according to the manufacturer's instructions. The genes responsible for HCH degradation (*lin* genes) were amplified by PCR using primers described previously by Kumari et al. (2002) (appendix 1, **Table S1**). The PCR products were sent for sequencing at Macrogen Europe Laboratory (Amsterdam, Netherlands). The resulting

sequences were translated to proteins using the NCBI Open Reading Frame (ORFs) finder tool (https://www.ncbi.nlm.nih.gov/orffinder/) using default settings. The resulting protein sequences were used for BLAST searches in the GenBank/EMBL databases using the BLASTp algorithm with default settings and later analyzed using the same procedure as that of 16S rRNA described in section **3.3.3**.

### 3.3.8. Genome sequencing of the bacterial isolates

Aliquots of 48h LB cultures grown at 30 ºC were used for genomic DNA extraction using Wizard genomic DNA purification kit (Promega, USA) and quantified using a Qubit fluorometer (Thermo Fisher Scientific, USA). NEBNex Ultra II FS DNA library kit (New England Biolabs, USA) was used to prepare a paired-end 300-bp library for genome sequencing on Illumina MiSeq platform according to the manufacturer's instructions. Sickle version 1.33 (Joshi & Fass, 2011) with a Phred quality score of > 30, was used for quality control and to trim the raw sequences. SPAdes version 3.15.2 (Bankevich et al., 2012) was used to perform *De novo* sequence assembly, while CheckM version 1.0.8 and RefineM version 0.0.25 (Parks et al., 2015) were used for quality check and to provide completeness and contamination information. Genome annotations were conducted using PROKKA version 1.14.5 (Seemann, 2014) and on the Rapid Annotation using Subsystems Technology tool kit (RASTtk) version 2.0 (Brettin et al., 2015). Default parameters settings were applied for all software used.

### 3.3.9. Nucleotide sequence accession numbers and protein sequence IDs

The nucleotide and protein sequence data were submitted to GenBank database. The 16S rDNA sequences were submitted under accession numbers MK736101.1 and MK736102.1. The *lin* genes nucleotide sequences were deposited under accession numbers MK883461 – MK883467 and MK908215 – MK908222 and their corresponding protein sequences were deposited under accession numbers QGJ16213.1 – QGJ16219.1 and QGJ16206.1 – QGJ16212.1 for *Sphingobium* sp. strain S6 and *Sphingobium* sp. strain S8 respectively. These whole-genome shotgun projects were been deposited to ENA/DDBJ/GenBank under accession numbers CAJHOG000000000 and CAJHOH000000000 for *Sphingobium* sp strain S6 and *Sphingobium* sp strain S8, respectively. The versions described in this paper are CAJHOG010000000.1 and CAJHOH010000000.1 for *Sphingobium* sp strain S6 and *Sphingobium* sp strain S8, respectively. Raw data is available at ENA under the accession numbers ERR4392070 and ERR4392071. All these were added as part of the Bioproject PRJEB39494.

## 3.4. Results

### 3.4.1. Enrichment and isolation of HCH-degrading bacterial strains

The contamination level of the soil sample as assessed by quantification of residual HCH isomers by GC-MS analysis were as follows: (in µg/g soil: α-HCH~3.02, β-HCH~6.11, γ-HCH~0.88, δ-HCH~122.5). In addition to HCH isomers, p,p' DDT, m,p'DDD, dieldrin, endrin, endrin ketone, isodrin, parathion E605, 1,2,4,5 tetrachlorobenzene and naphthalene were also detected in the collected soil samples, indicating heavy contamination levels at the site. Two yellow-pigmented HCH-degrading bacterial isolates (designated, strain S6 and strain S8) were obtained by enrichment culture and plate clearance assays. The colorimetric dechlorinase assay further confirmed the HCH degrading capacity of the two bacterial isolates for all HCH isomers as demonstrated by the color change of phenol red dye from red to yellow indicating chloride ion release as per the assay protocol (Phillips et al., 2001). Wells with β-HCH however, showed a slight color change after 24h incubation period indicating moderate degradation of β-HCH by both bacterial isolates. No color change was observed in the control wells (**Figure 3.1**).

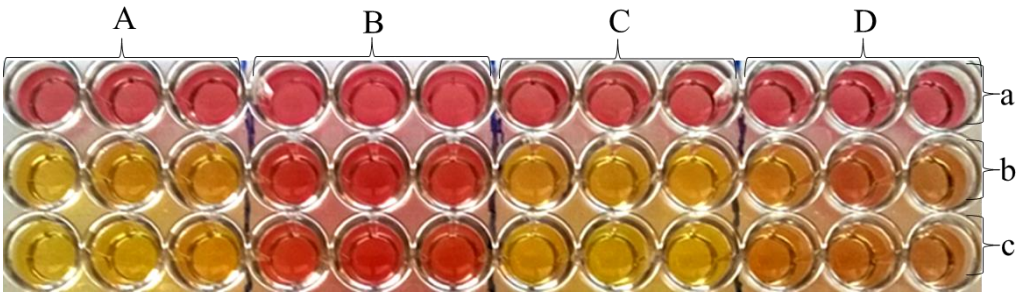


**Figure 3.1:** A Colorimetric assay used for testing HCH isomer degradation based on the dechlorination activity of haloalkane dehalogenase using cell-free extracts of the bacterial strains. The reaction mixture was incubated for 24hrs. Wells (A), (B), (C), and (D) represents 150µg/ml of each α-, β-, γ-, and δ-HCH respectively. Row (a) wells represents the control (buffer), while rows (b) and (c) wells represent active reaction mixtures containing cell-free extract from *Sphingobium* sp. strain S6 and *Sphingobium* sp. strain S8 respectively. The assays were conducted in triplicate.

### 3.4.2. Molecular identification and physiological properties of the bacterial isolates

Identification of the two bacterial isolates (strains S6 and S8) was done using 16S rDNA gene sequencing because of its robustness, accuracy, and reproducibility (Clarridge, 2004). Phylogenetic analysis based on 16S rDNA partial sequences revealed that the two bacterial isolates were affiliated with the genus *Sphingobium* and clustered together with *Sphingobium quisquiliarum* P25, a known HCH-degrader (Bala et al., 2010), *Sphingobium fuliginis* TKP, a

phenanthrene degrading bacterium (Prakash & Lal, 2006), and, *Sphingobium barthaii* KK22, a hydrocarbon-degrading bacterium (Maeda et al., 2015) with a posterior probability value of 86% (**Figure 3.2**). The 16S rDNA gene sequences exhibited the highest sequence identities with *S. quisquiliarum* P25 at 98.14% and 98.00% for strains S6 and S8 respectively. A summary of the phenotypic and biochemical properties of the two bacterial isolates (strains S6 and S8) with the closely related *Sphingobium* strains is shown in Table 3. Typically, they appeared yellow, circular with a diameter of ca. 2 mm, raised and with an entire margin on LB agar within 3–4 day of incubation at 30ºC. The two bacterial isolates could be distinguished from each other from their biochemical and physiological properties. Their zeta potential and water contact angle values also suggested that they had different surface properties possibly resulting from different membrane lipids (**Table 3.1**). Based on these results, the bacterial strains S6 and S8 were tagged as *Sphingobium* sp. strain S6 and *Sphingobium* sp. strain S8 respectively.

### 3.4.3. Biodegradation of HCH isomers by the bacterial strains

The two isolated *Sphingobium* strains degraded ~98% of α-HCH, ~99% of γ-HCH, ~94% of δ-HCH, and slightly more than 55% of β-HCH when exposed to an equal mixture of 34.4µM of each HCH isomer for 24 hours (**Figure 3.3**, appendix 1 **Table S2.1**). The degradation rates of γ-HCH were higher than those of α- and δ-HCH ($p < 0.041$) while no significant difference ($p > 0.12$) in the degradation rates of α- and δ-HCH was observed in both *Sphingobium* strains (**Figure 3.3**). β-HCH was observed to have the least removal rete. The removal rates of HCH isomers were therefore in the order γ-HCH > δ-HCH ≈ α-HCH > β-HCH. The degradation metabolites could, not be identified possibly due to low concentrations.

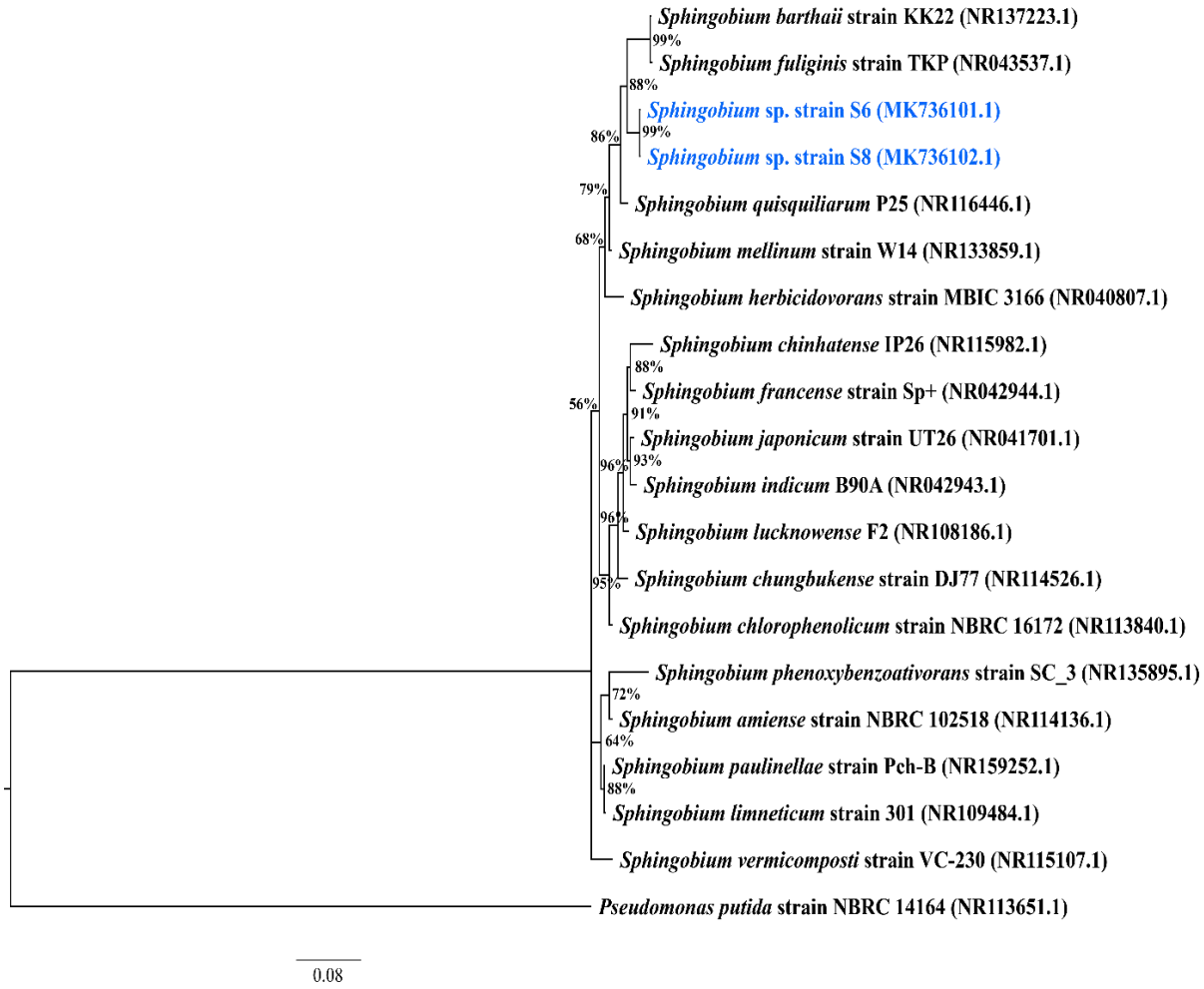


**Figure 3.2:** Phylogenetic tree based on 16S gene sequences showing the relationship between the two bacterial strains (*Sphingobium* sp. strain S6 and *Sphingobium* sp. strain S8) with related HCH degrading bacterial species. The tree was constructed using the Bayesian inference of phylogeny that is based on the Markov Chain Monte Carlo (MCMC) method in MrBayes. Numbers at the nodes indicate the percentage of posterior probabilities indicating the topological robustness of the Phylogenetic tree. *Pseudomonas putida* strain NBRC 14164 was used as an outgroup to root the tree.

**Table 3.1:** Comparative morphological and physiological characteristics of *Sphingobium* strains S6 and S8 with other phylogenetically closely related members of *Sphingobium* species.

Strains:1, *Sphingobium* sp. strain S6; 2, *Sphingobium* sp. strain S8 (data from this study); 3, *Sphingobium* quisquiliarum P25 (data from Bala et al., 2010); 4, *Sphingobium* fuliginis TKP (data from Prakash and Lal, 2006); 5, *Sphingobium* barthaii KK22 (data from Maeda et al 2015). Symbols: +, positive; W, weakly positive; –, negative; ND, no data available.

| **Characteristics** | 1* | 2* | 3 | 4 | 5 |
|---|---|---|---|---|---|
| **Morphological:** | | | | | |
| Colony shape<br>Colour | Circular<br>Yellow | Circular<br>Yellow | Circular<br>Yellow | Circular<br>Yellow | Circular<br>Yellow-light brown |
| Motility | – | – | – | – | + |
| Water contact angle (degree) | 82 | 66 | ND | ND | ND |
| Zeta potential (mV) | – 38 | – 43 | ND | ND | ND |
| **Physiological:** | | | | | |
| **Growth at** | | | | | |
| 1% NaCl | ++ | + | + | + | ND |
| 4% NaCl | – | – | W | + | ND |
| 8% NaCl | – | – | W | – | ND |
| pH 5 | – | – | W | + | + |
| pH 6 | ++ | ++ | W | + | + |
| **Assimilation of carbohydrates:** | | | | | |
| Glucose | ++ | + | + | + | + |
| Galactose | ++ | ++ | + | ND | + |
| Fructose | + | + | + | ND | + |
| Sucrose | – | – | + | – | |
| Cellobiose | – | – | + | ND | + |
| Mannitol | – | + | – | – | – |
| Raffinose | – | – | + | ND | – |
| Sorbitol | – | – | + | – | – |
| Trehalose | – | – | + | ND | + |
| L-Aspartic acid | ++ | + | ND | ND | ND |
| Methyl pyruvate | ++ | + | ND | ND | ND |
| p-Hydroxy-phenylacetic acid | ++ | + | ND | ND | ND |

*Data from this study: –, negative; +, weakly positive; + +, strong positive

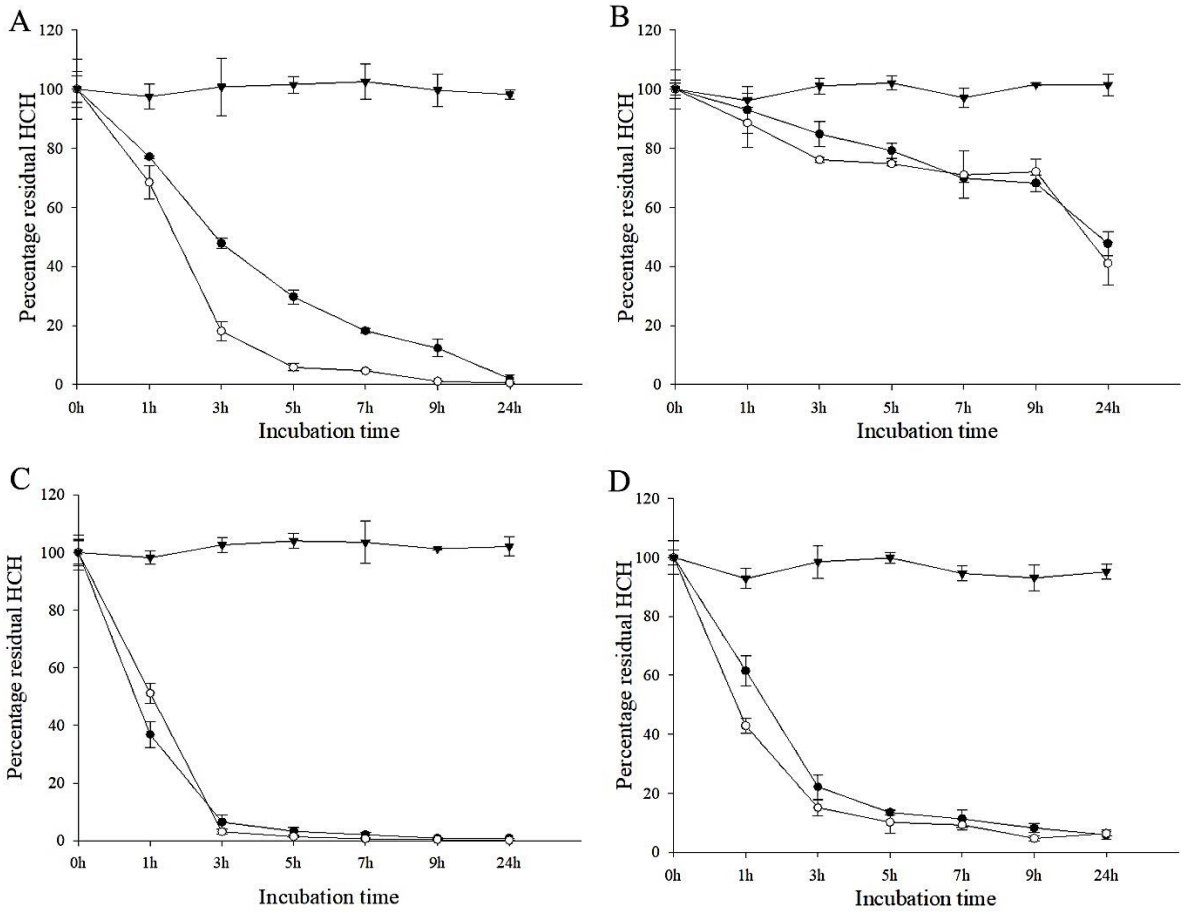


**Figure 3.3:** Degradation profiles of HCH isomers by the bacterial strains. Panels (A), (B), (C) and (D) represents the degradation profile of α-, β-, γ-, and δ-HCH respectively. ● (*Sphingobium* sp. strain S6), ○ (*Sphingobium* sp. strain S8) ▼ (Abiotic control). The reaction mixtures contained 10µg/ml (34.4µM) of each HCH isomer and the values are means of triplicate experiments

**Table 3.2:** Summary of the comparison of Lin genes protein sequences from *Sphingobium* sp. strain S6 and *Sphingobium* sp. strain S8 with their closest match from PDB and UniprotKB/TrEMBL databases

| *Lin* Gene | GenBank Accession No. (Protein IDs) | | Size (bp) (aa) | | Highest percent (%) sequence identity/ similarity (aa) | | Most closely related bacterial species (based on % protein sequence identity/similarity) | | |
|---|---|---|---|---|---|---|---|---|---|
| | **S6** | **S8** | **S6** | **S8** | **S6** | **S8** | **Bacteria** | **Accession No.** | **Reference** |
| ***LinA*** | MN649851.1 (QGJ16213.1) | MN649844.1 (QGJ16206.1) | 468 (156) | 450 (150) | 98.7/98.7 | 93.5/94.2 | *S. japonicum* UT26S | BAI96690.1 | (Nagata et al., 2010) |
| | | | | | | | *S. indicum* B90A | APL95055.1 | (Anand et al., 2012) |
| | | | | | | | *S. francense* Sp+ | AAU11089.2 | (Cérémonie et al., 2006) |
| | | | | | | | *Sphingomonas* sp. γ16-1 | CAI43919.1 | (Mohn et al., 2006) |
| | | | | | | | *Sphingomonas* sp. α1-2 | CAI43920.1 | (Boltner et al., 2005) |
| ***LinB*** | MN649852.1 (QGJ16214.1) | MN649845.1 (QGJ16207.1) | 888 (296) | 872 (291) | 98.6/99.3 | 95.9/96.9 | *P. aeruginosa* ITRC-5 | ABP93361.1 | (A.K. Singh et al., 2007) |
| | | | | | | | *Sphingobium* sp. TKS | AMK21182.1 | (Tabata et al., 2016) |
| ***LinC*** | MN649853.1 (QGJ16215.1) | MN649846.1 (QGJ16208.2) | 807 (250) | 750 (250) | 100/100 | 99.2/99.6 | *S. japonicum* UT26S | BAI95393.1 | (Nagata et al., 2010) |
| | | | | | | | *Sphingomonas* sp. NM05 | ABG77568.1 | (Manickam et al., 2008) |
| ***LinD*** | MN649854.1 (QGJ16216.1) | MN649847.1 (QGJ16209.1) | 1050 (346) | 1033 (344) | 99.4/100 | 99.1/99.4 | *S. japonicum* UT26S | sp\|D4Z909.1 | (Miyauchi et al., 1998) |
| ***LinE*** | MN649855.1 (QGJ16217.1) | MN649848.1 (QGJ16210.1) | 975 (321) | 951 (317) | 99.6/99.6 | 98.1/98.4 | *S. japonicum* UT26S | Q9WXE6.1 | (Miyauchi et al., 1999) |
| ***LinR*** | MN649856.1 (QGJ16218.1) | MN649849.1 (QGJ16211.2) | 922 (301) | 883 (308) | 98.6/99.0 | 97.2/97.9 | *S. japonicum* UT26S | Q9ZN79.3 | (Miyauchi et al., 2002) |
| | | | | | | | *S. baderi* LL03 | EQA99717.1 | (J. Kaur et al., 2013) |
| ***LinX*** | MN649857.1 (QGJ16219.1) | MN649850.1 (QGJ16212.1) | 750 (250) | 749 (250) | 100/100 | 100/ 100 | *S. japonicum* UT26S | BAI96692.1 | (Nagata et al., 2010) |

### 3.4.4. PCR amplification and analysis of Lin genes

The *lin* genes PCR amplicons from the respective gene primer sets were within the expected size range as reported in previous studies (Manickam et al., 2008; Nagata et al., 1999) (**Table 3.2**). Analysis of *lin* genes revealed that the two *Sphingobium* strains harbored all the six key *lin* genes necessary for the degradation of HCH. These included; five structural genes (*linA*, *linB*, *linC*, *linD*, and *linE*) and a regulatory gene *linR*. The translated protein sequences of the respective *lin* genes were compared to known sequences from UniprotKB/TrEMBL and PDB databases using the BLASTp algorithm. All the *lin* genes identified exhibited high levels of sequence similarities and sequence identities to *lin* genes from other HCH degrading sphingomonads with values ranging between 97% and 100%, particularly with those of *S. japonicum* UT26S (Nagata et al., 2010). Partial *linA* and *linB* sequences were, however, obtained for *Sphingobium* sp. strain S8 which could be responsible for the low similarity values observed (**Table 3.2**). Despite the high sequence similarities, minor mutations were identified in the Lin protein sequences, particularly on the N- and C-terminals (**Table 3.3**, appendix 1 **Figures S2.2**). Interestingly, LinB from the two *Sphingobium* strains (S6 and S8) were closely related to LinB*a* from *Pseudomonas aeruginosa* ITRC-5 (Singh et al., 2007). Five substitutions including residues, Val112, Val134, Met138, Val224, and Ser247 which are thought to lie within the active site of LinB were observed compared to those from *S. japonicum* UT26S (Nagata et al., 2010) and *S. francense* Sp+ (Cérémonie et al., 2006). In addition, Met138 were unique mutations observed in LinB from the two *Sphingobium* sp. isolates compared to the other HCH degrading bacteria (**Figure 3.4**).

**Table 3.3:** Unique amino acid substitutions identified in Lin genes protein sequences from *Sphingobium* sp. strain S6 and *Sphingobium* sp. strain S8 compared to closely related sequences from other organisms

| Protein Sequence | Notable amino acid substitutions | |
|---|---|---|
| | *Sphingobium* sp. strain S6 | *Sphingobium* sp. strain S8 |
| LinA | Arg144, Thr145 | Phe4, Gly10, Ser11, Asn13 |
| LinB | Leu13, **Met138** | **Met138**, Met282, Ala283, Arg284, Val289 |
| LinC | *** | Thr243, Asn244 |
| LinD | Asn336, Gln337 | Met24 |
| LinE | Phe11 | Met4, Pro313 |
| LinR | Pro10, Gln306 | Ser18, Cys295, Asp296, Arg297, Ser298, Gly299, Thr300 |
| LinX | *** | *** |

NB: (***): no mutations detected

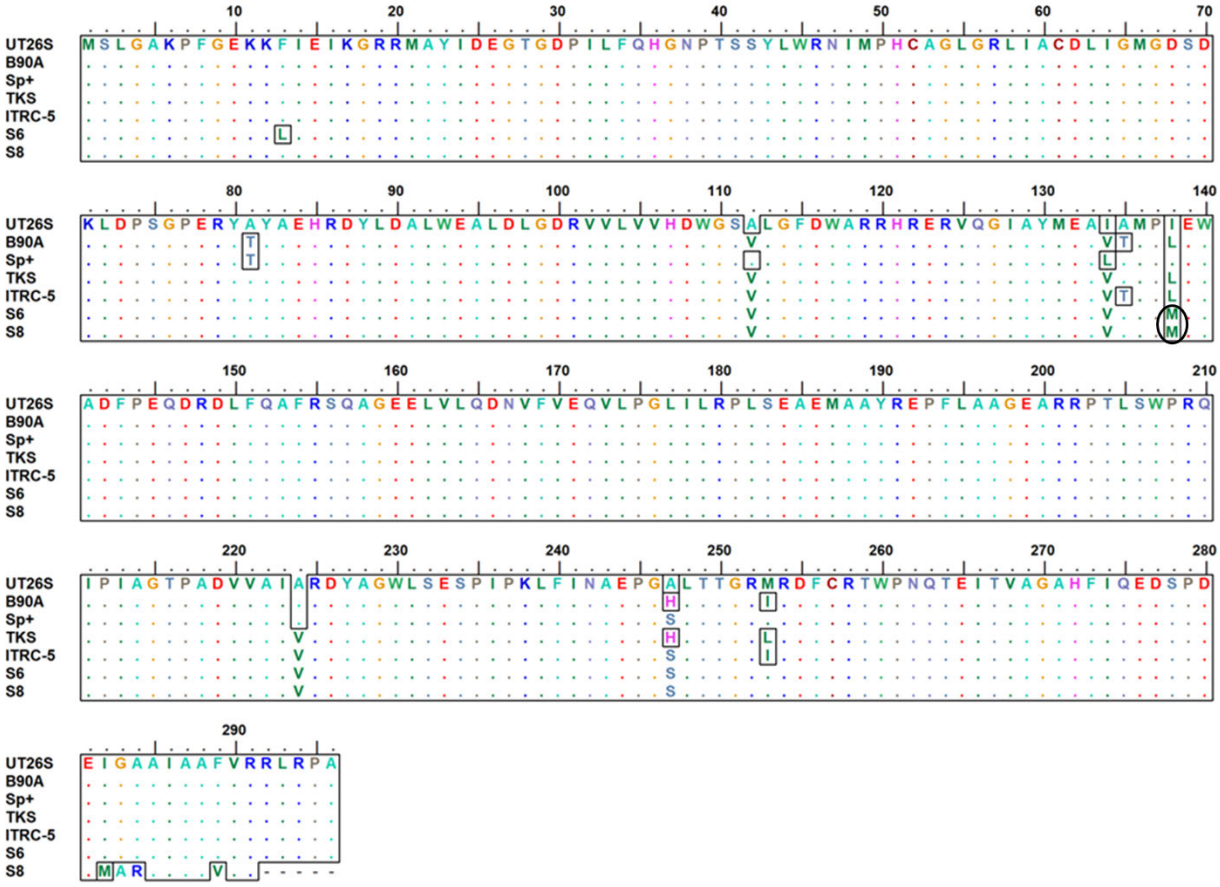


**Figure 3.4:** Multiple sequence alignment of haloalkane dehalogenase (LinB) of *Sphingobium* sp. strains (S6 and S8) and their homologs from known HCH-degrading bacteria. The LinB sequences and accession numbers are as follows: UT26S; *S. japonicum* UT26 (BAI96793.1), B90A; *S. indicum* B90A (APL96138.1), Sp+; *S. francense* Sp+ (AAX07227.1), TKS; *Sphingobium* sp. TKS (AMK21182.1), ITRC-5; *P. aeruginosa* ITRC-5 (ABP93361.1), S6; *Sphingobium* sp. Strain S6 (QGJ16214.1) and S8; *Sphingobium* sp. Strain S8 (QGJ16207.1).

### 3.4.5. Analysis of the draft genome sequences

The draft genomes of the two *Sphingobium* species had 42 and 44 contigs, with total lengths of 4,173,956bp and 4,170,555bp for *Sphingobium* sp strain S6 and *Sphingobium* sp strain S8 respectively. Both genomes had 99.2% completeness, 2.06% contamination, and %GC content of 62.4 and 62.53 for *Sphingobium* sp strain S6 and *Sphingobium* sp strain S8 respectively. The details of the final annotations are summarized in **Table 3.4**. Previous reports show that HCH-degrading Sphingomonads share the same degradation pathway that requires *linA* through *linF* genes (Boltner et al., 2005; Lal et al., 2010). Further analysis of the draft genomes revealed the presence of one copy each of *linA*, *linB*, *linC*, *linD*, *linE*, *linF*, *linG*, and *linH*, two copies each of *linJ*, *linR*, and *linX*. Annotation by RASTtk showed the presence of gene clusters for degradation of xenobiotic compounds such as 1,1,1-trichloro-2,2-bis(4-chlorophenyl) ethane (DDT), 1,4-dichlorobenzene, tetrachloroethene, 2,4-dichlorobenzoate, fluorobenzoate,

benzoate, toluene, and xylene. Gene clusters for the potential production of carotenoids were also predicted using antiSMASH version 6.0.0 (Blin et al., 2019).

## 3.5. Discussion

### 3.5.1. Identification of bacterial isolates and determination of HCH degradation

In the present study, two HCH-degrading bacteria were isolated from contaminated soil collected from a former obsolete pesticide store in, Kenya. Based on 16S rDNA sequencing the isolates were affiliated with members of the genus *Sphingobium*. A phylogenetic comparison of the isolates with previously described members of the genus *Sphingobium* (**Figure 3.2**) showed that the isolates were closely related to an established HCH-degrader *S. quisquiliarum* P25 (Bala et al., 2010), and were therefore designated *Sphingobium* sp. strains S6 and S8 respectively. The recent emergence of novel HCH-degrading sphingomonads from different geographical locations around the globe underscores the prominent role of this genus in HCH degradation (Boltner et al., 2005; Lal et al., 2006, 2010; Mohn et al., 2006; Nayyar et al., 2014). The water contact angle values of the two *Sphingobium* isolates (82º and 66º, **Table 3.1**) suggests that they have a moderately hydrophobic surface (Yuan et al., 2017). The outer membrane of sphingomonads are thought to contain glycosphingolipids in place of lipopolysaccharides (LPLs) which provides highly hydrophobic surface that would facilitate the assimilation of hydrophobic compounds like HCH (Boltner et al., 2005; Kawahara et al., 1999; White et al., 1996).

All four isomers of HCH were degraded by the isolated *Sphingobium* strains. More than 95% of α-, γ-, and δ-HCH and slightly more than 55% of β-HCH were degraded when the isolates were exposed to 34.4µM of each isomer in a mixture for 24 hours (**Figure 3.3**). The HCH removal rate of the isolates was in the order γ-HCH > δ-HCH ≈ α-HCH > β-HCH. The removal rates of the same isomers were not significantly different between the two bacterial isolates except for the degradation of α-HCH. The degradation capacity of these isolates is thought to result from their adaption to highly polluted soil from which they were isolated. These findings are consistent with previous studies in which HCH-degrading microbes were predominantly isolated from polluted environments (Boltner et al., 2005; Manickam et al., 2008; Mohn et al., 2006; Sahu et al., 1990; Senoo & Wada, 1989). *S. indicum* B90A isolated from sugarcane fields treated with commercial formulations of HCH in India, was the first bacterial strain reported to degrade all four isomers of HCH (Sahu et al., 1990). In their study, Sahu et al. (1990) reported that *S. indicum* B90A could degrade 28 µM of HCH isomers within 28 hours. Wu et al. (2007) also showed that *Sphingobium* sp. BHC-A, isolated from HCH contaminated upland

field in China (Ma et al., 2005), completely mineralized 17 μM each of γ-HCH, α- and δ-HCH, as well as β-HCH within 6, 10, and 12 hours respectively. More recently three *Sphingobium* species (namely; BHC-B, BHC-C, and BHC-D) isolated from a former industrial dumpsite in China were shown to degrade 170 μM of each HCH isomers over 7 days at different rates (Cao et al., 2013). On the other hand, *S. japonicum* UT26 isolated from γ-HCH contaminated upland field in Japan was demonstrated to completely mineralize 17 μM of γ-HCH within 4 hours (Senoo & Wada, 1989). *S. japonicum* UT26, however, only partially degraded α- and δ-HCH, but not β-HCH (Ma et al., 2005). The absence of β-HCH degradation capacity was also observed in *S. francense* Sp+ isolated from γ-HCH contaminated French soil (Dogra et al., 2004). *S. francense* Sp+ was, however, shown to completely mineralize 3.4μM γ-HCH supplied in a liquid medium as a sole carbon source within 3 days (Thomas et al., 1996). These findings display the diversity of HCH degradation in the environment.

**Table 3.4:** Summary of the draft whole-genome sequences of HCH degrading *Sphingobium* strains isolated from HCH contaminated site in Kitengela, Kenya. Phylogenetic-related neighbors were computed based on Average Nucleotide Identity (ANI) (Goris et al., 2007) analysis.

| Strains | NCBI accession no. | No. of contigs | $N_{50}$ (bp) | Average coverage (X) | Genome size (bp) | GC% | No. of rRNAs | No. of tRNAs | No. of tmRNA | No. of coding sequences | Transposon families | Closest Phylogenetic neighbors (% ANI)* |
|---|---|---|---|---|---|---|---|---|---|---|---|---|
| *Sphingobium* sp. strain S6 | CAJHOG000000000.1 | 44 | 538,820 | 48.72 | 4,173,956 | 62.40 | 3 | 49 | 1 | 4,015 | IS21(n=2)<br>ISNCY(n=1)<br>IS3(n=2)<br>IS5 (n=1)<br>IS630 (n=1)<br>IS256 (n=1)<br>IS481 (n=1) | *Sphingobium sp. starin S8 (99.96)*<br>*Sphingobium indicum B90A (85.93)*<br>*Sphingobium japonicum UT26S (85.51)*<br>*Sphingobium quisquiliarum P25 (83.88)*<br>*Sphingobium chlorophenolicum L-1 (83.65)* |
| *Sphingobium* sp. strain S8 | CAJHOH000000000.1 | 48 | 454,689 | 36.73 | 4,170,555 | 62.53 | 3 | 47 | 1 | 4,039 | IS21(n=2)<br>IS5 (n=1)<br>IS630 (n=1)<br>IS256 (n=1)<br>IS481 (n=1) | *Sphingobium sp. starin S6 (99.96)*<br>*Sphingobium indicum B90A (85.76)*<br>*Sphingobium japonicum UT26S (85.41)*<br>*Sphingobium quisquiliarum P25 (83.85)*<br>*Sphingobium chlorophenolicum L-1 (83.57)* |

### 3.5.2. Analysis of *lin* genes

The presence of *lin* genes is an indication of the presence of the common pathway reported for aerobic HCH degradation (Lal et al., 2006, 2010; Nagata et al., 2007; Nayyar et al., 2014). Most of the *lin* gene sequences identified from the two *Sphingobium* isolates showed high similarities (> 97) with related sequences from other HCH degraders (**Table 3.2**) except for a few mutations (**Table 3.3**). The presence of *lin* genes was further confirmed by the analysis of the draft genomes of the two *Sphingobium* isolates. Previous studies have revealed that HCH-degrading sphingomonads have substantially identical *lin* genes, implying that they have similar HCH degradation pathways (Boltner et al., 2005; Cao et al., 2013; Mohn et al., 2006; Pal et al., 2005). Horizontal gene transfer by plasmids, transposons, and other conjugative elements is thought to have resulted in the isolation of identical *lin* genotypes predominantly from sphingomonads across the globe (Boltner et al., 2005; Lal et al., 2006). The *lin* genes identified from this study had high similarities with those found in *S. japonicum* UT26 except *linB,* which showed differences at five positions (**Figure 3.4**) that are thought to lie within the active site. Similar differences were observed between LinB from *S. indicum* B90A/*Sphingobium* sp. BHC-A/*Sphingobium* sp. MI1205 and those from *S. japonicum* UT26/ *S. francense* Sp+ (Lal et al., 2010). These differences was shown to be important in B90A/BHC-A/MI1205 ability to degrade β-HCH to 2,3,5,6-tetrachlorocyclohexane-1,4-diol (TCDL) through 2,3,4,5,6-pentachlorocyclohexanol (PCHL) , a property that is missing in UT26/SP+ (Ito et al., 2007; Lal et al., 2010). Site-directed mutagenesis suggests that the presence of Val134 and His247 within the active site increases the activity of LinB in B90/BHC-A/MI1205 for the conversion of β-HCH to PCHL and PCHL to TCDL (Ito et al., 2007). Other amino acids that have been shown to play a key role in the degradation of β-HCH within the active site of LinB from B90/BHC-A/MI1205 include, Thr81, Val112, Thr135, Leu138 and Ile253 (Ito et al., 2007; Lal et al., 2010). The presence of Val134, Ser247 and unique mutation, Met138 in LinB observed from this study could be responsible for the moderate degradation capacity of β-HCH observed in the two *Sphingobium* strains. Further investigations are however needed to validate this hypothesis.

### 3.6. Conclusion

Two HCH-degrading *Sphingobium* strains (S6 and S8) that are closely related to *S. quisquiliarum* P25, a known HCH-degrading bacteria were isolated. The two strains could degrade all the four HCH isomers and also harbored *lin* genes with high sequence similarity to those reported from *S. japonicum* UT26 except LinB which had five mutations compared to that found in *S. japonicum* UT26. The observed LinB mutations are thought to be important for the moderate β-HCH degradation capacity of the two bacterial isolates. This research, therefore, adds to the diversity of HCH degraders and that of LinB sequences which would aid in unraveling the molecular mechanism of degradation and bioremediation of the recalcitrant β-HCH. The availability of the genome sequences of the two *Sphingobium* species would add valuable information on the diversity of HCH degraders and that of *lin* genes that would provide insights into the molecular mechanism of HCH degradation.

# CHAPTER FOUR

## 4.0 Mycelial mediated translocation of hexachlorocyclohexane (HCH) in a water unsaturated system

### 4.1. Abstract

The ability of filamentous fungi to translocate material across their mycelial networks enables them to flourish in heterogeneous environments like soil. By growing hyphal networks, mycelial fungi have been shown to access resources from remote locations and transport them across air-gaps and pores in soil. This property enables them to tolerate harsh and toxic conditions that are inhospitable to other microorganisms like bacteria. Recent studies have demonstrated the role of mycelial networks in the translocation of water, nutrients, and other nonessential compounds such as polycyclic aromatic hydrocarbons (PAHs). In the present study, we investigated the role of mycelia as transport networks for organochlorine pesticides using hexachlorocyclohexane (HCH) isomers as model compounds. To achieve this, a laboratory-based microcosm system was developed to simulate the air-water interface in soil, while a non-white-rot fungus (non-WRF) previously isolated from HCH-contaminated soil was used as a model organism. The fungus was identified as *Fusarium equiseti* by a combination of ITS gene sequencing and whole genome sequencing. The draft genome was 37.88 Mb in size with 12,311 predicted protein-coding sequences, 261 tRNA sequences, and gene clusters previously described in other *Fusarium* species. The fungus poorly degraded HCH isomers in liquid culture with HCH removal rate in the order $\beta > \alpha > \delta > \gamma$, while 1,3,5-trichlorobenzene and 1,3,5-trichloromethoxy benzene were identified as degradation metabolites. Quantification of HCH amounts in the lab-based microcosm systems after the exclusion of vapor-phase transport demonstrated active mycelia as the main path for HCH transport. Our results revealed isomer-specific transport of HCH in the order $\beta \approx \delta < \alpha < \gamma$ that was likely influenced by their octanol-air partition coefficients (log $K_{OA}$) and solubilities. The isomers with lower log $K_{OA}$ (< 7.8) were more effectively mobilized along active mycelium. Mycelial mediated dispersal of HCH, therefore, provides the potential to improve their bioavailability and bio-accessibility in heterogeneous environments.

## 4.2. Introduction

Microbial degradation of hexachlorocyclohexane (HCH) is an important process in bioremediation and has attracted attention as an ecofriendly method for cleaning up polluted sites (Guillén-Jiménez et al., 2012; Nagpal et al., 2008; Zhang et al., 2020). While both bacteria (Lal et al., 2010; Nagata et al., 2007; Nayyar et al., 2014; Nayyar & Lal, 2016) and fungi (Guillén-Jiménez et al., 2012; Nagpal et al., 2008; Sagar & Singh, 2011; Singh & Kuhad, 1999, 2000) are important HCH degraders in soil, complete mineralization of HCH has only been reported in bacteria (Lal et al., 2006, 2010). However, bacterial degradation is normally limited by the tendency of organic contaminants (such as HCH) to adsorb onto organic matter, thereby decreasing their accessibility to degraders (Furuno et al., 2010, 2012; Harms et al., 2011). In contrast to bacteria, mycelial fungi possess non-specific extra-cellular enzyme system that enables them to co-metabolically degrade complex mixtures of contaminants even in conditions inhospitable for bacterial growth (Nagpal et al., 2008; Wick et al., 2010). Mycelial growth provides deeper penetration into soil particles and a large surface area for absorption, thus enhancing the bioavailability of poorly soluble compounds such as HCH (Nagpal et al., 2008; Sagar & Singh, 2011). HCH biodegradation by fungi has extensively been studied using white-rot fungi (WRF), which have been shown to possess an efficient enzyme system for the degradation of a variety of xenobiotic compounds (Kaur et al., 2016; Mougin et al., 1996; Singh & Kuhad, 1999, 2000). Despite the high HCH degradation efficiency, WRF are slow growing and require an oxygen-rich environment for their growth (Nagpal et al., 2008; Sagar & Singh, 2011). The use of non-white-rot fungi (non-WRF) for bioremediation has therefore attracted attention because of their rapid growth without the need for an oxygen-rich environment. Their mycelial structures therefore provide deeper penetration in soil and a larger surface area for absorption of contaminants (Guillén-Jiménez et al., 2012; Nagpal et al., 2008). In this context, several HCH degrading non-WRF including *Fusarium verticillioides* AT-100 (Guillén-Jiménez et al., 2012), *Fusarium poae*, *Fusarium solani* (Sagar & Singh, 2011) and *Conidiobolus* 03-1-56 (Nagpal et al., 2008) have recently been reported.

The soil environment exhibits physical and temporal heterogeneities ranging from the nanometer to the kilometer scale (Wick et al., 2010; Young & Crawford, 2004). To adapt to a such heterogeneous environment, filamentous fungi develop a dense network of mycelial structures which enable them to optimally exploit new resources in a patchy resource environment (Boswell et al., 2002; Heaton et al., 2012). Despite the hyphal microscopic nature (with diameters in the

range of 2 – 10µm), fungi are among the largest living organisms in soil with reported network lengths of between $10^2$ and $10^4$m $g^{-1}$ of topsoil (Furuno et al., 2012; Ritz & Young, 2004). Fungi are therefore thought to represent up to 75% of soil microbial biomass with a dry biomass of 0.05 – 1 mg $g^{-1}$ of dry soil (Furuno et al., 2012; Ritz & Young, 2004; Wick et al., 2010). The ability of fungal mycelia to grow over surfaces and through pores and air gaps, coupled with the secretion of hydrophobins (small hydrophobic proteins) on their hyphal surfaces, enable them to cross the water-air barrier and to grow between soil particles (Wessels, 1996; Wick et al., 2010; Wösten et al., 1999). Their growth in patchy environments like soil is facilitated by intracellular translocation of material (nutrients) across the mycelial network (Bebber et al., 2007; Boswell et al., 2002; Darrah et al., 2006). To sustain their mycelial networks, filamentous fungi have evolved a highly polarized internal cellular architecture that supports hyphal tip extension (Darrah et al., 2006; Furuno et al., 2012; Wick et al., 2010). Translocation of hyphal cellular material involves a complex extended vacuole that forms interconnected networks, linked by tubules that are thought to act as channels ("fungal pipelines") for active and diffusive longitudinal transport over distances of millimeters to centimeters (Darrah et al., 2006; Furuno et al., 2012; Glass et al., 2004).

Strong adsorption of xenobiotic compounds and reduced mobility of bacterial degraders particularly in water and nutrient-deficient zones, limits the bioavailability of organic contaminates in soil (Harms et al., 2011; Semple et al., 2004). Transport of organic contaminants to active degraders at substantial mass fluxes is therefore necessary for their efficient transformation by microorganisms (Furuno et al., 2012; Wick et al., 2010). Active translocation of cellular material by fungal mycelia observed in previous studies (Darrah et al., 2006; Furuno et al., 2012), led to the exploration of their ability to transport non-essential compounds such as hydrophobic organic contaminants (Furuno et al., 2012). To this end, fungal mycelia have recently been reported to take up and actively transport otherwise immobile polycyclic aromatic hydrocarbons (PAH) in water-unsaturated soil over distances of centimeters (Furuno et al., 2012; Schamfuß et al., 2013, 2014). These studies demonstrated increased bioavailability of PAH to degrading bacteria following mycelial transport. In the present study, we used GC chemical analysis and a non-white-rot soil fungal species (*Fusarium* sp.) isolated from HCH-contaminated soil as model organisms to test the hypothesis that mycelial structures are effective transport vectors for HCH isomers. To our knowledge, our data demonstrate for the first-time active transport of HCH isomers along fungal

mycelia. In addition, our data suggest isomer fractionation during transport that is correlated with their differences in physicochemical properties such as log $K_{OA}$ and solubility.

## 4.3. Materials and Methods

### 4.3.1. Chemicals and reagents

Hexane (LiChrosolv grade), acetone (99.8%), γ-HCH (97%), and HCH Mix (HCH analytical standard mixture of isomers, α: β: γ: δ = 1:1:1:1), were either purchased from Sigma (Munich, Germany) or Merck (Darmstadt, Germany) and were of analytical grade. PCR primers used were purchased from Integrated DNA Technologies (IDT, Iowa USA), while kits necessary for PCR amplification were purchased from Roche (Mannheim, Germany).

### 4.3.2. Isolation and identification of the fungal strain

Inverted Petri dish microcosms previously described by Bravo et al. (2013) served as the isolation system of the fungal strain. For this purpose, five grams of moist HCH-contaminated soil was placed at the center of the Petri dish cover, leaving a 5mm air gap between the soil sample and the target agar (**Figure 4.1**). A minimum salt medium (MSM) previously described by Senoo & Wada, (1989) supplemented with 100 µg/mL HCH was used as the target agar. The composition of the MSM was (in $gL^{-1}$): 1 g $K_2HPO_4$, 1 g $KH_2PO_4$,1 g $NH_4NO_3$, 0.2 g $MgSO_4.7H_2O$, 5 mg $Fe(SO_4)$, 5 mg $Na_2MoO_4.2H_2O$, 5 mg $MnSO_4.4H_2O$ and pH set at 7 (Senoo & Wada, 1989). The microcosms were incubated in the dark at 25 ºC until fungal hyphae touched the target agar (~7 days). Fresh mycelia from the periphery of the target agar were repeatedly (~5 to 6 times) sub-cultured on potato dextrose agar (PDA) and observed under a microscope to obtain pure cultures. A fungal isolate designated as strain-K3 was obtained following several subsequent purification steps. For molecular identification of the fungal isolate, fresh mycelium obtained from the periphery of a 7-day PDA culture plate overgrown with the fungus was used for genomic DNA (gDNA) extraction using Wizard genomic DNA purification kit (Promega, USA), then quantified using a Qubit fluorometer (Thermo Fisher Scientific, USA). The extracted gDNA was subjected to PCR amplification and gene sequencing of the internal transcribed spacer (ITS) region using the universal ITS1 (5'…TCCGTAGGTGAACCTGCGG…3') and ITS4 (5'…TCCTCCGCTTATTGATATGC…3') primers according to Guillén-Jiménez et al. (2012). The ITS sequence was used for BLAST searches in the GenBank database at NCBI using the BLASTn algorithm with default settings, the database set at ITS from fungi type and reference

material, and optimized for highly similar sequences (Altschul et al., 1990). Twenty homologous ITS sequences with sequence identities of 99.82 – 100% and sequence coverage of 99 – 100% were retrieved from the database and analyzed using the Bayesian phylogenetic approach in MrBayes, version 3.1.2 (Huelsenbeck & Ronquist, 2001) as described in section **3.3.3**.

### 4.3.3. Genome sequencing of the fungal strain

Fresh mycelium obtained from the periphery of a 7 days culture plate overgrown with the fungus was used for genomic DNA extraction using Wizard genomic DNA purification kit (Promega, USA), then quantified using a Qubit fluorometer (Thermo Fisher Scientific, USA). Paired-end 300-bp library for genome sequencing on Illumina MiSeq platform was prepared using the NEBNext Ultra II FS DNA library prep kit (New England Biolabs, USA) according to the manufacturer's instructions. This resulted in a total of 2,602,796 paired-end reads. Sickle version 1.33 (Joshi & Fass, 2011), with a Phred quality score of >30 was used for quality control and to trim the sequences. *De novo* sequence assembly was performed using SPAdes version 3.15.2 (Bankevich et al., 2012), while QUAST version 5.0.2 (Gurevich et al., 2013) and BUSCO version 5.0.0 (Simão et al., 2015) with fungi_odb10 database were used for quality check and completeness of gene space within the assembly. The MAKER pipeline v2.31.11 (Cantarel et al., 2008) was used to perform genome annotation. AUGUSTUS version 3.4.0 (Stanke et al., 2006) and SNAP version 2013 11 29 (Korf, 2004) were used for *ab-initio* gene prediction, using *Fusarium graminearum* PH-1 (accession number: AACM00000000.2) as the training species. For all software used, default parameter settings were applied. The whole-genome shotgun project was deposited to ENA/DDBJ/GenBank under accession number CAJSTJ000000000. The version described here is the first version CAJSTJ010000000.1. Raw data is available at ENA sequence reads archive (SRA) under the BioProject number PRJEB39686, BioSample number SAMEA7112172, and SRA number ERR4398881.

### 4.3.4. HCH degradation assay in liquid medium

HCH biodegradation assays were performed in 100 mL head space GC vials containing 20 ml MSM (Senoo & Wada, 1989) supplemented with 100 µg $mL^{-1}$ of each HCH isomer. To prepare the fungal inoculum, 20 mycelial discs (Ø 10mm) scraped off from the periphery of a 7-day PDA culture plate were homogenized in 20 mL MSM. Aliquots of 2 mL of the fungal suspension were then added to the reaction mixture. Controls were prepared by adding 2 mL of killed (autoclaved)

fungal suspension to the reaction. The vials were incubated in a rotary shaker at 25 ºC and 150 rpm. At specific time intervals (0, 7, 14, 21, and 28 days) the experimental and control vials were used for extraction and GC analysis of residual HCH in the reaction mixture. All experiments were conducted in triplicate and the computed results are means of triplicate samples.

### 4.3.5. Quantification of HCH transport along fungal mycelia

The experiment was conducted in a laboratory-based microcosm system designed to mimic air-water interfaces in soil according to Schamfuß et al. (2014) (**Figure 4.2**). The fungal isolate K3 from this study was used as a model organism. Circular PDA agar patches (P1, P3, and P4, Ø 10 mm) were placed on either side of the curved MSM agar patch (P2) leaving gaps of 8 and 2 mm between them. An aliquot of 25 µg (10 µL) of each HCH isomer dissolved in dimethyl sulfoxide (DMSO) was placed inside a well (Ø 5 mm) dug out of PDA patch P1 and covered with (F)PDA (Ø 10mm) freshly overgrown with mycelium from the fungal isolates. A mechanical barrier consisting of agar patch P2 and a Petri dish (Ø 5.5 cm) was placed between agar patch P1 and P3 to prevent airborne HCH transport. In the control setups, the MSM agar patch (P2) that served as the mechanical barrier was amended with 0.2g $L^{-1}$ of the fungicide, cycloheximide to prevent mycelial growth across the P2 agar patch. To further minimize gaseous HCH concentration, four agar patches (Ø 10 mm) containing 0.06 g $mL^{-1}$ activated charcoal were included in the microcosm setup. Parallel experiments including those with active mycelia and killed mycelia were prepared to distinguish active HCH transport and transport due to passive diffusion. For all the microcosm setups HCH extraction from agar patch P3 and P4 and quantification by gas chromatography was conducted in four replicates after a 14-day incubation period.

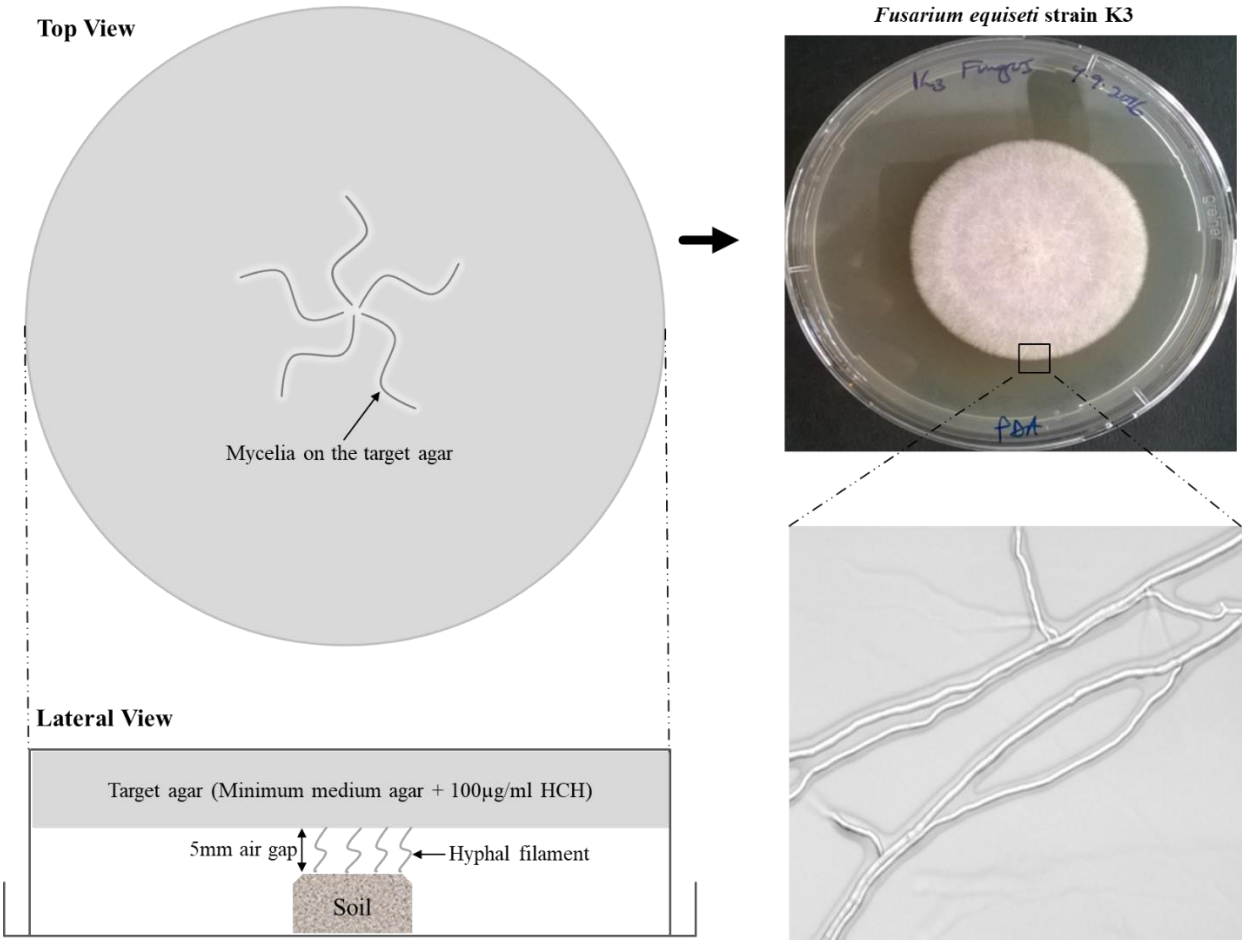


**Figure 4.1:** An illustration of the inverted Petri dish system that was used in the isolation of fungi (adapted from Bravo et al., 2013) and photographs of culture plates and microscopy of the fungal isolates.

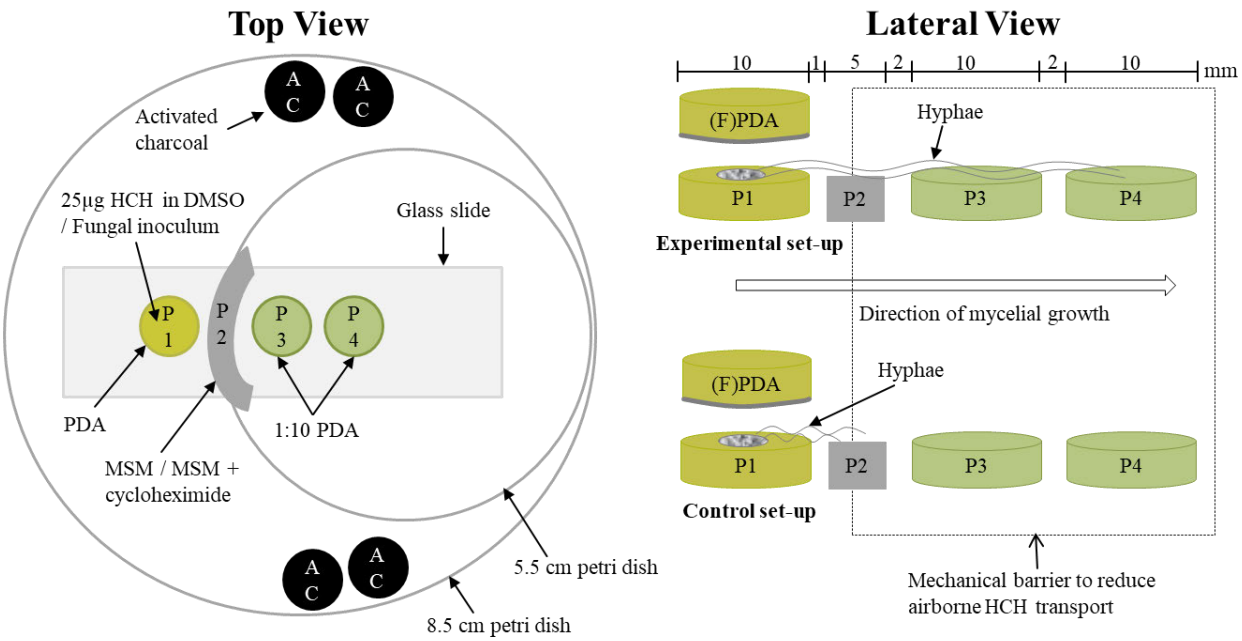


**Figure 4.2:** Scheme of the lab-based microcosm model used for the investigation of mycelial-mediated transport of HCH. The agar patches were placed on top of a glass slide that had three small cavities. Twenty-five µg of each HCH isomer were placed inside a well (Ø 5 mm) dug in the middle of P1 agar patch. (F)PDA patch cut from 7-day-old culture plates of the respective fungal isolates was placed on top of agar patch P1from the side overgrown with mycelia. A curved MSM agar patch (P2) was placed between agar patch P1 and P3 to create a mechanical barrier for the gas-phase transport of HCH together with the lid of the Petri dish (Ø 5.5 cm). Four activated charcoal agar patches were included in the setup to minimize gaseous HCH concentration. Adapted from Schamfuß et al., (2014).

### 4.3.6. Extraction and analytical methods

#### 4.3.6.1. Quantification of HCH degradation

To monitor HCH degradation in liquid culture, triplicate bottles were sacrificed by the addition of a few drops of concentrated HCl and prepared for extraction of residual HCH. On day zero, the cultures were extracted thrice with 5 mL of the extraction solvent (hexane containing 0.31 µg $L^{-1}$ DDT as the internal standard). For every extraction step, the bottles were then frozen at -20 ºC overnight to separate the solvent (extract) and the aqueous phase (culture). The extract was then transferred into clean glass vials and dried with Sodium sulfate. On the subsequent time points (7, 14, 21, and 28 days) the grown mycelia were separated from the medium by centrifugation at 10,000 x g. The mycelial mats were washed twice with 10 mL of distilled water to remove adsorbed HCH. The mycelial washings and the medium were separately extracted thrice with 5 mL of the extraction solvent. The mycelial mats were crushed with sodium sulfate in clean 20 mL

headspace GC vials and extracted once with 10 mL and twice with 5 mL of the extraction solvent. Extracts from the different repetition steps were pooled and prepared for GC-MS analysis. A hundred µL of the extract was mixed with 10 µL of 4-chlorobenzotrichloride and analyzed by GC (HP 7890 Series GC, Agilent) with 20 m 0.18 mm 18 µm column (Agilent). Helium was used as a carrier gas with a flow rate of 1 mL/min.

#### 4.3.6.2. Quantification of HCH transport

To quantify the translocation of HCH along fungal mycelia, agar patches P3 and P4 and their associated overlaying mycelium were separately transferred into clean glass vials and crushed with sodium sulfate. These were then extracted with 15 mL hexane/acetone (3:1, v/v) containing 0.31 µg $L^{-1}$ DDE internal standard by shaking overnight on a horizontal shaker and analyzed by GC as described in section 4.3.6.1. Subsequently, the net amounts of HCH transported by active transport $A_{active}$ were computed by comparing the net amounts transported by live mycelia $A_{mycelium}$ and killed mycelia $A_{biomass}$ at position $i$ = 3 and 4, and time $t$ = 14 days according to equations:

$$A_{air}(i, t) = A_{mycelium,\ control}(i, t), A_{biomass,\ control}(i, t) \quad \text{eq. 1}$$

$$A_{mycelium}(i, t) = A_{mycelium,\ test}(i, t) - A_{mycelium,\ control}(i, t) \quad \text{eq. 2}$$

$$A_{biomass}(i, t) = A_{biomass,\ test}(i, t) - A_{biomass,\ control}(i, t) \quad \text{eq. 3}$$

$$A_{active}(i, t) = A_{mycelium}(i, t) - A_{biomass}(i, t) \quad \text{eq. 4}$$

Where:

$A_{air}$ is the amount of HCH recovered from the control set-ups in presence of live or killed mycelia.

$A_{mycelium,\ test}$ is the amount of HCH recovered from the experimental set-ups in presence of live mycelia.

$A_{biomass,\ test}$ is the amount of HCH recovered from the experimental set-ups in presence of killed mycelia.

Thus, $A_{air}$ is attributed to air-borne transport while $A_{biomass}$ is the net contribution of passive diffusion (eq. 3). Therefore, to compute the net amount of active mycelial transport, $A_{biomass}$ was subtracted from $A_{mycelium}$ (eq. 3). HCH transport by gas-phase diffusion ($A_{air}$), biomass-based diffusion ($A_{biomass}$) and active transport ($A_{active}$) could therefore be distinguished.

### 4.3.7. Data analysis

Statistical significance testing of the various experimental treatments (experimental setups and controls; $p < 0.05$) was performed on HCH concentrations using analysis of variance (one-way ANOVA) and Tukey's HSD (honestly significant difference) in R (version 4.2.0). The differences between individual means were computed with the student's t-test. The line graphs were plotted in sigma plot version (14.0) while the box plots were plotted using gg plot in R (version 4.2.0).

## 4.4. Results

### 4.4.1. Isolation and identification of the fungal strain

Identification of the fungal isolate relied on internal transcribed spacer (ITS)-5.8S rRNA gene sequencing. A BLAST search (Altschul et al., 1990) of ITS-5.8S rRNA partial sequences revealed that the fungal isolates was affiliated to *Fusarium equiseti*, with sequence identities >99%. Further analysis by phylogeny (**Figure 4.3**), based on homologous ITS-5.8S rRNA sequence of nineteen *Fusarium* species obtained from BLAST searches showed that the fungal isolate clustered with members of *F. equiseti* with a posterior probability of 51%. The fungus was more closely related to *F. equiseti* strain UOA/HCPF 47B (KC254029.1) and *Fusarium* sp. isolate RM33 (MG664720.1) with posterior probability values of 83% and 92% respectively (**Figure 4.3**). From the tree topology, the fungus was likely to be new member of *F. equiseti* clade. The ITS-5.8S rRNA gene sequence of the fungal isolate was deposited to GenBank at NCBI where it was tagged as *Fusarium equiseti* strain K3 under accession numbers MK734071.1.

### 4.4.2. Genome sequencing of the fungal strain

The genome assembly of *F. equiseti* strain K3 resulted in 206 contigs with a total length of 37,882,472 bp ($N_{50}$ contig length of 601,073 bp and 48.03% GC). Annotation of the draft genome resulted in 12,311 predicted protein-coding sequences while analysis of the predicted protein-coding sequences with BUSCO (Gurevich et al., 2013) and the fungi_odb10 database ( with a total of 758 genes) resulted in 749 genes (98.8%) as complete single-copy genes, 3 genes (0.4%) as complete duplicated genes, 3 genes (0.4%) as fragmented genes and 3 genes (0.4%) as missing genes. A total of 261 tRNA genes were predicted using ARAGORN version 1.2.36 (Laslett, 2004) and a total of 34 putative secondary metabolites biosynthetic gene clusters previously reported for other *Fusarium* species were predicted using antiSMASH version 6.0.0 (Blin et al., 2019). These included clusters likely to produce; non-ribosomal peptides (Bonsch et al., 2016; Wollenberg et

al., 2017), polyketides (Janevska et al., 2016; Miyamoto et al., 2010; Studt et al., 2012), and terpenes (Brock et al., 2013; Miyamoto et al., 2010).

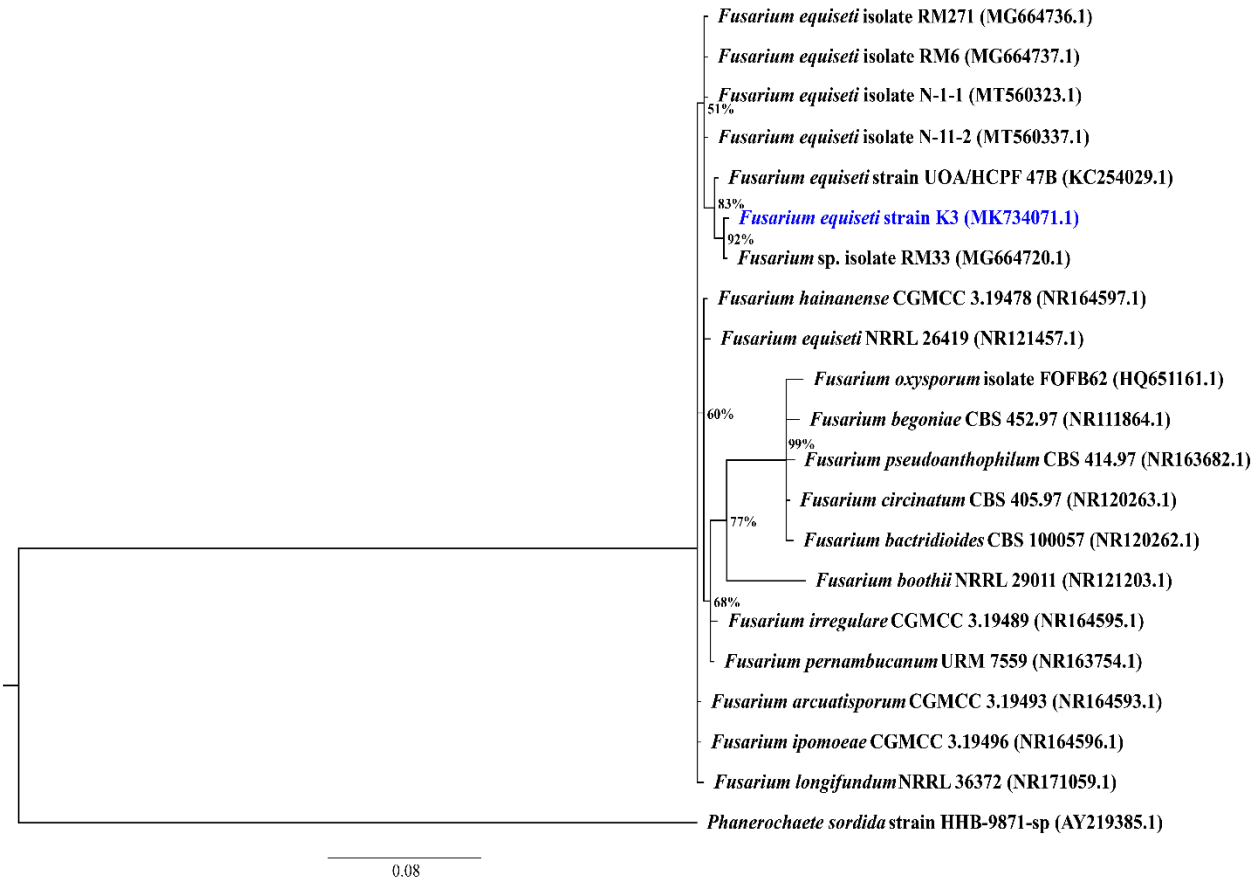


**Figure 4.3:** A phylogenetic tree based on internal transcribed spacer (ITS), 5.8S rRNA gene sequences depicting the evolutionary relationship of *Fusarium equiseti* strain K3 (734071.1) with other *Fusarium* species. The tree was constructed in MrBayes, a program for Bayesian inference of phylogeny that is based on Markov Chain Monte Carlo (MCMC) method. The topographical robustness of the tree is indicated by the percentage posterior probabilities (calculated from 1,000 samples) at the nodes. The tree was rooted using *Phanerochaete sordida* strain HHB-9871-sp (AY219385.1).

### 4.4.3. Biodegradation of and identification of degradation metabolites

Gas chromatography (GC) analyses of residual HCH in the degradation cultures were conducted to demonstrate the biodegradation of the pesticide by the *Fusarium* strain. The difference between HCH levels in the controls and fungal inoculated cultures over the incubation period (28 days) indicated the capacity of the fungus to degrade HCH isomers. The results revealed the degradation of 35.4% ±6.4%, 51.0% ±12.2%, 28.4% ±2.1%, and 36.9% ±13.3% of 100 µg $mL^{-1}$ of each α-, β-,

γ-, and δ-HCH respectively (**Figure 4.4**). Interestingly, the fungus appeared to better degrade the more recalcitrant HCH isomer (β-HCH) with the degradation of isomers in the order β > δ > α > γ. ANOVA revealed statistically significant differences in the degradation of the respective HCH isomers [$F(3,8) = 10.39$; $N = 12$, $p < 0.0039$]. GC-MS analysis of the cell-free extract revealed the presence of two degradation metabolites in the fungal growth medium after 14 days. The metabolites were identified by comparing their mass spectral fragmentation patterns to those in the national institute of standards and technology (NIST) mass spectral library (Stein et al., 2008). The first metabolite showed a fragmentation pattern with ion fragments of m/z 180, 145, 109, and 75 identical to that of 1,3,5-trichlorobenzene, while the second metabolite with ion fragments of m/z 195, 143, and 97 was identified as 1,3,5-trichloromethoxy benzene (**Figure 4.5**). To our knowledge, we report for the first time the presence of these two metabolites in a fungal HCH degradation culture.

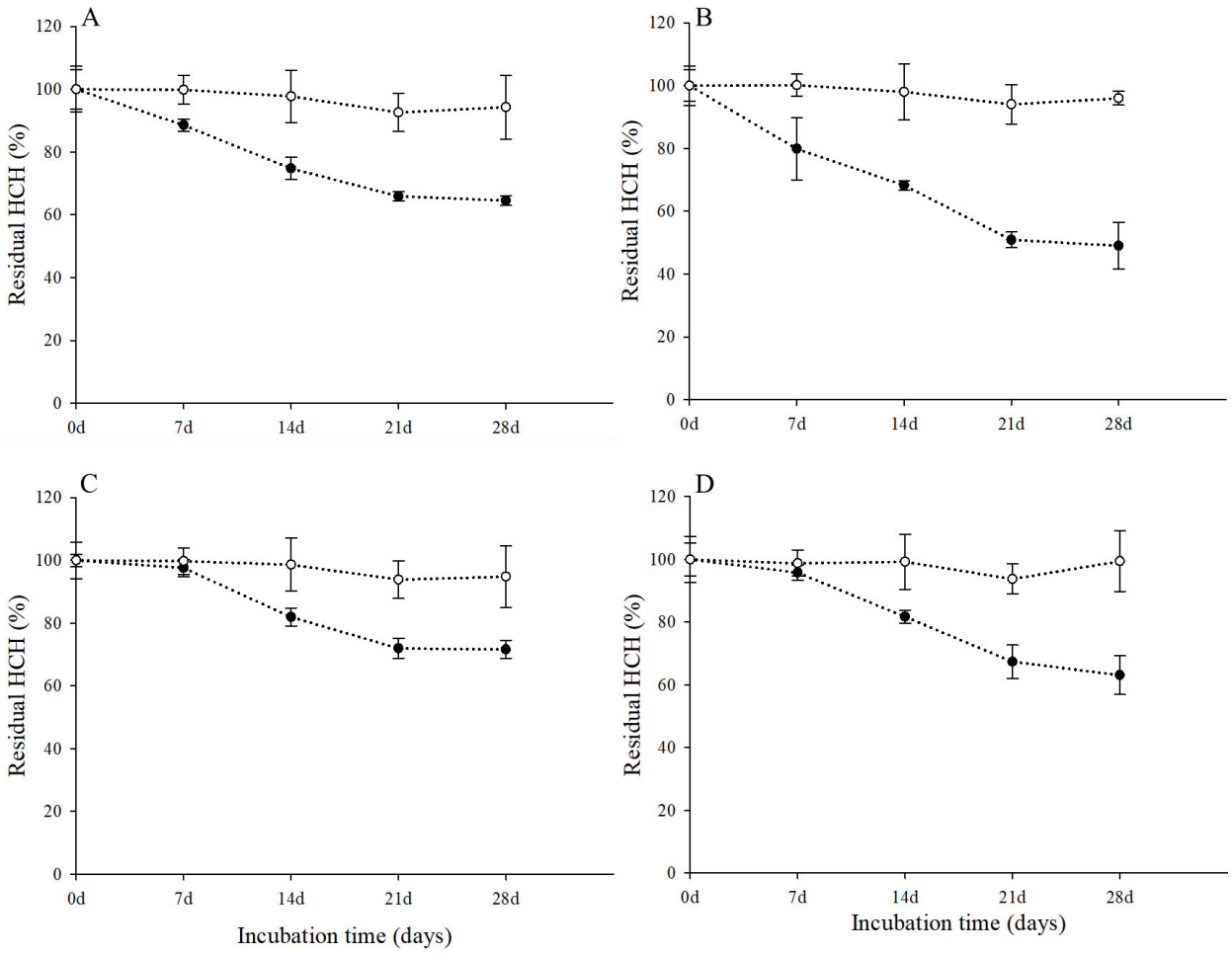


**Figure 4.4:** HCH degradation profile by *F. equiseti* strain K3. Panels A, B, C, and D represents α-HCH, β-HCH, γ-HCH, and δ-HCH respectively. Fungal culture (●), Control (○).

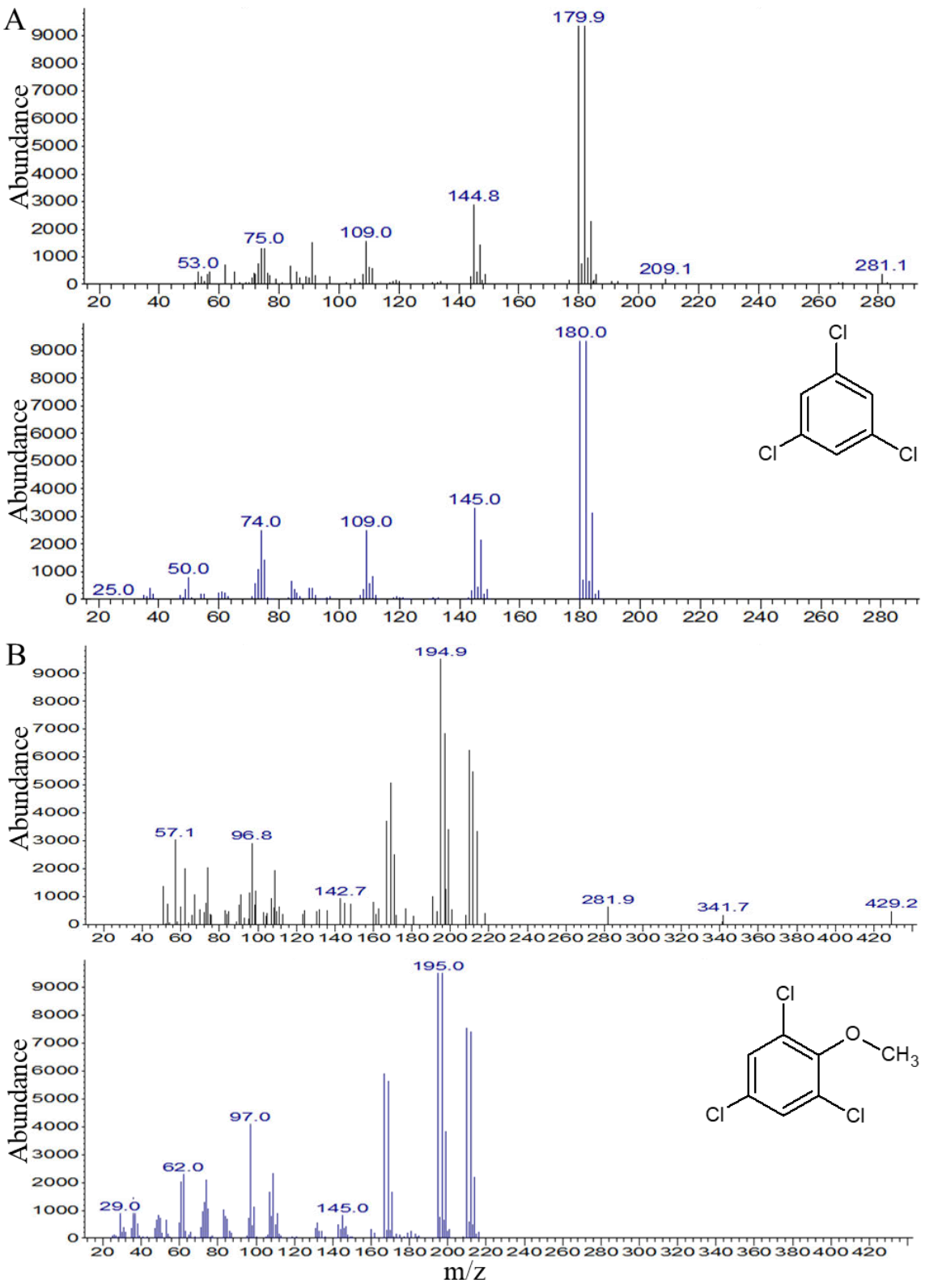


**Figure 4.5:** GC-MS profiles of two metabolites identified as (A) 1,3,5-trichlorobenzene and (B) 1,3,5-trichloromethoxy benzene.

### 4.4.4. Quantification of mycelial HCH transport in porous media

Quantification of HCH at positions P3 and P4 (**Figure 4.2**) after exclusion of gas-phase transport (cf. eq. 2) revealed amounts in the range of 0.1µg, 0.1µg, 0.2µg and 0.1µg at position P3 (~1.8cm distance) and 0.4µg, 0.1µg, 0.6µg, and 0.1µg at position P4 (~3cm distance) for α-, β-, γ-, and δ-HCH respectively (**Figure 4.6**, **Table 4.1**). The increase in HCH amounts with distance in presence of active mycelia clearly revealed the effect of mycelia-based transport of HCH. Nearly equal amounts of β- and δ-HCH isomers were recovered at positions P3 and P4 ($p > 0.4$), while significantly higher amounts ($p < 0.02$) of α- and γ- HCH isomers were recovered at position P4 than P3 (**Figure 4.6**). This suggests that α- and γ-HCH were better transported along mycelial structures than β- and δ-HCH isomers. The low or negative HCH amounts computed for biomass-based transport (cf. eq. 3, **Table 4.1**), indicated that passive diffusion did not significantly influence the transport process along mycelial structures. To further assess the influence of mycelia-mediated translocation of HCH, the transport processes, $A_{\text{mycelium}}$ and $A_{\text{biomass}}$ were correlated with HCH's octanol-air partition coefficient (log $K_{OA}$) (**Figure 4.7**). Log $K_{OA}$ was chosen because of its role as a key descriptor of chemical partitioning between air and the ambient organic phases (for our case, hyphal structures and agar patches used in the experiment) (Shoeib & Harner, 2002). A plot of net HCH amounts against log $K_{OA}$ revealed no correlation ($r = -0.2$) at position P3 and a strong negative correlation ($r = -0.8$) at position P4 for $A_{\text{mycelium}}$. These results, therefore, suggest that isomers with high log $K_{AO}$ (8.84 and 8.88 for δ- and β-HCH) are poorly translocated along mycelia compared to isomers with low log $K_{OA}$ (7.61 and 7.85 for α- and γ-HCH). Therefore, the transport of HCH isomers was in the order $\beta \approx \delta < \alpha < \gamma$. The difference in the transport rates ($p < 0.003$) observed between α- and γ-HCH, however, was likely due to their differences in solubility (10ppm for α-HCH and 17ppm for γ-HCH). In contrast, no correlation ($r = -0.2$) was observed for biomass-based transport ($A_{\text{biomass}}$) further indicating the insignificant role played by passive diffusion of HCH isomers along dead mycelia in the transport process. The observed transport effect in presence of fungal mycelia ($A_{\text{mycelium}}$) was therefore likely due to the metabolic activity of live mycelia. HCH transport may not have greatly been influenced by degradation due to the poor HCH degradation capacity of the fungus, however, further research on degradation during transport is required.

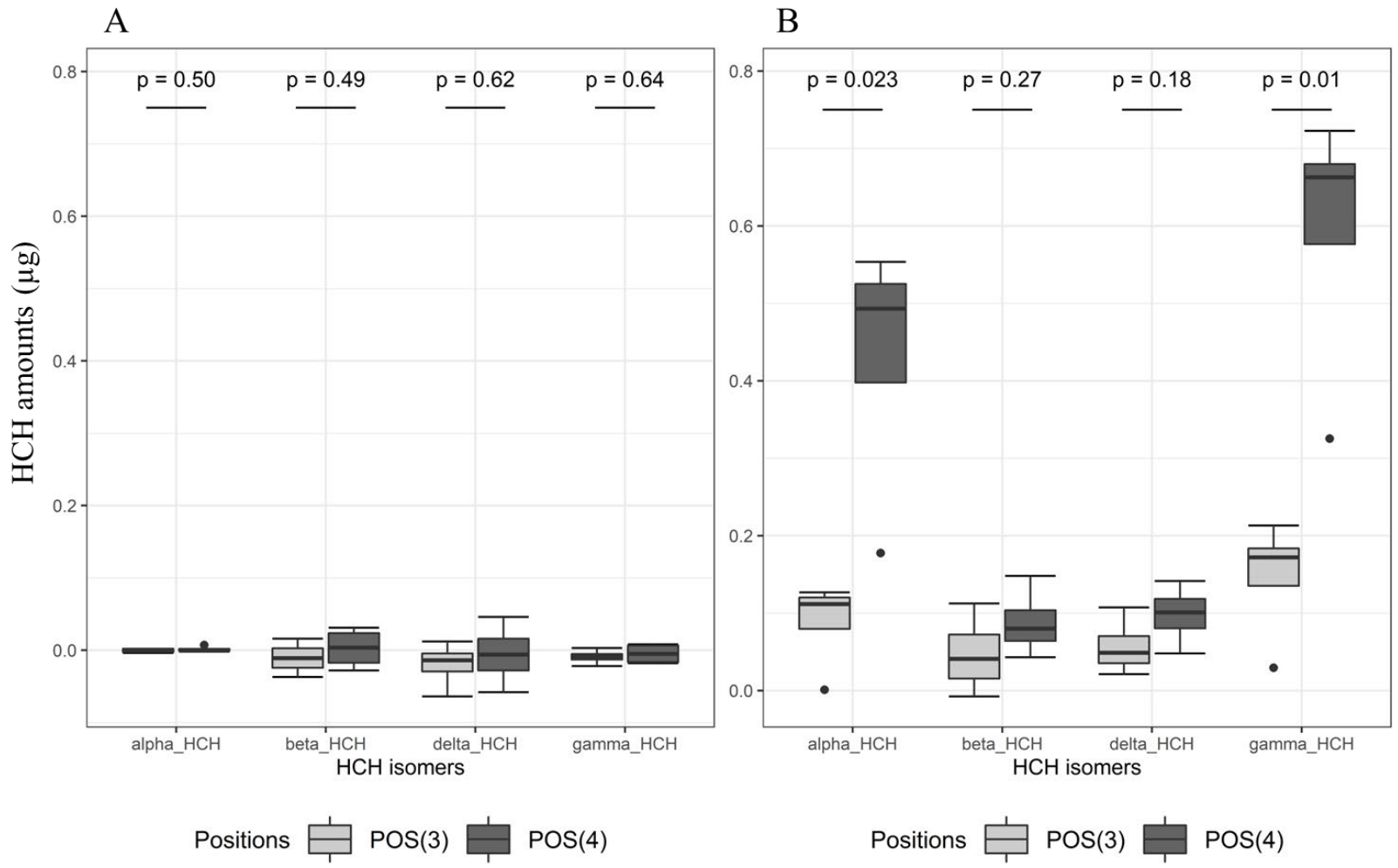


**Figure 4.6:** An illustration of HCH transport quantification. Amounts of HCH isomers in µg recovered from agar patch P3 and P4. $A_{biomass}$ (cf. eq. 3; panel A), and $A_{mycelium}$ (cf. eq. 2; panel B) after 14 day-incubation period in presence of mycelial structures *F. equiseti* strain K3.

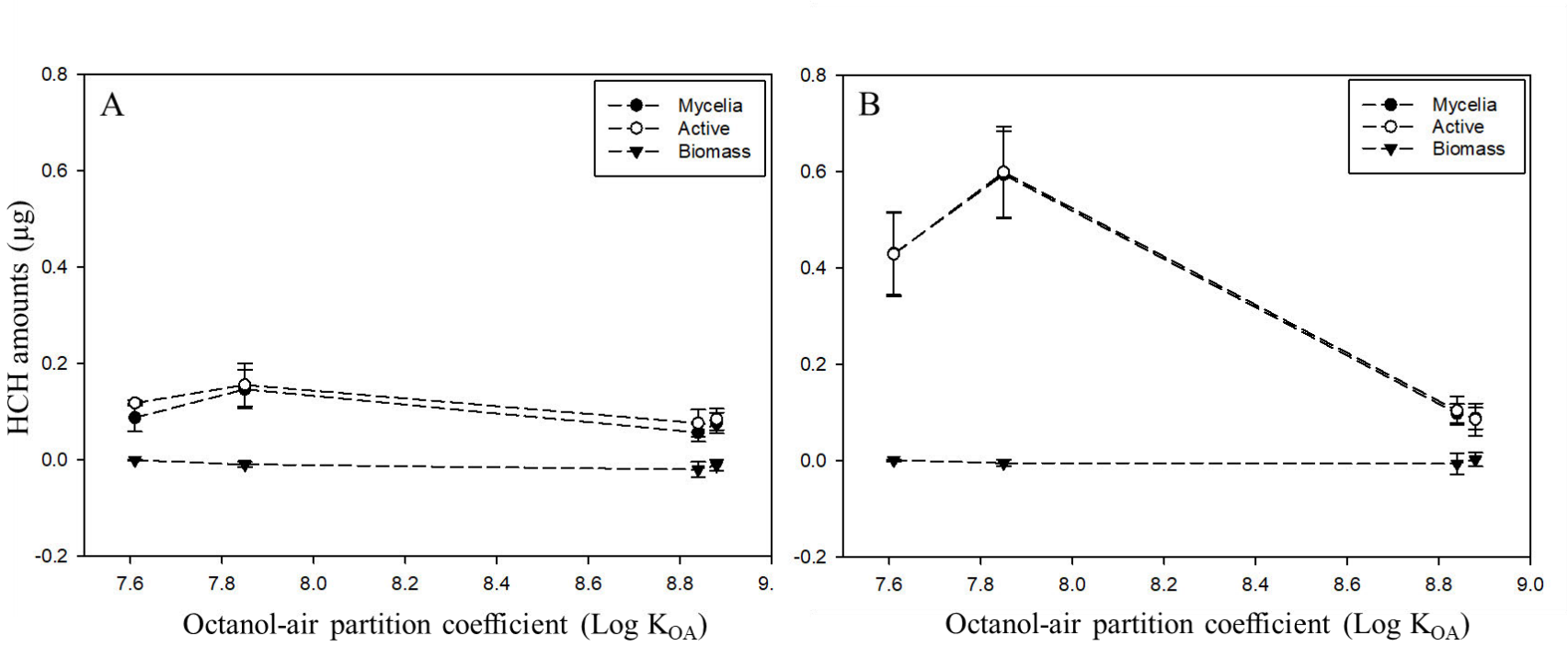


**Figure 4.7:** Profiles of the net amounts of HCH isomers translocated for $A_{mycelium}$ (●), $A_{biomass}$ (▼) and $A_{active}$ (○) at positions P3 (panel A) and P4 (panel B) in *F. equiseti* strain K3 plotted against log $K_{OA}$ of the respective HCH isomers. No significant difference ($p > 0.05$) was observed between $A_{mycelium}$ and $A_{active}$. Data represents the means of four replicates after 14 day-incubation period.

**Table 4.1:** Average amounts (µg) of HCH isomers at positions 3 and 4 transported by live mycelia (cf. eq. 2, $A_{mycelium}$), biomass-based diffusion (cf. eq. 3, $A_{biomass}$) and active mycelia (cf. eq. 4, $A_{active}$).

| HCH Isomers | HCH concentration (µg) | | | | | |
|---|---|---|---|---|---|---|
| | $A_{mycelium}$ | | $A_{biomass}$ | | $A_{active}$ | |
| | Position 3 | Position 4 | Position 3 | Position 4 | Position 3 | Position 4 |
| α HCH | 0.09 ±0.06 | 0.43 ±0.17 | -0.0005 ±0.003 | 0.0010 ±0.004 | 0.12 ±0.01 | 0.43 ±0.18 |
| β HCH | 0.06 ±0.05 | 0.09 ±0.04 | -0.0109 ±0.023 | 0.0024 ±0.028 | 0.08 ±0.05 | 0.09 ±0.07 |
| γ HCH | 0.15 ±0.08 | 0.60 ±0.18 | -0.0093 ±0.010 | -0.0050 ±0.014 | 0.16 ±0.09 | 0.60 ±0.19 |
| δ HCH | 0.06 ±0.04 | 0.10 ±0.04 | -0.0198 ±0.032 | -0.0061 ±0.043 | 0.08 ±0.06 | 0.10 ±0.06 |

## 4.5. Discussion

### 4.5.1. Identification and determination of HCH degradation of the fungus

The fungus was isolated from HCH-contaminated soil and exhibited a high percentage sequence homology (99.8%) with the genus *Fusarium*. As demonstrated by the phylogenetic tree topology (**Figure 4.3**), the ITS sequence of the fungus clustered together with those of *F. equiseti* suggesting it to be a new member of this clade. On the other hand, analysis of the genome sequence revealed the presence of 34 secondary metabolites biosynthetic gene clusters previously reported for other *Fusarium* species such as *F. fujikuroi* (Brock et al., 2013; Janevska et al., 2016; Studt et al., 2012) and *F. heterosporum* (Sims et al., 2005) The fungus was therefore tagged as *F. equiseti* strain K3. Chemical analysis of residual HCH isomers in the culture medium revealed the removal of approximately 35%, 51%, 28%, and 37% of 100 µg/mL of each α-, β-, γ-, and δ-HCH respectively in the fungal culture over 28 days, while HCH removal was not observed in the controls (**Figure 4.4**). Further analysis of cell-free extract by GC-MS revealed the presence of two degradation metabolites identified as 1,3,5-trichlorobenzene and 1,3,5-trichloromethoxy benzene (**Figure 4.5**).

Though studies relating to the degradation of organochlorine pesticides have been focused on white rot fungi because of their efficient enzyme system (Rigas et al., 2009; Shah et al., 1992; Singh & Kuhad, 1999, 2000), there are a few reports related to the use of non-white rot fungi (Guillén-Jiménez et al., 2012; Nagpal et al., 2008; Sagar & Singh, 2011). HCH degradation by non-white rot fungi was first reported in the phycomycetes *Conidiobolus*, which was demonstrated to completely mineralize 5 µg/mL lindane in liquid culture in 5 days (Nagpal et al., 2008). Subsequently, Sagar & Singh, (2011) reported degradation of 59% and 57% 100 µg/mL lindane by *F. solani* and *F.poae* respectively in liquid culture in 10 days, while *F. verticillioides* was reported to degrade 28% of 50 µg/mL lindane in 11 days (Guillén-Jiménez et al., 2012). Therefore, the partial degradation of HCH isomers observed in this study is consistent with HCH degradation rates previously observed for other *Fusarium* species. It has previously been proposed that the partial degradation observed could be due to non-specific nature of the fungal enzymes and/or enzyme inhibition by the degradation metabolites (Guillén-Jiménez et al., 2012; Murthy & Manonmani, 2007).

Several metabolites have previously been identified in HCH degradation microbial cultures under both oxic and anoxic conditions (Lal et al., 2010; Phillips et al., 2005). γ-pentachlorocyclohexane (γ-PCCH) has been reported as the metabolite generated in the first step of aerobic HCH degradation through dehydrochlorination (Nagata et al., 2007; Pal et al., 2005; Phillips et al., 2005). Singh & Kuhad, (2000) however, identified tetrachlorocyclohexene (TCCH) and tetrachlorocyclohexenol (TCCOL) as the initial lindane degradation products in two white rot fungi *C. bulleri* and *P. sordida*. They therefore proposed that lindane degradation in the two fungi would proceed by reductive dechlorination to TCCH followed by hydroxylation to TCCOL. They however attributed the failure to identify other degradation metabolites to low concentrations in the culture media and high polarity (Singh & Kuhad, 2000). More recently, Guillén-Jiménez et al. (2012) identified γ-PCCH and benzoic acid derivatives in lindane degradation cultures of *F. verticillioides*. They, therefore, proposed that the fungus would degrade HCH via PCCH to phenolic compounds that would then undergo carboxylation under aerobic conditions (Guillén-Jiménez et al., 2012). The identification of 1,3,5-trichlorobenzene and 1,3,5-trichloromethoxy benzene in the present study therefore suggests that several subsequent dechlorination steps and a hydroxylation step were likely employed by *F. equiseti* strain K3 in the degradation of HCH isomers. The failure to identify a complete profile of metabolites did not allow for the proposition of a possible HCH degradation mechanism in the fungus, thus, further research is required.

### 4.5.2. Quantification of mycelial HCH transport

Mycelial microorganisms have previously been shown to access nutrients from remote locations and transport them across air-gaps to support their apical growth (Furuno et al., 2012; Wick et al., 2010). Though most research has been focused on the role of mycelia as transport networks for nutrients (Bago et al., 2002; Whitfield, 2007; Worrich et al., 2017), their role in the translocation of contaminants such as polycyclic aromatic hydrocarbons (PAHs) was demonstrated in the hyphae of the soil oomycete *Pythium ultimum* (Furuno et al., 2012; Schamfuß et al., 2013). The model system used in the present study was developed such that gas-phase HCH transport could be excluded (**Figure 4.2**). Therefore, following the exclusion of gas-phase transport, active mycelia ($A_{\text{mycelium}}$) of the *Fusarium* species transported up to 0.4µg α-HCH, 0.1 µg β-HCH, 0.6 µg γ-HCH, and 0.2 µg δ-HCH over 3cm (P4) within 14 days (**Figure 4.6, Table 4.1**). The low/negative HCH amounts computed in presence of dead mycelia ($A_{\text{biomass}}$, **Table 4.1**) indicated

the minor role played by passive diffusion in the transport process. This suggests that the presence of active mycelia was necessary for the translocation of HCH to occur. These results are consistent with previous studies where active mycelia were reported to act as transport vectors "pipelines" for PAHs (Furuno et al., 2012; Schamfuß et al., 2013). To establish the role of mycelia in the translocation of the PAH phenanthrene (PHE), Furuno et al. (2012) demonstrated a more effective distribution of PHE in the presence of active mycelia.

The transport mechanism of PAHs has been demonstrated to include their uptake by the fungal hyphae into lipid vesicles (Furuno et al., 2012; Schamfuß et al., 2013; Verdin et al., 2005) and subsequent streaming of the PAH-enriched cytoplasmic vesicles (Furuno et al., 2012; Schamfuß et al., 2013). It has previously been demonstrated that hyphal growth is facilitated by the accumulation of vesicles at the hyphal tip (Steinberg, 2007) according to "the vesicle supply center" model of hyphal growth initially proposed by Bartnicki-Garcia et al. (1989). Therefore, the recovery of higher amounts of HCH isomers at position P4 than P3 is likely due to the accumulation of the isomers at the hyphal tip of the growing mycelia. Correlation of the transport process with log $K_{OA}$ revealed that HCH transport ($A_{mycelium}/A_{active}$) increased with distance, particularly for α- and γ-HCH (P3 to P4, cf. **Figure 4.6**) and was negatively correlated to log $K_{OA}$ ($r = -0.8$) (**Figure 4.7**). This suggests that the transport of HCH isomers is influenced by their physicochemical properties. We, therefore, speculate that the high amounts of HCH observed at position P4 was likely due to an overlay of vesicle-bound and diffusive transport (Furuno et al., 2012; Heaton et al., 2010) along mycelial structures. It has been shown previously that biological activity is necessary for both transport processes because mycelial fungi employ energy-dependent mechanisms for both vesicle movement and cytoplasmic streaming (Heaton et al., 2010; Steinberg, 2007). These observations, therefore, demonstrate that the mycelial structures of the *Fusarium* species translocated HCH isomers in the water-unsaturated heterogeneous system. Our study hence provides for the first-time evidence for the role of fungal mycelia in the translocation of HCH isomers. Due to their ubiquitous nature and transport capacity, these results underpin the central role of mycelial activity in the dispersal of hydrophobic pollutants in soil, which may improve their bio-accessibility to potential bacterial degraders.

### 4.6. Conclusion

A non-white rot fungus *F. equiseti* strain K3 was isolated from HCH-contaminated soil and could partially degrade HCH isomers. The identified degradation metabolites suggest HCH degradation by dechlorination and hydroxylation. The fungus could preferentially translocate HCH isomers in porous media in the order $\beta \approx \delta < \alpha < \gamma$, suggesting that it can potentially act as transport network for HCH in soil. These findings add to our knowledge of the potential role of non-white rot fungi in the bioremediation of HCH. Further research is however required to characterize the degradation mechanism and the catabolic enzymes responsible for HCH degradation. The availability of this genome would provide invaluable insights into these efforts. In addition, further investigation on the mechanism of HCH transport and the effect of degradation during the transport process would be necessary to fully understand its effectiveness as transport network for HCH.

# CHAPTER FIVE

## 5.0 Mycelial nutrient transfer facilitates bacterial co-metabolic degradation of an organochlorine pesticide in nutrient-deprived environments

### 5.1. Abstract

Biotransformation of soil organochlorine pesticides (OCP) is often impeded by a lack of nutrients relevant for bacterial growth and/or co-metabolic OCP biotransformation. By providing space-filling mycelia, fungi promote contaminant biodegradation by facilitating bacterial dispersal and the mobilization and release of nutrients in the mycosphere. We here tested whether mycelial nutrient transfer from nutrient-rich to nutrient-deprived areas facilitates bacterial OCP degradation in a nutrient-deficient habitat. The legacy pesticide hexachlorocyclohexane (HCH), a non-HCH-degrading fungus (*Fusarium equiseti* K3), and a co-metabolically HCH-degrading bacterium (*Sphingobium* sp. S8) isolated from the same HCH-contaminated soil were used in spatially structured model ecosystems. Using 13C-labelled fungal biomass and protein-based stable isotope probing (protein-SIP), we traced the incorporation of $^{13}C$ fungal metabolites into bacterial proteins while simultaneously determining the biotransformation of the HCH isomers. The relative isotope abundance (RIA, 7.1 – 14.2%), labeling ratio (LR, 0.13 – 0.35), and the shape of isotopic mass distribution profiles of bacterial peptides indicated the transfer of 13C-labeled fungal metabolites into bacterial proteins. Distinct 13C incorporation into the haloalkane dehalogenase (linB) and 2,5-dichloro-2,5-cyclohexadiene-1,4-diol dehydrogenase (LinC), as key enzymes in metabolic HCH degradation, underpin the role of mycelial nutrient transport and fungal-bacterial interactions for co-metabolic bacterial HCH degradation in heterogeneous habitats. Nutrient uptake from mycelia increased HCH removal by twofold as compared to bacterial monocultures. Fungal-bacterial interactions hence may play an important role in the co-metabolic biotransformation of OCP or recalcitrant micropollutants (MPs).

## 5.2. Introduction

Despite its ban or restricted use in many parts of the world, the organochloride pesticide hexachlorocyclohexane (HCH) continues to pose a serious environmental risk (Mohn et al., 2006; Sharma et al., 2006) due to its toxicity and environmental persistence (Lal et al., 2006; Mohn et al., 2006; Singh & Lal, 2009; Singh & Kuhad, 1999). Commercial production of HCH typically results in a mixture of four major isomers (α-HCH (60 – 70%), β-HCH (5 – 12%), γ-HCH (10 – 12%), δ-HCH (6 – 10%)) (Kumar & Pannu, 2018; Lal et al., 2006), of which only γ-HCH has insecticidal activity while the other isomer are discarded as HCH-muck, thereby generating stockpiles of persistent toxic waste (Kumar & Pannu, 2018; Lal et al., 2006, 2010; Nayyar & Lal, 2016). Microorganisms including fungi (Bumpus et al., 1985; Phillips et al., 2005; Singh & Kuhad, 1999) and bacteria (Dogra et al., 2004; Lal et al., 2010; Pal et al., 2005) can degrade HCH isomers. However, an elaborate degradation pathway and the respective catabolic enzymes for complete mineralization of HCH have only been reported for bacterial members of the family sphingomonadaceae under ideal laboratory conditions (Dogra et al., 2004; Lal et al., 2006, 2010; Pal et al., 2005). Microbial degradation in heterogeneous environments though emerges from manifold biotic and abiotic factors including redox conditions, moisture, and – in cases of co-metabolic degradation – the presence and spatial availability of auxiliary organic growth substrates to potential degraders (Harms et al., 2011; Rijnaarts et al., 1990; Wick, 2020). Contrary to bacteria, mycelial fungi are highly adapted to heterogeneous habitats. Due to their space-filling mycelial structures, they translocate resources within their networks from nutrient-rich to nutrient-deficient patches (Jennings, 1987; Nazir et al., 2010).

Fungi and bacteria thereby often share the same microhabitat and contribute to nutrient cycling and other biogeochemical processes (Deveau et al., 2018; Nazir et al., 2010; Worrich et al., 2017), such as the biotransformation of organic contaminants (Harms et al., 2011; Kohlmeier et al., 2005; Wick et al., 2010). In the mycosphere (i.e. the microhabitat that surrounds fungal hyphae and mycelia), bacteria and fungi may compete for the same substrates and, depending on the organisms and habitat conditions, their interactions may be either ecologically neutral, competitive, or cooperative (Espinosa-Ortiz et al., 2021; Haq et al., 2014) and range from apparently random physical to specific commensal or symbiotic associations (Deveau et al., 2018). Mycelia e.g. have been shown to actively transport polycyclic aromatic hydrocarbons (PAH) thus improving their bioavailability to bacterial degradation in unsaturated environments (Furuno et al., 2012;

Schamfuß et al., 2013, 2014). They may further serve as transport vectors for bacteria and phage-bacteria couples (You et al., 2022), thus improving the access of bacteria to otherwise poorly available nutrients and contaminants(Kohlmeier et al., 2005; Wick et al., 2007). Fungi are also known to shape bacterial community structures surrounding the hyphosphere by secreting carbonaceous compounds that can be utilized by fungus-associated bacteria (Boer et al., 2005; Frey-Klett et al., 2007; Nazir et al., 2010; Schamfuß et al., 2013). They thereby exude carbon substrates such as phenols, citrate, or oxalate that may serve as auxiliary carbon sources for pollutant-degrading bacteria (Wick et al., 2010).

Co-metabolic degradation offers the benefit of contaminant removal even at trace quantities since the degrader is not reliant on the contaminant for carbon or energy source (Hazen, 2010; Wick, 2020). However, the role of fungal resource transfer to bacteria for improved bacterial activity and co-metabolic contaminant degradation in contaminated oligotrophic microhabitats remains vastly underexplored. In microbial ecology, stable isotope probing of proteins (protein-SIP) has become a valuable technique that allows the identification of key metabolic actors and functional interactions in microbial communities (Jehmlich et al., 2016; Sachsenberg et al., 2015; Taubert et al., 2011). Protein-SIP combines meta-proteomics based on mass spectrometry and stable isotope probing techniques to sensitively detect the assimilation of labeled target substrate (such as $^{13}C$) at peptide level (Jehmlich et al., 2016; Sachsenberg et al., 2015). The information gleaned from mass spectrometry data includes relative isotope abundance (RIA), labeling ratio (LR), and the shape of the isotopic distribution (Sachsenberg et al., 2015). The RIA describes the percentage of the heavy isotope (i.e., $^{13}C$) atoms in a peptide, which provides information on the incorporation of the labeled substrate into biomass. The LR describes the ratio of labeled to unlabeled peptides which relate to protein turnover following the addition of the labeled substrate (Lünsmann et al., 2016; Sachsenberg et al., 2015).

In the present study, we used spatially fragmented laboratory model ecosystems to test the hypothesis whether mycelial nutrient transfer from eutrophic habitats promotes co-metabolic degradation of HCH by bacteria in oligotrophic contaminated environments. A non-HCH-degrading soil fungus *Fusarium equiseti* K3 and a co-metabolically HCH degrading bacterium *Sphingobium* sp. S8 isolated from the same HCH contaminated soil were used. Strain S8 was placed onto a nutrient-free HCH-treated agar patch that was separated from the fungal inoculum

by an air gap. $^{13}$C-labeled mycelia of strain K3 were allowed to overgrow the bacterial region. Using a combination of metaproteomics and stable isotope labeling and analyses (Jehmlich et al., 2016), we traced the incorporation of $^{13}$C of fungal origin into bacterial proteins responsible for both housekeeping and co-metabolic HCH degradation respectively, and simultaneously followed by chemical analytics. Our results demonstrate that mycelial fungi facilitate bacterial degradation of contaminants in nutrient-deficient environments by providing C-substrates to bacteria, thus enhancing their biotransformation capacity.

## 5.3. Material and Methods

### 5.3.1. Chemicals

Hexane (LiChrosolv grade), Acetone (99.8%), and γ-HCH (97%) were either purchased from Sigma (Munich, Germany) or Merck (Darmstadt, Germany) and were of analytical grade. $^{13}$C-glucose (D-glucose$^{13}C_6$, 99%) was obtained from Cambridge Isotope Laboratories, Inc, (USA) The analytical standard containing a mixture of the HCH isomers, $\alpha$: $\beta$: $\gamma$: $\delta$ = 1:1:1:1 was obtained from Merck (Darmstadt, Germany).

### 5.3.2. Organisms, media, and culture conditions

The ascomycete *Fusarium equiseti* K3 was isolated from HCH-contaminated soil collected from a former obsolete pesticide store in Kitengela, Kenya (GPS: 01.49 S, 37.048E), and its draft genome sequence was described earlier (Khan et al., 2021). The fungus was not found to degrade HCH (see below). Fungal pre-cultures were cultivated at 25ºC on potato dextrose agar (PDA; Difco) prior to the transfer to $^{13}$C glucose/glucose-containing MSM agar. The HCH degrading bacterium *Sphingobium* sp. S8 was isolated from the same soil as the fungus and its draft genome sequence was described by Khan et al (Khan et al., 2022). The bacterium was cultivated on Luria-Bertani (LB) (DSMZ) agar medium treated with γ-HCH (97%; Sigma) to a final concentration of 100 µg/ml. To prepare the inoculum of the S8 strain, a 72-h old culture ($OD_{600}$ ~1.5) of strain S8 in LB medium was centrifuged at 12000 g at 15°C for 10 min, the cell pellet washed twice with MSM medium, and resuspended in the same medium to a concentration of 7.2 x$10^8$ cells $mL^{-1}$.

### 5.3.3. Inhibition test

The absence of mutual fungal-bacterial inhibition was assessed using a standard procedure as described before (Yang et al., 1994). Briefly, a fungal mycelium was inoculated in the middle of

a PDA plate, and four spots of bacterial suspension (10 µL) inoculated onto the agar surface around the fungal inoculum at a distance of 1cm. The plates were later incubated at 25ºC and mutual growth or growth inhibition was analyzed by visual inspection and microscopy.

### 5.3.4. Microcosm set-up

Laboratory microcosms consisted of spatially separated nutrient-rich (NR) and nutrient-deficient (ND) zones that were separated by 2 mm air gaps (**Figure 5.1A**). To create NR zones, two patches (Ø 1 cm) were cut from a minimum salt medium (MSM) (Senoo & Wada, 1989) agar plate supplemented with 10% w/v $^{13}$C glucose/glucose as sole carbon source as described below. The two patches (patches 1 & 3; **Figure 5.1A**) were placed in a Petri dish (Ø 8.5 cm) at a distance of 1.4 cm apart. To represent a ND zone an MSM agar patch (l x w x h: 1 x1 x 0.5 cm; patch 2) was placed between them, leaving a 2 mm air gap on either side (**Figure 5.1A**). Patch 2 served as a spot for HCH spiking (in the case of HCH degradation setups) and bacterial inoculation. Fungal strain K3 was inoculated on patch 1 and allowed to grow until its hyphae touched the edges of patch 2 (after ca. 3d). Fifty µL (i.e., ≈ 3.6 x $10^7$ cells) HCH degrading strain S8 in MSM medium was applied to patch 2 of the microcosm. The microcosms were then incubated at 25 ºC in the dark until the mycelia had overgrown the patches (ca. 10d) and subsequently subjected to protein and HCH extraction and analysis.

### 5.3.5. Analysis of fungal nutrient transfer to bacteria

#### 5.3.5.1. Preparation of microcosms and inoculation

Patch 1 (**Figure 5.1A**) was spiked with $^{13}$C glucose by liquefying MSM medium agar at 95°C in a water bath and subsequently transferring a five mL aliquot into a sterile tube containing 0.5 g of $^{13}$C glucose. The tube was then warmed at constant shaking at 750 rpm in a thermomixer (Eppendorf, Germany) at 95°C until complete glucose dissolution. Two droplets of 200 µL each of the $^{13}$C-glucose-agar (i.e., 40 mg glucose) were then placed into the Petri dishes (Ø 8.5 cm) at a distance of 1.4 cm apart and allowed to solidify under a sterile laminar flow hood to form patches 1 & 3) (**Figure 5.1A**) while patch 2 was used an inoculation spot for the HCH degrading bacteria.

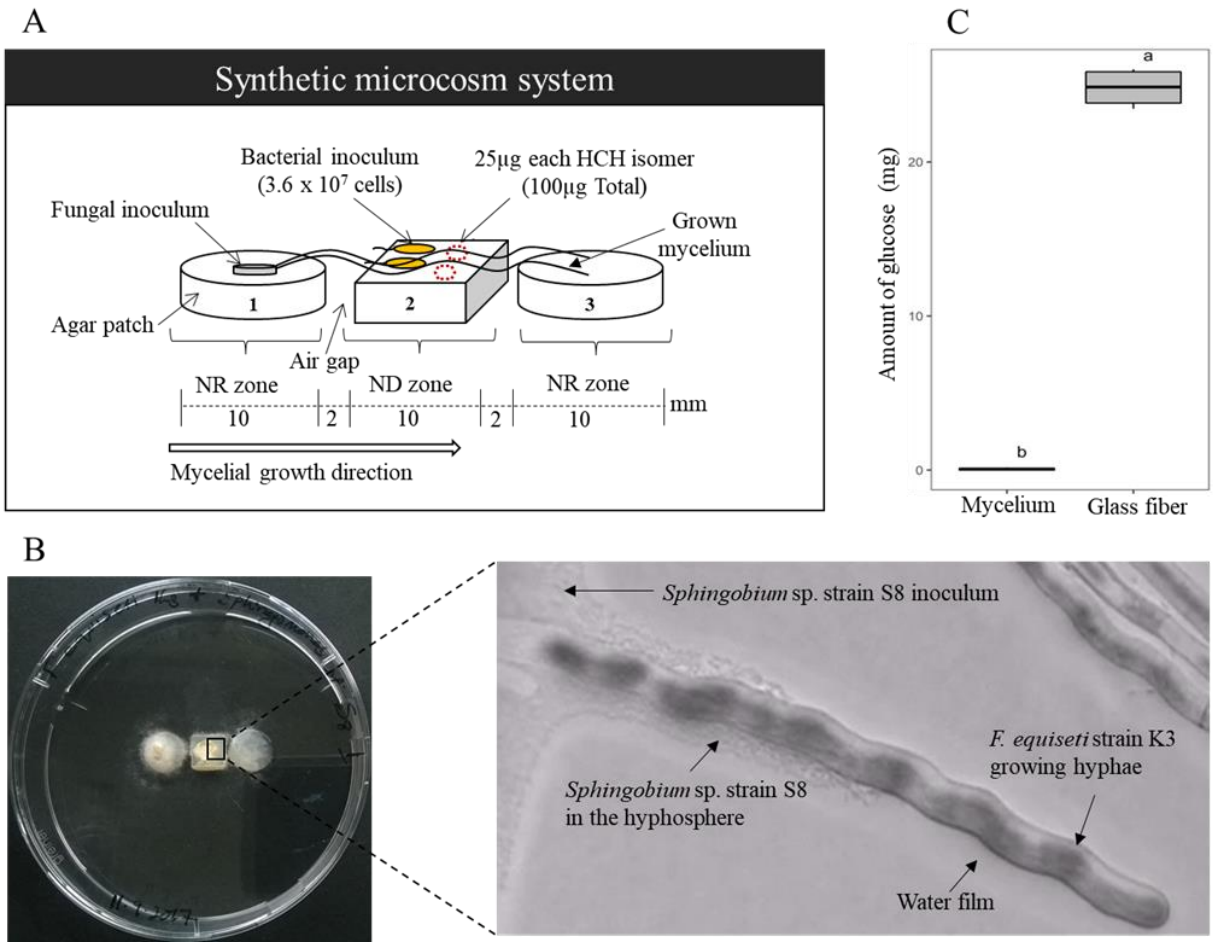


**Figure 5.1:** Fragmented synthetic microcosms to assess mycelial nutrient transfer and its effect on co-metabolic bacterial HCH degradation.

(A) Scheme of the microcosm consisting of two nutrient rich (NR) agar patches (patch1 and patch 3) and a nutrient-deficient agar patch 2 (ND zone) separated by air gaps to mimic unsaturated soil habitats. The fungus was inoculated to patch 1 and allowed to overgrow bacteria on patch 2 in presence of HCH. (B) Bird's view of the setup placed in a Petri dish and micrographs of *Sphingobium* sp. S8 growing as biofilm in close proximity to growing hyphae of F. equiseti K3 on patch 2. (C) Glucose content measured on patch 2 after 10 days in the presence of F. equiseti K3 and glass fiber. Different lowercase letters indicate statistically significant difference between the treatment groups ($p < 0.05$, $n = 3$).

Parallel control setups including glass fiber experiments to mimic mycelial structures "Glass fibre" and control experiments with bacteria directly growing on a $^{13}$C-glucose enriched (~20 mg) agar patch "Control" were prepared (**Figure 5.2**). Following a 10d incubation period, the microcosms were subjected to protein and glucose extraction from patch 2 and analysed as described below. All experiments were performed in triplicate. Identical setups in the absence of bacteria served to

quantify the glucose amounts transported by diffusion or capillary forces along glass fibers from patch 1 to patch 2 in the presence and absence of glass fibers after 10d. To do so, patch 2 was weighed and transferred into a 15 mL Falcon tube (Corning, USA). Subsequently, 5 mL of hot water and 3 mL of 1N HCl were added and the tube vigorously shaken for 5 minutes. The suspension was then filtered and the glucose concentration measured by pulsed amperometric detection (PAD).

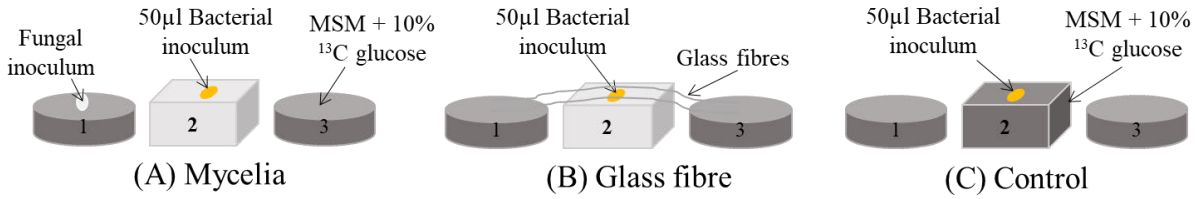


**Figure 5.2:** A scheme of different microcosm setups (A) "mycelia"; mycelium + bacteria, (B) "glass fiber"; glass fiber + bacteria, (C) "control"; positive control used in the labeling experiment. The three agar patches were placed in a raw with 2mm gaps between them to mimic nutrient-rich and nutrient deficient pockets in soil.

#### 5.3.5.2. Protein extraction, sample preparation

After harvest, patch 2 (**Figure 5.1A**) was transferred to sterile 10 mL glass tubes containing 2 mL of 1x PBS buffer pH 7.4, the tubes vortexed for 1 min and then sonicated (3 times for 30 s with 1 min pause each time) in a sonication bath (SONOREX SUPER RK 255 H, BANDELIN, Germany) at 35kHz ultrasound wave. The cell suspension was then transferred into 2 mL tubes and centrifuged at 16,000g and 4°C (Eppendorf, Germany) to pellet the cells. The cells were lysed in 50 µL lysis buffer (10 mM Tris; 5 mM EDTA; 0.29% NaCl; and 0.4% SDS) and processed as previously described (Jehmlich et al., 2010). A Bradford assay was used to estimate protein concentrations. For the SDS-PAGE, 75 µg of protein was precipitated with an equal volume of 20% trichloroacetic acid (TCA, Sigma) for 16 h at 4°C. The proteins were then separated in a 12% acrylamide gel using the Hoefer$^{TM}$ mini–Vertical Electrophoresis system (Thermo Fisher Scientific, USA) and the Laemmli-buffer system (Jehmlich et al., 2010). The protein bands were visualized by staining the gel in colloidal Coomassie Brilliant blue G-250 (Roth, Kassel, Germany). Protein bands were excised from the gel and subjected to in-gel tryptic digestion as described previously (Jehmlich et al., 2010). Tryptic peptides of all gel slices were then extracted for LC-MS/MS analysis.

#### 5.3.5.3. Protein-SIP analysis and evaluation

Peptides were analyzed by LC-MS/MS as described before (Sachsenberg et al., 2015): after tryptic digestion of the samples, the resulting peptides were subjected to a shotgun proteomics workflow (nanoLC-MS/MS). Briefly, peptide lysate was injected into a nanoLC system (UltiMate 3000, Dionex, Thermo Fisher Scientific). Peptides were first trapped for 3 min on a C18-reverse phase trapping column (Acclaim PepMap® 100, 75 µm x 2 cm, particle size 3 µM, nanoViper, Thermo Fisher Scientific), followed by separation on a C18-reverse phase analytical column (Acclaim PepMap® 100, 75 µm x 25 cm, particle size 3 µM, nanoViper, Thermo Fisher Scientific) with a solvent flow-rate of 300 nL/min and a column temperature of 35°C. Eluting peptides were ionized by a nano ion source (Advion, TriVersa Nanomate, Ithaca, NY, USA) and analyzed at the Q Exactive HF mass spectrometer (Thermo Fisher Scientific) (cf. appendix 2 **S1.1** for detailed description). Proteome Discoverer (v1.4.1.14, Thermo Scientific) was used for protein identification and the acquired MS/MS spectra were searched with the SequestHT algorithm against the UniProt reference proteome of *Sphingobium* sp. and *Fusarium equiseti*. Trypsin served as cleavage enzyme, allowing a maximum of two miss cleavages. The precursor mass tolerance (MS) was set to 10 ppm, and the fragment mass tolerance (MS/MS) was 0.05 Da. Carbamidomethylation of cysteine was considered as fixed and oxidation of methionine was set as dynamic modification. Peptide spectrum matches (PSM`s) were validated using percolator with a false discover rate (FDR) <1% and quality filtered for XCorr ≥2.25 [for charge state +2] and ≥2.5 [for charge state +3]. Identified proteins were grouped by applying the strict parsimony principle. Identification of $^{13}$C-labeled peptides and quantification of $^{13}$C incorporation was done by comparing measured and expected isotopologue patterns, chromatographic retention time, and fragmentation patterns using MetaProSIP as previously described (Sachsenberg et al., 2015). Proteome data from the genomes of *Sphingobium* sp. S8 and *Fusarium equiseti* K3 were used as a decoy input file in the MetaProSIP pipeline. Data was evaluated by calculating the relative isotope abundance (RIA) and the labeling ratio (LR) of the labeled peptides.

### 5.3.6. Analysis of co-metabolic HCH degradation

#### 5.3.6.1. HCH quantification

Similar setups as described above in presence of unlabeled glucose were used to quantify the effects of mycelial C-substrate transfer on bacterial degradation of *α*-, *β*-, *γ*-, and *δ*-HCH isomers, where 10 µL of a HCH mix dissolved in acetone containing 25µg of each isomer and fifty µL (i.e.,

≈ 3.6 x 107 cells) of bacterial cells suspended in MSM media were simultaneously placed to patch 2 (**Figure 5.1A**). Four circular agar patches containing activated carbon (60 mg $mL^{-1}$) were included in the microcosms to decrease the gaseous phase concentration of HCH. After a 10d incubation period, the patches (patch 1 – 3 and the activated carbon agar patches) were separately transferred into clean 40 mL screw cap septum glass vials (Thermo Scientific, USA), crushed with 10–15 g of dried sodium sulfate, and then extracted with hexane/acetone (3:1, v/v) containing 0.31 $\mu gL^{-1}$ dichlorodiphenyldichloroethylene (DDE) as an internal standard. One hundred µL of the extract was mixed with 10µL of 4-chlorobenzotrichloride as injection standard and analyzed by GC (HP 7890 Series GC, Agilent, USA) with a 20 m 0.18mm (18µm film thickness) HP5MS capillary column (Agilent, USA). Helium was used as a carrier gas at a flow rate of 1 mL $min^{-1}$. Quadruplicate setups including an abiotic setup, a fungus-only, and a bacteria-only setup, were also tested as controls (**Figure 5.3,** appendix 2 **S1.2**).

#### 5.3.6.2. Data analysis

To account for possible variations of the amounts of the HCH isomer added (e.g., due to volatilization, varying dissolution properties of the isomers), the amounts of the individual isomers recovered immediately after application onto patch 2 were taken as the initial amounts of HCH ($A_{t0}$). Subsequently, HCH amounts ($A_{deg,\,t10}$), and the residual ($F_{res,\,t10}$) and degraded fractions ($F_{deg,\,t10}$) of added HCH after 10 d were derived from equations 1– 4 (cf. appendix 2, **S2.3** for details). $A_{t10}$ is the residual amounts of HCH, $A_{abiotic,\,t10}$ the residual HCH amounts in the abiotic control, $A_{P1,\,t10\ or\ P2,\,t10\ or\ P3,t10}$ the residual HCH amounts on patches 1, 2 or 3, and $A_{AC,t10}$ the residual HCH amount on activated charcoal.

$$A_{t10} = A_{P1,t10} + A_{P2,t10} + A_{P3,t10} + A_{AC,t10} \qquad \text{eq. 1}$$

$$A_{deg,t10} = A_{abiotic,t10} - A_{t10} \qquad \text{eq. 2}$$

$$F_{deg,t10}\,(\%) = (A_{deg,t10}/A_{abiotic,t10}) * 100 \qquad \text{eq. 3}$$

$$F_{res,\,t10}\,(\%) = (A_{t10} / A_{abiotic,\,t10}) * 100 \qquad \text{eq. 4}$$

Statistical testing of the experimental treatments (abiotic, fungal-monoculture, bacterial-monoculture, and fungal-bacterial co-culture; $p < 0.05$) was performed on residual HCH concentrations ($A_{t10}$) using analysis of variance (one-way ANOVA) and Tukey's HSD (honestly

significant difference) in R (v 4.2.0). The significance of differences between individual means was computed using the student's t-test.

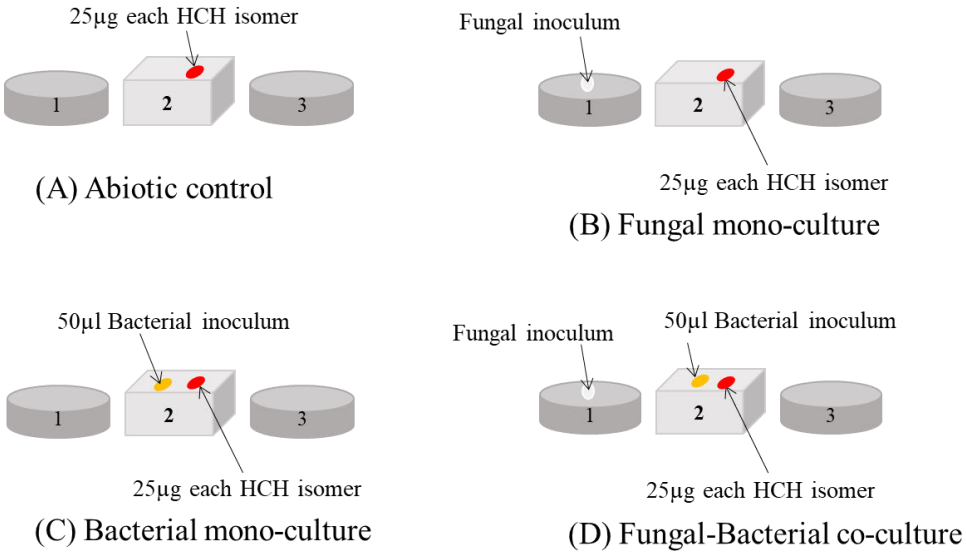


**Figure 5.3:** Different setups used in HCH degradation experiment; (A) abiotic control, (B) fungal monoculture, (C) bacterial monoculture, and (D) fungal-bacteria co-culture. Three agar patches were placed in a row with 2mm air gaps between them to mimic nutrient-rich and nutrient-deficient contaminated pockets in soil.

## 5.4. Result

### 5.4.1. Uptake of hyphal nutrients analyzed by protein-SIP

In a spatially heterogeneous laboratory ecosystem, we assessed whether mycelial nutrient transfer from nutrient-rich to nutrient-deprived areas facilitates bacterial co-metabolic HCH degradation in a nutrient-deficient habitat. Using $^{13}$C-labelled fungal biomass and protein-SIP, we observed higher protein contents and stable isotope enriched proteins in *Sphingobium* sp. S8 in presence of fungal hyphae (protein content: 0.45 mg) as compared to controls in presence of glass fiber (0.37 mg) and the absence of hyphal or glass fiber transport (0.29 mg; appendix 2 **Table S2.1**). The relative isotope abundance (RIA, **Figure 5.4**), the labeling ratio (LR; **Figure 5.4**) and the shape of isotopic spectral patterns (**Figure 5.5**) evidenced $^{13}$C enrichment of the total bacterial proteome (RIA = 10.9 – 93.9%; LR = 0.15 – 0.57) and selected proteins (RIA = 10.1 – 92%; LR = 0.17 – 0.59) (appendix 2 **Table S2.2**). Constitutively expressed bacterial proteins from core cellular and metabolic processes were selected out of 87 labeled proteins for assessing $^{13}$C incorporation in our treatments (**Figure 5.4** and appendix 2 **Table S2.2**): the chaperone DnaK (RIA = 9.4%; LR =

0.13), the ATP synthase subunit-β (RIA = 10.4%; LR = 0.24), and the peptidoglycan-associated lipoprotein (RIA = 14.2%; LR = 0.14).

To quantify fungal impacts on the expression of central enzymes of bacterial HCH degradation, the $^{13}C$ incorporation into two enzymes responsible for the initial steps of HCH degradation was quantified (Figs. 2&3); i.e. the haloalkane dehalogenase (LinB; RIA = 9.5%; LR = 0.35) and the 2,5-dichloro-2,5-cyclohexadiene-1,4-diol dehydrogenase (Lin C; RIA = 7.1%; LR = 0.34). LinB and LinC exhibited significant labeling and hence were built on $^{13}C$ enriched substrates upon hyphal transfer. As expected, observed RIA (88% – 96%) and LR (0.38 – 0.82) values in hyphal nutrient transfer experiments were different ($p < 9.8 \times 10^{-5}$) in cells cultivated on $^{13}C$ glucose agar. Control experiments applying glass fibers to link patches 1 and 2 instead of mycelia were further performed assuming that abiotic fibers may not actively transfer $^{13}C$ glucose and, hence, would not lead to increased RIA and LR. Likely due to capillary effects, efficient glucose transport to patch 2 was observed leading to clear glucose enrichment (≈24.8 mg) as found in additional abiotic glucose transport experiments (**Figure 5.1C)**. By contrast, no hyphal glucose transfer to bacteria-free patch 2 (< 0.14 mg) was measured (**Figure 5.1C**), hence suggesting that $^{13}C$ enrichment of the proteins in the fungal transfer experiments was due to fungal metabolites. Such assumption is further backed by RIA and LR values of glass fiber experiments, where RIA (86% – 97%) was similar to bacterial cultivation experiments on $^{13}C$ glucose agar. As RIA reflects the extent to which a labeled substrate is used for biomass production (Sachsenberg et al., 2015), high RIA values in glass fiber transfer and $^{13}C$ glucose growth experiment reflect direct assimilation of $^{13}C$ glucose by the bacteria (Taubert et al., 2012). Lower RIA values, however, were observed in presence of mycelia as a likely result of the assimilation of partially labeled fungal metabolites (Sachsenberg et al., 2015; Taubert et al., 2012). The LR in the mycelial transfer experiments were similar or lower than LR in the glass fiber transfer experiments (LR = 0.15 – 0.34; **Figure 5.4**) yet clearly lower than on $^{13}C$ glucose agar (LR = 0.38 – 0.82). Peptide mass spectra patterns also reflected $^{13}C$ protein incorporation (**Figure 5.5**) and allowed for the visual distinction between direct assimilation of the labeled substrate (**Figure 5.5B, C**) or utilization from partially labeled metabolites (**Figure 5.5A**) secreted by other organisms (Sachsenberg et al., 2015). The skewed isotopic incorporation pattern (**Figure 5.5A**) in presence of mycelia, therefore, suggests assimilation of partially labeled substrates (Taubert et al., 2012).

### 5.4.2. HCH biodegradation by *Sphingobium* sp. S8

The effects of mycelial C-substrate transfer on bacterial HCH degradation were further quantified. Lower residual HCH fractions ($F_{res, t10}$; eq. 4) of all HCH isomers were found in fungal-bacterial co-cultures ($F_{res, t10}$ = 19% – 45%) than in bacterial ($F_{res, t10}$ = 50% – 72%) or fungal ($F_{res, t10}$ = 92% – 99%) mono-cultures after 10 days of incubation (appendix 2 **Table S2.4)**. No difference in $F_{res, t10}$ ($p < 0.05$) was observed between the fungal monoculture and abiotic control setups (**Figure 5.6**) suggesting that increased HCH degradation in presence of fungal-bacterial co-cultures was due to increased bacterial activity. To distinguish between abiotic and biotic losses, the HCH fractions lost by microbial activity ($F_{deg, t10}$) were calculated (eq 3) revealing that 71 % ($\alpha$-HCH), 57 %, ($\beta$-HCH), 75% ($\gamma$-HCH), and 81% ($\delta$-HCH) were degraded by fungal-bacterial activity (**Figure 5.7**). For the $\alpha$-, $\beta$-, $\gamma$-, and $\delta$-HCH isomers this results in ca. 1.9-, 1.1-, 1.6- and 1.6-fold better degradation than by a bacterial monoculture (**Figure 5.7,** appendix 2 **Table S2.6**) and reveals significant ($p < 0.05$) influence of C-substrate transfer on the degradation of the $\alpha$-, $\gamma$-, and $\delta$-HCH, yet not of $\beta$-HCH. Batch biodegradation experiments performed in parallel revealed that *Sphingobium* sp. S8 co-metabolically degraded $\beta$-HCH less efficiently (~59% of 34.4 µM $\beta$-HCH in 24 h; cf. **Section 3.4.3**) than the other isomers (~100 % removal; cf. **Section 3.4.3**). The low degradation efficiency of $\beta$-HCH that is independent of additional substrates may hence explain the poor effect of hyphal transfer on the β-HCH biodegradation.

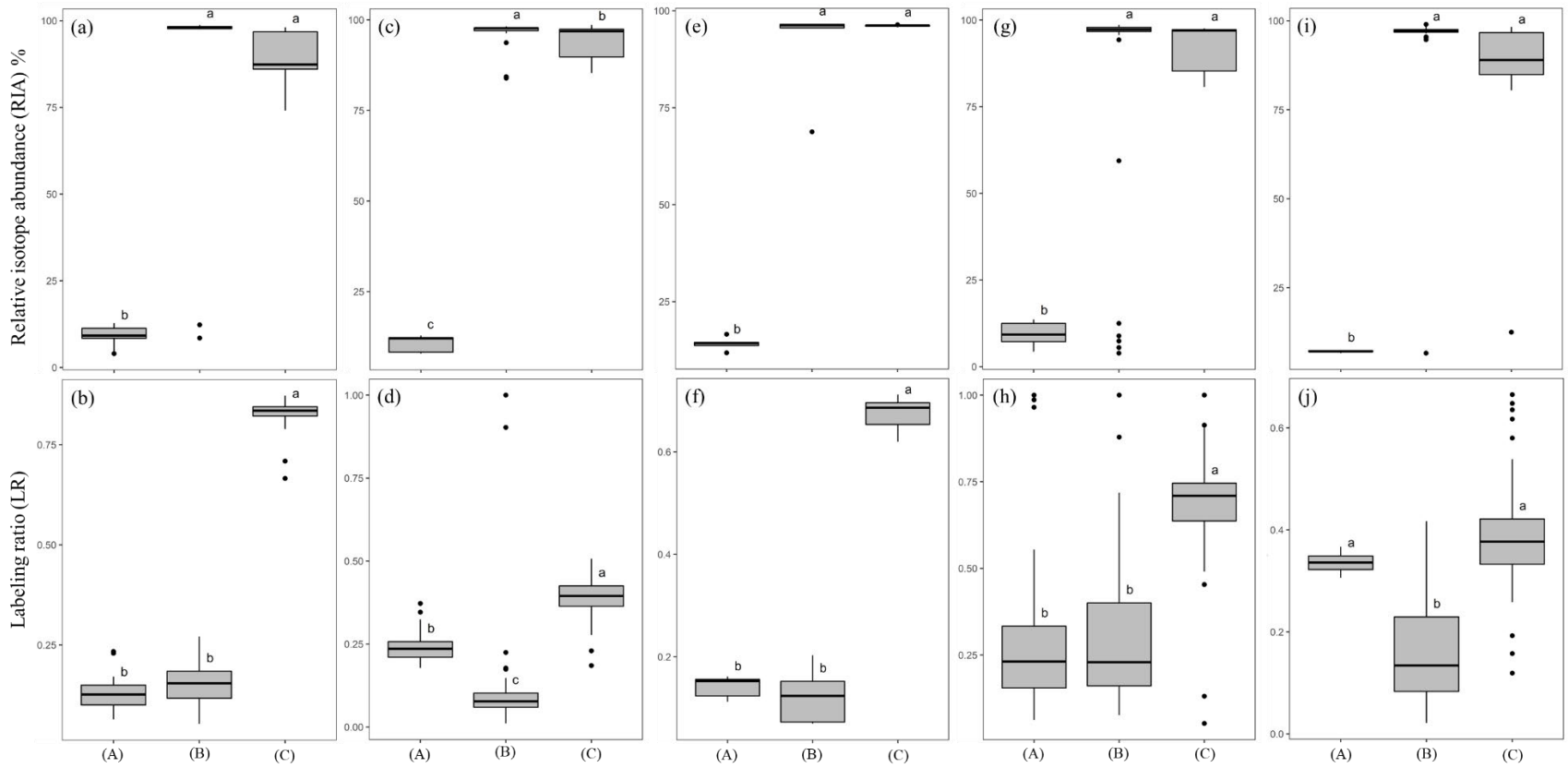


**Figure 5.4:** Relative isotope abundance (RIA, Figs. 2a, c, e, g, i) and labeling ratio (LR, Figs. 2b, d, f, h, j) of housekeeping and key HCH degrading proteins of *Sphingobium* sp. S8 in presence of mycelia (A), glass fiber (B), and bacteria grown on 10% w/v 13C glucose agar (C). Figs. 2 a,b: Chaperone DnaK protein, Figs. 2c&d: ATP synthase β-subunit, Figs. 2e&f: peptidoglycan associated lipoprotein, Figs. 2g & h: haloalkane dehalogenase (LinB), and Figs. 2i & j: dichloro-2,5-cyclohexadiene-1,4-diol dehydrogenase (LinC) respectively. Different lowercase letters indicate statistically significant difference between the treatment groups ($p < 0.05$, $n = 3$).

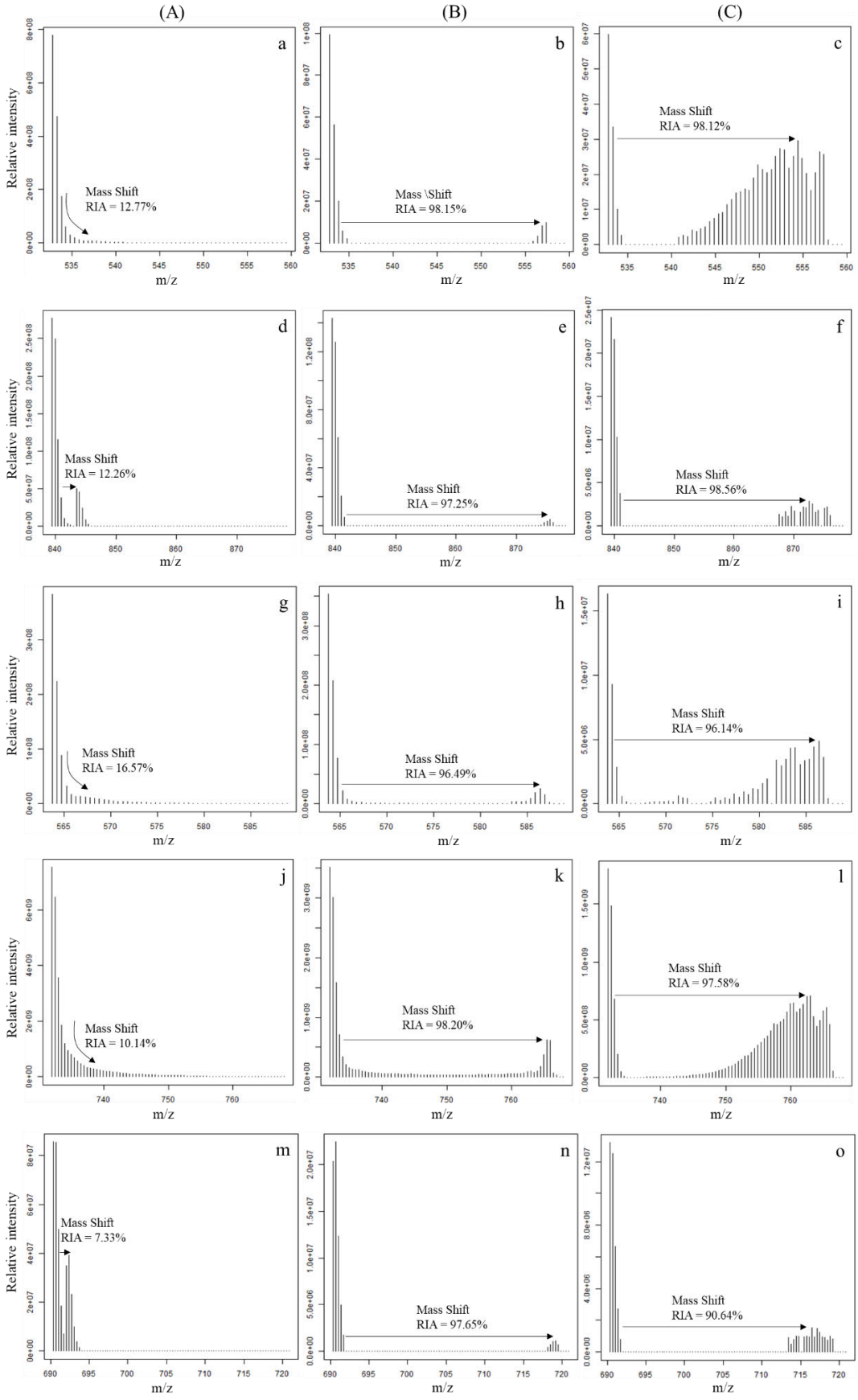
(A)
(B)
(C)
a
b
c
d
e
f
g
h
i
j
k
l
m
n
o
Relative intensity
m/z
Mass Shift
RIA = 12.77%
Mass \Shift
RIA = 98.15%
Mass Shift
RIA = 98.12%
Mass Shift
RIA = 12.26%
Mass Shift
RIA = 97.25%
Mass Shift
RIA = 98.56%
Mass Shift
RIA = 16.57%
Mass Shift
RIA = 96.49%
Mass Shift
RIA = 96.14%
Mass Shift
RIA = 10.14%
Mass Shift
RIA = 98.20%
Mass Shift
RIA = 97.58%
Mass Shift
RIA = 7.33%
Mass Shift
RIA = 97.65%
Mass Shift
RIA = 90.64%

**Figure 5.5:** Representative mass spectra showing ion mass distribution of peptides from selected proteins on setups in presence of mycelia (A), glass fiber (B), and bacteria grown on 10% w/v 13C glucose agar (C) bacteria. Figs. 3a, b, c: peptide sequence TTPSIVAFTK of Chaperone DnaK protein; Figs. 3d, e, f: peptide sequence LVLEVAQHLGENTVR of ATP synthase β subunit; Figs. 3g, h, i: peptide sequence VTIEGHADER of peptidoglycan associated lipoprotein; Figs. 3j, k, l: peptide sequence DYAGWLSESPIPK of haloalkane dehalogenase; Figs. 3m, n, o: peptide sequence RGANVVVADIVEAAAEETVR of 2,5-dichloro-2,5-cyclohexadiene-1,4-diol dehydrogenase.

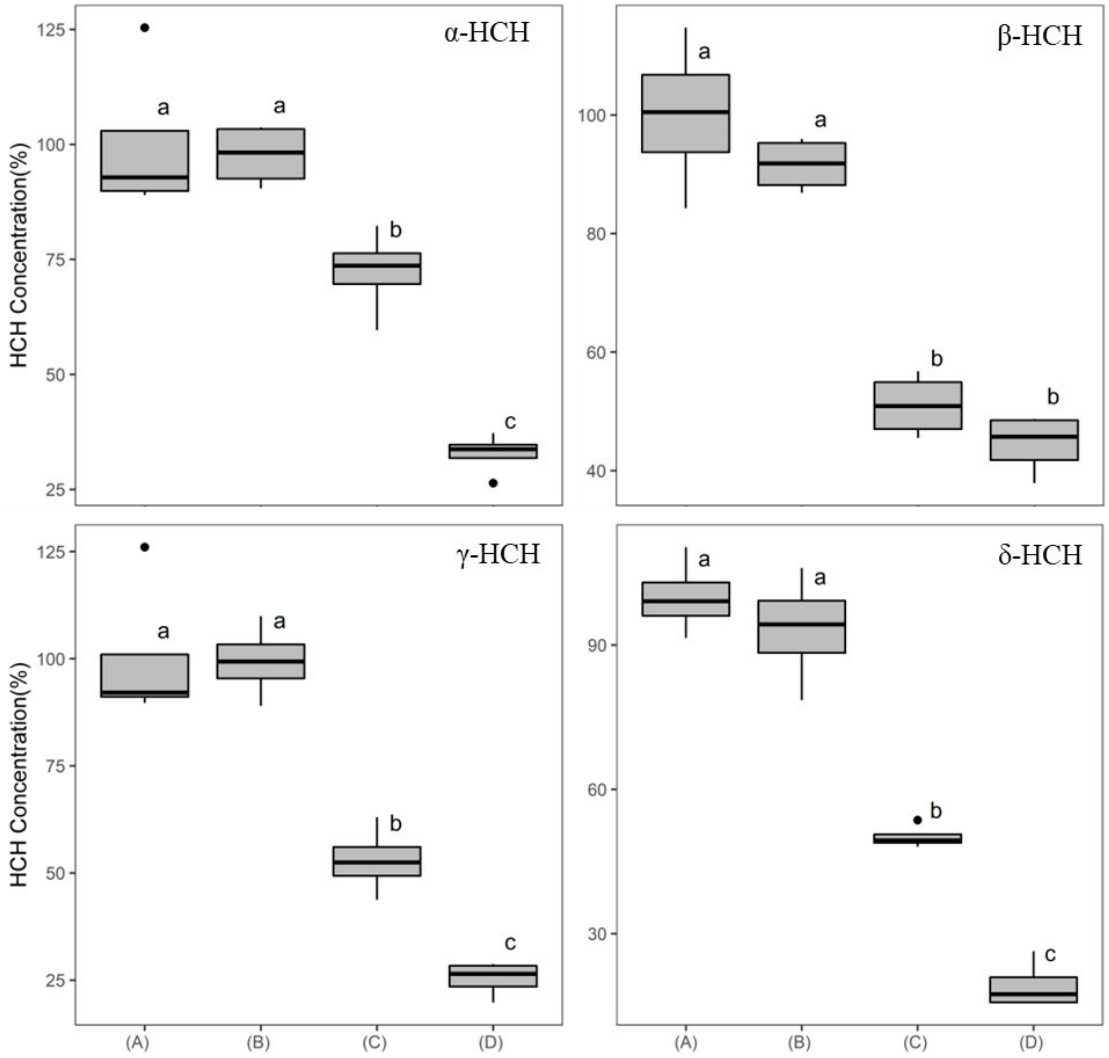


**Figure 5.6:** Residual fractions of HCH isomers after 10 days of incubation (Fres, t10) in an abiotic control (A) and in presence of a fungal mono-culture (B), a bacterial mono-culture (C), and fungal-bacterial co-culture (D). Letters a, b, and c indicate statistical significance ($p < 0.05$, $n = 4$).

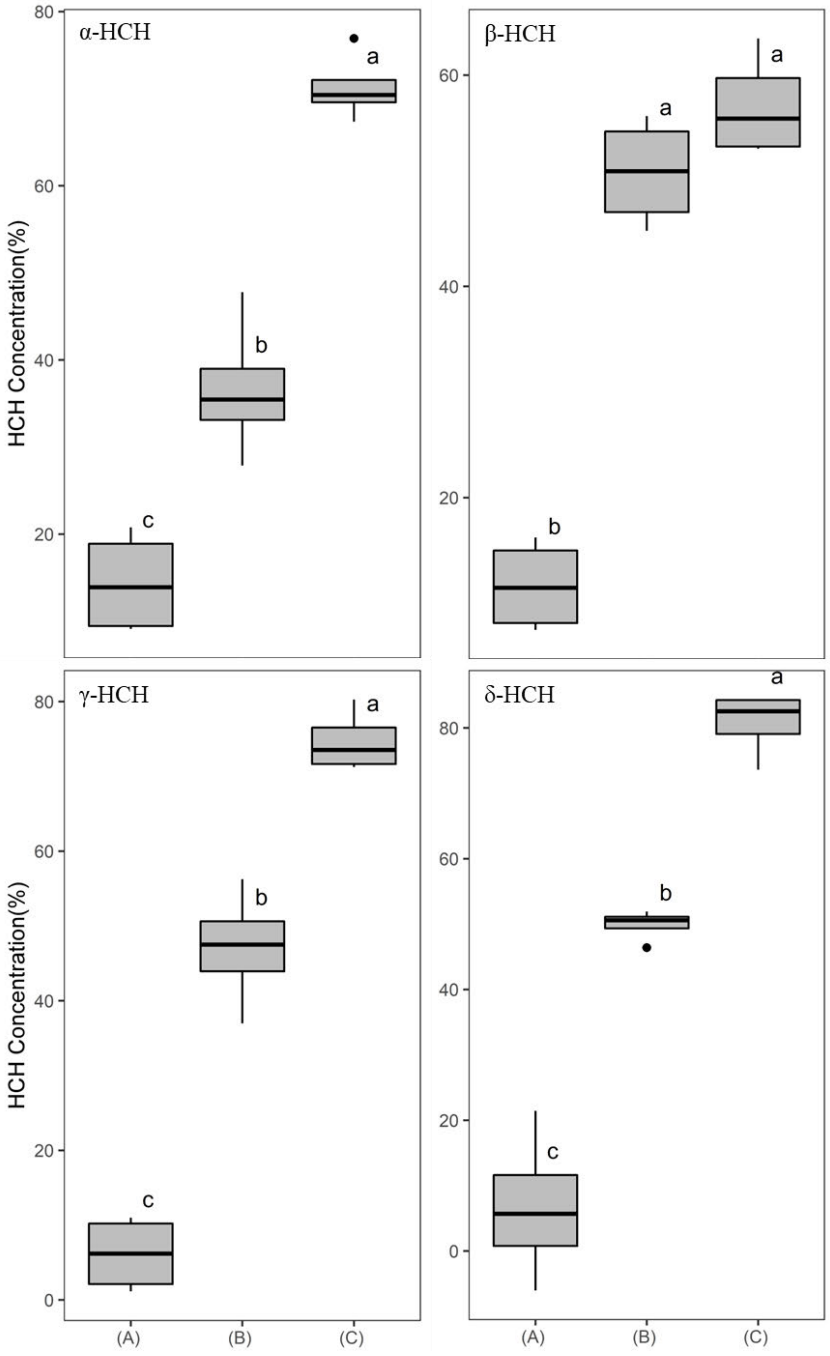


**Figure 5.7:** Fractions of HCH isomers degraded after 10 days of incubation (Fdeg, t10) in presence of a fungal mono-culture (B), a bacterial mono-culture (C), and fungal-bacterial co-culture (D). Different lowercase letters indicate statistically significant difference between the treatment groups ($p < 0.05$, $n = 4$).

## 5.5. Discussion

### 5.5.1. Hyphal transport and bacterial uptake of fungal metabolites

Using $^{13}$C-labelled fungal biomass and protein-SIP, we traced the incorporation of $^{13}$C fungal metabolites into proteins of HCH degrading *Sphingobium* sp. S8. Our findings suggest that mycelial metabolite transfer to nutrient-deficient habitats promoted bacterial growth and co-metabolic HCH in a spatially structured model ecosystem. The $^{13}$C-metabolite transfer was detected by relative isotope abundance, the labeling ratio, and the shape of isotopic mass distribution profiles of the bacterial proteins. Mycelial transport typically exhibited lower RIA than in fungus-free controls that provided $^{13}$C glucose at different bioavailability **(Figure 5.1**), either by glass fiber transfer or upon growth on $^{13}$C glucose agar (**Figures. 5.4 a, c, e, g,** and **i**). The LR upon metabolite transport were similar or even higher (Chaperone DnaK (**Figure. 5.4 d**) and LinB (**Figure 5.4 j**)) than in glass fiber experiments. As the LR reflects the extent of protein turnover and hence bacterial growth (Sachsenberg et al., 2015), suggests efficient activation of the bacterial metabolism and HCH biotransformation by fungal metabolites. $^{13}$C incorporation into key enzymes of co-metabolic HCH degradation (i.e., LinB and LinC) thereby provides a direct link between hyphal metabolite transport and co-metabolic bacterial HCH degradation in fragmented habitats (**Figure 5.7**). This study hence provides for the first time direct molecular evidence for the role of fungal-bacterial interactions for co-metabolic contaminant degradation in an otherwise nutrient-deprived environment. In natural environments fungal-bacterial associations (Espinosa-Ortiz et al., 2021; Worrich et al., 2017) can develop neutral, competitive (antagonistic) or synergistic (Espinosa-Ortiz et al., 2021; Little et al., 2008) relationships. In a synergistic relationship as in our experiment, fungal compounds have been found to stimulate bacterial growth in the hyphosphere (Espinosa-Ortiz et al., 2021; Harms et al., 2011; Morris et al., 2013; Nazir et al., 2010) by providing low molecular weight organic acids (LMWOAs) such as acetic acid and oxalic acid (Van Hees et al., 2006), carbohydrates, polyols, peptides, and amino acids (Sun et al., 1999; Van Hees et al., 2006). Although we didn't characterize the metabolome of fungal strain K3, we speculate that similar metabolites may have led to the observed HCH degradation effects. The observed active mycelial growth and the proximity of *Sphingobium* sp. S8 biofilms to fungal hyphae (**Figure 5.1 B**) suggests that C-substrate assimilation of strain S8 occurred by extracellular biotrophy (Leveau & Preston, 2008) in the hyphosphere of *Fusarium equiseti* K3 as has been reported earlier in other systems (Bassler & Losick, 2006; Kim et al., 2008; Worrich et al., 2017).

Such an assumption is further supported by the fact that *Sphingobium* sp. S8 (Khan et al., 2022) and *Fusarium equiseti* K3 (Khan et al., 2021) had been isolated from the same organochloride pesticide-contaminated soil.

### 5.5.2. Co-metabolic degradation of HCH isomers

In similar setups as used for protein-SIP experiments (**Figure 5.3**), we determined mycelial transport effects on bacterial HCH degradation by quantifying residual concentrations of the *α*-, *β*-, *γ*-, and δ-isomers of HCH. After 10 days of incubation, we did not find HCH removal by *Fusarium equiseti* K3, yet clearly increased bacterial HCH degradation in presence of mycelia (**Figures 5.6 & 5.7**) led to 1.6-1.9-fold faster biodegradation of *α*-, *γ*-, and *δ*-HCH. The least benefit (1.1-fold increase) was observed for *β*-HCH. *β*-HCH is the most recalcitrant of the HCH isomers tested, due to its equatorially substituted chlorine atoms that form a barrier to the enzymatic dehydrochlorination preferring axial chlorine atoms (Lal et al., 2010; Nayyar et al., 2014; Nayyar & Lal, 2016; Willett et al., 1998). *Sphingobium* sp. S8 could not effectively degrade HCH isomers in absence of an additional carbon source (**Figure 5.7**). In the presence of 1% glucose in liquid batch experiments, however, it showed 59-100% removal of all HCH isomers (cf. **Section 3.4.3**) indicating its reliance on additional carbon sources for HCH degradation. Combining protein-SIP with the HCH degradation, our study, therefore, underpins the role of fungal exudates for efficient co-metabolic bacterial HCH degradation as also had been proposed for pesticide degradation in porous media (Ellegaard-Jensen et al., 2014; Knudsen et al., 2013). Co-metabolic degradation is thought to be a critical process for the removal of xenobiotic compounds at both trace and bulk concentrations (Kumar & Pannu, 2018; Nzila, 2013; Saez et al., 2017). Benimeli et al. (2007) for instance, demonstrated simultaneous consumption of glucose and *γ*-HCH by *Streptomyces* sp. M7 with increased *γ*-HCH removal at high glucose concentrations (Benimeli et al., 2007). Similarly, Álvarez et al. (2012) demonstrated increased *γ*-HCH removal by *Streptomyces* strains in the presence of root exudates as an additional carbon source (Álvarez et al., 2012). In addition, HCH degradation in sphingomonads has mostly been conducted in the presence of varying percentages of Luria-Bertani (LB) broth or glucose as additional carbon sources (Boltner et al., 2005; Mohn et al., 2006).

## 5.6. Conclusion

In our study, we observed the commensal incorporation of fungus-derived $^{13}C$ labels into bacterial peptides. The presence of $^{13}C$ labeled bacterial peptides indicated the availability of fungal exudates for bacterial uptake and hence nutrient transfer. The labeled bacterial peptides belonged to both housekeeping enzymes and enzymes relevant to HCH degradation. The labeling of bacterial haloalkane dehalogenase (LinB) and 2,5-dichloro-2,5-cyclohexadiene-1,4-diol dehydrogenase (LinC) involved in HCH degradation indicates the functional relevance of mycelial nutrient transfer to HCH degradation by bacteria. This was indicated by improved HCH degradation ($p<0.05$) in the presence of fungus and bacteria compared to either bacteria (up to 2 times increase) or mycelia (up to 12 times increase) alone for all four HCH isomers. Our data thereby underpin the relevance of the mycosphere as a habitat for the efficient degradation of organic contaminants. Since co-metabolic contaminant degrading microorganisms in the mycosphere may not rely on the contaminants for growth, they also may degrade chemicals at minute concentrations (‘micropollutants’) and down to proposed cleanup endpoints in the parts per trillion range (Hazen, 2010).

# CHAPTER SIX

# 6.0 GENERAL DISCUSSION, CONCLUSION, AND RECOMMENDATIONS

## 6.1. General discussion

The toxicity of HCH isomers to non-target organisms including humans has been demonstrated in several reports (Abolhassani et al., 2019; Jayaraj et al., 2016; Mortazavi et al., 2019; Nolan et al., 2012). Due to their toxicity and persistence in the environment, there is an increased interest to utilize microorganisms in the bioremediation of HCH-contaminated sites (Benimeli et al., 2007; Phillips et al., 2005). However, the utilization of microorganisms for bioremediation requires an understanding of the biochemistry, physiology, molecular aspects, and ecology of the microbial system (Lal et al., 2010; Singh & Kuhad, 1999; Wick, 2020). This thesis, therefore, describes the isolation and characterization of two HCH-degrading *Sphingobium* species and an ascomycete fungus *F. equiseti* from HCH-contaminated soil collected from an obsolete pesticide store in Kitengela, Kenya. Subsequently, laboratory model systems were used to demonstrate the capacity of mycelia as transport networks for HCH isomers and improved HCH degradation facilitated by mycelial nutrients transfer to co-metabolically degrading bacteria. The implications of these findings are discussed in this final chapter and the recommendations for further research are proposed.

### 6.1.1. Bacterial HCH degradation and analysis of lin genes

The two bacterial strains identified as *Sphingobium* strain S6 and *Sphingobium* strain S8 were members of the Sphingomodaceae family and were closely related to *S. quisquiliarum* P25, a known HCH-degrading bacteria that was previously isolated from HCH dump site in India (Bala et al., 2010). Both isolates could degrade all four HCH isomers and also harbored *lin* genes highly similar to those described previously (Boltner et al., 2005; Lal et al., 2010; Nagata et al., 2007; Nayyar et al., 2014). The growing number of phylogenetically distinct HCH degrading sphingomonads isolated from polluted sites from diverse geographical locations demonstrates their remarkable adaptability for degradation of the contaminant (Boltner et al., 2005). The adaptation of Sphingomodaceae to the degradation of HCH and other recalcitrant compounds is not known, however, their unusual outer membrane composition has been proposed as one of the contributing factors (Boltner et al., 2005; White et al., 1996). Their outer membrane is thought to contain

glycosphingolipids in place of lipopolysaccharides (LPLs) which provides a highly hydrophobic surface that would facilitate the assimilation of hydrophobic compounds like HCH (Boltner et al., 2005; Kawahara et al., 1999; White et al., 1996).

Horizontal gene transfer of HCH catabolic genes (*lin* genes) facilitated by transposable elements is thought to be the other factor contributing to the adaptation of sphingomonads to HCH degradation (Boltner et al., 2005). The identification of highly conserved *lin* genes in different sphingomonads as in the present study is thought to imply the distribution of lin genes by frequent horizontal gene transfer (Boltner et al., 2005). The availability of a genome inventory for these organisms has enabled a comparative analysis of their genome architecture that would facilitate a deeper understanding of their biochemistry, physiology, and genetics (Nayyar & Lal, 2016). The isolation of the two *Sphingobium* species in this study coupled with the determination of their genome sequences would therefore add to the diversity of HCH degraders and that of *lin* genes which would aid in unraveling the molecular mechanism of degradation and bioremediation of the recalcitrant HCH.

### 6.1.2. Impact of mycelial mediated transport of HCH

The fungus identified as *F. equiseti* strain K3 is a non-white rot (non-WRF) fungus belonging to the division Ascomycota. The fungus could partially degrade HCH isomers conceivably by dechlorination and hydroxylation reaction. The synthetic lab microcosms revealed that the fungus could preferentially translocate HCH isomers in porous media in the order $\beta \approx \delta < \alpha < \gamma$. Most research relating to the degradation of organochlorine pesticides has been focused on white rot fungi (WRF) because of their efficient enzyme system (Rigas et al., 2009; Shah et al., 1992; B. K. Singh & Kuhad, 1999, 2000). However, WRF are slow growing and need an oxygen-rich environment for their growth (Nagpal et al., 2008; Sagar & Singh, 2011). Therefore, to overcome the challenges associated with WRF, there is a growing interest in the search for non-WRF with HCH degradation capacity (Nagpal et al., 2008; Sagar & Singh, 2011).

The degradation rates of organic contaminants are mostly dependent on their physicochemical properties and their accessibility to degrading organisms(Semple et al., 2003; Wick, 2020). However, organic contaminants tend to adsorb onto the mineral or soil organic matter by physical and/or chemical means once they enter the soil. The strong sorption of HCH onto soil particles may reduce its bioavailability and therefore influences its bioremediation efficiency (Chen et al.,

2015). The microcosm model used in the present study demonstrates that active mycelia could act as a continuous for the translocation of the insoluble chemical over air-filled gaps. This property could have an impact on the bioavailability of HCH, particularly in water unsaturated environments lacking continuous water paths. Fungi are therefore better suited for bioremediation because they possess efficient extracellular enzyme systems for the degradation of organic contaminants (Nagpal et al., 2008; Sagar & Singh, 2011). In addition, their mycelial structures provide deeper penetration and a large surface area for absorption that can enhance the bioavailability of poorly soluble organic contaminants (Nagpal et al., 2008; Sagar & Singh, 2011).

### 6.1.3. Impact of mycelial C-substrate transfer to HCH degrading Bacteria

The synthetic microcosm system used in this study coupled with protein-SIP analysis demonstrated the incorporation of fungus-derived $^{13}C$-labelled substrates into bacterial proteins. The labeling of HCH catabolic enzymes (Lin B and Lin C) indicated the functional relevance of mycelial nutrient transfer to bacterial degradation of HCH. This was further demonstrated by the observed improved HCH degradation in presence of fungal-bacterial co-cultures. Previous reports have demonstrated improved degradation of certain contaminants using a combined fungal-bacterial co-culture treatment compared to either, alone (Espinosa-Ortiz et al., 2021; Knudsen et al., 2013; Xu et al., 2007). The enhanced pollutant degradation is thought to result from increased enzyme production by one or both partners or secretion of secondary metabolites that promotes pollutant degradation by either of the partners (Espinosa-Ortiz et al., 2021). There is, however, increasing data that demonstrate the capacity of fungal mycelia to provide favorable microhabitats for bacteria through the exudation of carbonaceous compounds (Nazir et al., 2010; Worrich et al., 2017; L. Zhang et al., 2016). This resource transfer has been shown to increase bacterial activity in harsh contaminated environments and is considered to be an effective strategy for microbial survival in hostile environments while simultaneously promoting contaminant degradation (Espinosa-Ortiz et al., 2021; Worrich et al., 2017, 2018). The utilization of fungal-bacterial systems for bioremediation could therefore lead to synergistic associations that would facilitate more efficient removal of organic contaminants such as HCH (Espinosa-Ortiz et al., 2021).

## 6.2. Conclusions

i. The isolation of the two HCH-degrading *Sphingobium* species described in chapter 3 further underpins the important role of Sphingomodaceae family in the degradation of HCH. In addition, the identification of highly conserved *lin* genes implies that they utilize a similar HCH catabolic pathway previously described in other sphingomonads. The characterization of the two bacteria coupled with the availability of their genome sequences would add valuable information on the diversity of HCH degraders and that of *lin* genes that would provide insights into the molecular mechanism of HCH degrading enzymes.

ii. The isolated *Fusarium* species described in chapter 4 partially degraded all four HCH isomers and the metabolites identified suggest that the degradation process proceed by dechlorination and hydroxylation. The mycelial structures of the fungus were also demonstrated to translocate HCH isomers and the translocation process was influenced by the physicochemical properties of the individual isomers.

iii. The presence of $^{13}$C-labeled bacterial peptides observed in chapter 5 indicated the incorporation of fungus-derived $^{13}$C-labelled substrates into bacterial proteins. In addition, the labeling of bacterial enzymes (LinB and LinC) involved in HCH degradation indicated the functional relevance of mycelial nutrient transfer to HCH degradation by bacteria. This was further indicated by the significant improved HCH degradation in presence of fungus and bacteria as compared to either bacteria or mycelia alone. These results, therefore, imply that mycosphere processes could play an important role in the development of biotechnological approaches for improved bioremediation of HCH.

## 6.3. Recommendations

i. The lin genes identified in the two *Sphingobium* species were highly conserved, however, LinB revealed a unique mutation at position 138. Therefore, additional studies on the degradation efficiency of this enzyme and the binding mechanism to its respective substrate through molecular cloning, protein expression, protein assays, protein modeling, and molecular docking are necessary.

ii. Due to the failure in the identification of other degradation metabolites from the fungal culture, further research would be necessary to fully understand its degradation mechanism.

In addition, despite the observed HCH translocation along the mycelial structure, further research would be necessary to establish the effect of degradation on the transport process.

iii. Finally, the observed improved bacterial activity and HCH degradation resulting from mycelial nutrient transfer need additional research to identify the specific fungal exudates that would support bacterial growth in the hyphosphere. Fungal-bacterial co-cultures can potentially be used to improve the bioremediation of HCH contaminated sites in Kenya through bioaugmentation. However, further research in actual soil environment is needed to establish potential bottlenecks and how to circumvent them.

## REFERENCES


Abhilash, P. C., Jamil, S., Singh, V., Singh, A., Singh, N., & Srivastava, S. C. (2008). Occurrence and distribution of hexachlorocyclohexane isomers in vegetation samples from a contaminated area. *Chemosphere*, *72*(1), 79–86. https://doi.org/10.1016/j.chemosphere.2008.01.056

Abolhassani, M., Asadikaram, G., Paydar, P., Fallah, H., Aghaee-Afshar, M., Moazed, V., Akbari, H., Moghaddam, S. D., & Moradi, A. (2019). Organochlorine and organophosphorous pesticides may induce colorectal cancer; A case-control study. *Ecotoxicology and Environmental Safety*, *178*, 168–177. https://doi.org/10.1016/j.ecoenv.2019.04.030

Aislabie, J., & Lloyd-Jones, G. (1995). A review of bacterial-degradation of pesticides. *Soil Research*, *33*(6), 925–942. https://doi.org/10.1071/sr9950925

Altschul, S. F., Gish, W., Miller, W., Myers, E. W., & Lipman, D. J. (1990). Basic local alignment search tool. *Journal of Molecular Biology*, *215*(3), 403–410. https://doi.org/10.1016/S0022-2836(05)80360-2

Alvarez, A., Benimeli, C., Saez, J., Fuentes, M., Cuozzo, S., Polti, M., & Amoroso, M. (2012). Bacterial bio-resources for remediation of hexachlorocyclohexane. *International Journal of Molecular Sciences*, *13*(12), 15086–15106. https://doi.org/10.3390/ijms131115086

Álvarez, A., Yañez, M. L., Benimeli, C. S., & Amoroso, M. J. (2012). Maize plants (Zea mays) root exudates enhance lindane removal by native Streptomyces strains. *International Biodeterioration & Biodegradation*, *66*(1), 14–18. https://doi.org/10.1016/j.ibiod.2011.10.001

Anand, S., Sangwan, N., Lata, P., Kaur, J., Dua, A., Singh, A. K., Verma, M., Kaur, J., Khurana, J. P., Khurana, P., Mathur, S., & Lal, R. (2012). Genome Sequence of *Sphingobium indicum* B90A, a hexachlorocyclohexane-degrading bacterium. *Journal of Bacteriology*, *194*(16), 4471–4472. https://doi.org/10.1128/JB.00901-12

ATSDR. (2002). ATSDR's Toxicological Profiles. *Web Version*. CRC Press. https://doi.org/10.1201/9781420061888

Aucha, J., Wandiga, S., Abong'o, D., Madadi, V., & Osoro, E. (2017). Organochlorine pesticides residue levels in air and soil from Nairobi and Mount Kenya regions, Kenya. *IOSR Journal of Applied Chemistry*, *10*, 05–11. https://doi.org/10.9790/5736-1007020511

Awasthi, N., Ahuja, R., & Kumar, A. (2000). Factors influencing the degradation of soil-applied endosulfan isomers. *Soil Biology and Biochemistry*, *32*(11), 1697–1705. https://doi.org/10.1016/S0038-0717(00)00087-0

Bacci, E., Cerejeira, MariaJ., Gaggi, C., Chemello, G., Calamari, D., & Vighi, M. (1992). Chlorinated dioxins: Volatilization from soils and bioconcentration in plant leaves. *Bulletin of Environmental Contamination and Toxicology*, *48*(3). https://doi.org/10.1007/BF00195639

Bago, B., Pfeffer, P. E., Zipfel, W., Lammers, P., & Shachar-Hill, Y. (2002). Tracking metabolism and imaging transport in arbuscular mycorrhizal fungi. Metabolism and transport in AM fungi. *Plant and Soil*, *244*(1), 189–197. https://doi.org/10.1023/A:1020212328955

Bala, K., Sharma, P., & Lal, R. (2010). *Sphingobium quisquiliarum* sp. Nov., a hexachlorocyclohexane (HCH)-degrading bacterium isolated from an HCH-contaminated soil. *International Journal of Systematic and Evolutionary Microbiology*, *60*(2), 429–433. https://doi.org/10.1099/ijs.0.010868-0

Bankevich, A., Nurk, S., Antipov, D., Gurevich, A. A., Dvorkin, M., Kulikov, A. S., Lesin, V. M., Nikolenko, S. I., Pham, S., Prjibelski, A. D., Pyshkin, A. V., Sirotkin, A. V., Vyahhi, N., Tesler, G., Alekseyev, M. A., & Pevzner, P. A. (2012). SPAdes: A new genome sssembly algorithm and its applications to single-cell sequencing. *Journal of Computational Biology*, *19*(5), 455–477. https://doi.org/10.1089/cmb.2012.0021

Bartnicki-Garcia, S., Hergert, F., & Gierz, G. (1989). Computer simulation of fungal morphogenesis and the mathematical basis for hyphal (tip) growth. *Protoplasma*, *153*(1), 46–57. https://doi.org/10.1007/BF01322464

Bassler, B. L., & Losick, R. (2006). Bacterially speaking. *Cell*, *125*(2), 237–246. https://doi.org/10.1016/j.cell.2006.04.001

Bebber, D. P., Hynes, J., Darrah, P. R., Boddy, L., & Fricker, M. D. (2007). Biological solutions to transport network design. *Proceedings of the Royal Society B: Biological Sciences*, *274*(1623), 2307–2315. https://doi.org/10.1098/rspb.2007.0459

Beland, F. A., Farwell, S. O., Robocker, A. E., & Geer, R. D. (1976). Electrochemical reduction and anaerobic degradation of lindane. *Journal of Agricultural and Food Chemistry*, *24*(4), 753–756. https://doi.org/10.1021/jf60206a019

Benimeli, C. S., González, A. J., Chaile, A. P., & Amoroso, M. J. (2007). Temperature and pH effect on lindane removal by Streptomyces sp. M7 in soil extract. *Journal of Basic Microbiology*, *47*(6), 468–473. https://doi.org/10.1002/jobm.200700242

Bidlan, R., Afsar, M., & Manonmani, H. K. (2004). Bioremediation of HCH-contaminated soil: Elimination of inhibitory effects of the insecticide on radish and green gram seed germination. *Chemosphere*, *56*(8), 803–811. https://doi.org/10.1016/j.chemosphere.2004.01.015

Blin, K., Shaw, S., Steinke, K., Villebro, R., Ziemert, N., Lee, S. Y., Medema, M. H., & Weber, T. (2019). antiSMASH 5.0: Updates to the secondary metabolite genome mining pipeline. *Nucleic Acids Research*, *47*(W1), W81–W87. https://doi.org/10.1093/nar/gkz310

Bochner, B. R. (1989). Sleuthing out bacterial identities. *Nature*, *339*(6220), 157–158. https://doi.org/10.1038/339157a0

Boer, W. de, Folman, L. B., Summerbell, R. C., & Boddy, L. (2005). Living in a fungal world: Impact of fungi on soil bacterial niche development. *FEMS Microbiology Reviews*, *29*(4), 795–811. https://doi.org/10.1016/j.femsre.2004.11.005

Boltner, D., Moreno-Morillas, S., & Ramos, J.-L. (2005). 16S rDNA phylogeny and distribution of lin genes in novel hexachlorocyclohexane-degrading *Sphingomonas* strains. *Environmental Microbiology*, *7*(9), 1329–1338. https://doi.org/10.1111/j.1462-5822.2005.00820.x

Bonsch, B., Belt, V., Bartel, C., Duensing, N., Koziol, M., Lazarus, C. M., Bailey, A. M., Simpson, T. J., & Cox, R. J. (2016). Identification of genes encoding squalestatin S1 biosynthesis

and in vitro production of new squalestatin analogues. *Chemical Communications*, *52*(41), 6777–6780. https://doi.org/10.1039/C6CC02130A

Boschker, H. T. S., Nold, S. C., Wellsbury, P., Bos, D., de Graaf, W., Pel, R., Parkes, R. J., & Cappenberg, T. E. (1998). Direct linking of microbial populations to specific biogeochemical processes by $^{13}$C-labelling of biomarkers. *Nature*, *392*(6678), Article 6678. https://doi.org/10.1038/33900

Boswell, G. P., Jacobs, H., Davidson, F. A., Gadd, G. M., & Ritz, K. (2002). Functional consequences of nutrient translocation in mycelial fungi. *Journal of Theoretical Biology*, *217*(4), 459–477. https://doi.org/10.1006/jtbi.2002.3048

Boyle, A. W., Häggblom, M. M., & Young, L. Y. (1999). Dehalogenation of lindane (γ-hexachlorocyclohexane) by anaerobic bacteria from marine sediments and by sulfate-reducing bacteria. *FEMS Microbiology Ecology*, *29*(4), 379–387. https://doi.org/10.1111/j.1574-6941.1999.tb00628.x

Bravo, D., Cailleau, G., Bindschedler, S., Simon, A., Job, D., Verrecchia, E., & Junier, P. (2013). Isolation of oxalotrophic bacteria able to disperse on fungal mycelium. *FEMS Microbiology Letters*, *348*(2), 157–166. https://doi.org/10.1111/1574-6968.12287

Brettin, T., Davis, J. J., Disz, T., Edwards, R. A., Gerdes, S., Olsen, G. J., Olson, R., Overbeek, R., Parrello, B., Pusch, G. D., Shukla, M., Thomason, J. A., Stevens, R., Vonstein, V., Wattam, A. R., & Xia, F. (2015). RASTtk: A modular and extensible implementation of the RAST algorithm for building custom annotation pipelines and annotating batches of genomes. *Scientific Reports*, *5*(1), 8365. https://doi.org/10.1038/srep08365

Brock, N. L., Huss, K., Tudzynski, B., & Dickschat, J. S. (2013). Genetic dissection of Sesquiterpene biosynthesis by *Fusarium fujikuroi*. *ChemBioChem*, *14*(3), 311–315. https://doi.org/10.1002/cbic.201200695

Bumpus, J. A., Tien, M., Wright, D., & work(s):, S. D. A. R. (1985). Oxidation of persistent environmental pollutants by a white rot fungus. *Science, New Series*, *228*(4706), 1434–1436.

Calvelo Pereira, R., Monterroso, C., Macías, F., & Camps-Arbestain, M. (2008). Distribution pathways of hexachlorocyclohexane isomers in a soil-plant-air system. A case study with Cynara scolymus L. and Erica sp. Plants grown in a contaminated site. *Environmental Pollution*, *155*(2), 350–358. https://doi.org/10.1016/j.envpol.2007.11.009

Camacho-Pérez, B., Ríos-Leal, E., Rinderknecht-Seijas, N., & Poggi-Varaldo, H. M. (2012). Enzymes involved in the biodegradation of hexachlorocyclohexane: A mini review. *Journal of Environmental Management*, *95 Suppl*, S306-318. https://doi.org/10.1016/j.jenvman.2011.06.047

Cantarel, B., Korf, I., Robb, S., Parra, G., Ross, E., Moore, B., Holt, C., Sánchez Alvarado, A., & Yandell, M. (2008). MAKER: An easy-to-use annotation pipeline designed for emerging model organism genomes. *Genome Research*, *18*, 188–196. https://doi.org/10.1101/gr.6743907

Cao, L., Xu, J., Li, M., Wu, G., Wang, J., Guan, Y., He, J., Li, S., & Hong, Q. (2013). Characterization and analysis of three newly isolated hexachlorocyclohexane (HCH)-degrading strains. *International Biodeterioration & Biodegradation*. http://dx.doi.org/10.1016/j.ibiod.2013.08.023

Cérémonie, H., Boubakri, H., Mavingui, P., Simonet, P., & Vogel, T. M. (2006). Plasmid-encoded γ-hexachlorocyclohexane degradation genes and insertion sequences in *Sphingobium francense* (ex-*Sphingomonas paucimobilis* Sp+). *FEMS Microbiology Letters*, *257*(2), 243–252. https://doi.org/10.1111/j.1574-6968.2006.00188.x

Chen, H., Gao, B., Wang, S., & Fang, J. (2015). Microbial Degradation of Hexachlorocyclohexane (HCH) Pesticides. In *Advances in Biodegradation and Bioremediation of Industrial Waste*. CRC Press.

Chen, X., Wei, S., Ji, Y., Guo, X., & Yang, F. (2015). Quantitative proteomics using SILAC: Principles, applications, and developments. *Proteomics*, *15*(18), 3175–3192. https://doi.org/10.1002/pmic.201500108

Clarridge, J. E. (2004). Impact of 16S rRNA gene sequence analysis for identification of bacteria on clinical microbiology and infectious diseases. *Clinical Microbiology Reviews*, *17*(4), 840–862. https://doi.org/10.1128/CMR.17.4.840-862.2004

Concha-Graña, E., Turnes-Carou, M. I., Muniategui-Lorenzo, S., López-Mahía, P., Prada-Rodríguez, D., & Fernández-Fernández, E. (2006). Evaluation of HCH isomers and metabolites in soils, leachates, river water and sediments of a highly contaminated area. *Chemosphere*, *64*(4), 588–595. https://doi.org/10.1016/j.chemosphere.2005.11.011

Cutright, T., & Erdem, Z. (2012). Overview of the Bioremediation and the Degradation Pathways of DDT. *Undefined*. https://www.semanticscholar.org/paper/Overview-of-the-Bioremediation-and-the-Degradation-Cutright-Erdem/49ce85fb2c39f256a4c1db965eb61999013b1ffa

Darrah, P. R., Tlalka, M., Ashford, A., Watkinson, S. C., & Fricker, M. D. (2006). The Vacuole System is a significant intracellular pathway for longitudinal solute transport in Basidiomycete fungi. *Eukaryotic Cell*, *5*(7), 1111–1125. https://doi.org/10.1128/EC.00026-06

Delcour, I., Spanoghe, P., & Uyttendaele, M. (2015). Literature review: Impact of climate change on pesticide use. *Food Research International*, *68*, 7–15. https://doi.org/10.1016/j.foodres.2014.09.030

Deveau, A., Bonito, G., Uehling, J., Paoletti, M., Becker, M., Bindschedler, S., Hacquard, S., Hervé, V., Labbé, J., Lastovetsky, O. A., Mieszkin, S., Millet, L. J., Vajna, B., Junier, P., Bonfante, P., Krom, B. P., Olsson, S., van Elsas, J. D., & Wick, L. Y. (2018). Bacterial–fungal interactions: Ecology, mechanisms and challenges. *FEMS Microbiology Reviews*, *42*(3), 335–352. https://doi.org/10.1093/femsre/fuy008

Dogra, C., Raina, V., Pal, R., Suar, M., Lal, S., Gartemann, K.-H., Holliger, C., Meer, J. R. van der, & Lal, R. (2004). Organization of lin genes and IS6100 among different strains of hexachlorocyclohexane-degrading *Sphingomonas paucimobilis*: Evidence for Horizontal Gene Transfer. *Journal of Bacteriology*, *186*(8), 2225–2235. https://doi.org/10.1128/JB.186.8.2225-2235.2004

Dorsey, A. (2005). Toxicological profile for alpha-, beta-, gamma-, and delta-hexachlorocyclohexane. https://www.atsdr.cdc.gov/toxprofiles/tp43.pdf

Dubus, I. G., Hollis, J. M., & Brown, C. D. (2000). Pesticides in rainfall in Europe. *Environmental Pollution*, *110*(2), 331–344. https://doi.org/10.1016/S0269-7491(99)00295-X

Edgar, R. C. (2004). MUSCLE: Multiple sequence alignment with high accuracy and high throughput. *Nucleic Acids Research*, *32*(5), 1792–1797. https://doi.org/10.1093/nar/gkh340

Elcey, C. D., & Kunhi, A. A. M. (2010). Substantially enhanced degradation of hexachlorocyclohexane isomers by a microbial consortium on acclimation. *Journal of Agricultural and Food Chemistry*, *58*(2), 1046–1054. https://doi.org/10.1021/jf9038259

Elfvendahl, S., Mihale, M., Kishimba, M. A., & Kylin, H. (2004). Pesticide pollution remains severe after cleanup of a stockpile of obsolete pesticides at Vikuge, Tanzania. *Ambio*, *33*(8), 503–508. https://doi.org/10.1579/0044-7447-33.8.503

Ellegaard-Jensen, L., Knudsen, B. E., Johansen, A., Albers, C. N., Aamand, J., & Rosendahl, S. (2014). Fungal-bacterial consortia increase diuron degradation in water-unsaturated systems. *The Science of the Total Environment*, *466–467*, 699–705. https://doi.org/10.1016/j.scitotenv.2013.07.095

Endo, R., Kamakura, M., Miyauchi, K., Fukuda, M., Ohtsubo, Y., Tsuda, M., & Nagata, Y. (2005). Identification and characterization of genes involved in the downstream degradation pathway of gamma-hexachlorocyclohexane in *Sphingomonas paucimobilis* UT26. *Journal of Bacteriology*, *187*(3), 847–853. https://doi.org/10.1128/JB.187.3.847-853.2005

Espinosa-Ortiz, E. J., Rene, E. R., & Gerlach, R. (2021). Potential use of fungal-bacterial co-cultures for the removal of organic pollutants. *Critical Reviews in Biotechnology*, *0*(0), 1–23. https://doi.org/10.1080/07388551.2021.1940831

Finlay, R. D. (2008). Ecological aspects of mycorrhizal symbiosis: With special emphasis on the functional diversity of interactions involving the extraradical mycelium. *Journal of Experimental Botany*, *59*(5), 1115–1126. https://doi.org/10.1093/jxb/ern059

Francis, A. J., Spanggord, R. J., & Ouchi, G. I. (1975). Degradation of lindane by *Escherichia coli*. *Applied Microbiology*, *29*(4), 567–568.

Frey-Klett, P., Garbaye, J., & Tarkka, M. (2007). The mycorrhiza helper bacteria revisited. *New Phytologist*, *176*(1), 22–36. https://doi.org/10.1111/j.1469-8137.2007.02191.x

Fuentes, M. S., Benimeli, C. S., Cuozzo, S. A., & Amoroso, M. J. (2010). Isolation of pesticide-degrading actinomycetes from a contaminated site: Bacterial growth, removal and dechlorination of organochlorine pesticides. *International Biodeterioration & Biodegradation*, *64*(6), 434–441. https://doi.org/10.1016/j.ibiod.2010.05.001

Fuentes, M. S., Benimeli, C. S., Cuozzo, S. A., Sáez, J. M., & Amoroso, M. J. del R. (2010). Microorganisms capable to degrade organochlorine pesticides. In *Current Research, Technology and Education Topics in Applied Microbiology and Microbial Biotechnology*. Formatex Research Centre. https://ri.conicet.gov.ar/handle/11336/111569

Furuno, S., Foss, S., Wild, E., Jones, K. C., Semple, K. T., Harms, H., & Wick, L. Y. (2012). Mycelia promote active transport and spatial dispersion of polycyclic aromatic hydrocarbons. *Environmental Science & Technology*, *46*(10), 5463–5470. https://doi.org/10.1021/es300810b

Furuno, S., Päzolt, K., Rabe, C., Neu, T. R., Harms, H., & Wick, L. Y. (2010). Fungal mycelia allow chemotactic dispersal of polycyclic aromatic hydrocarbon-degrading bacteria in water-unsaturated systems. *Environmental Microbiology*, *12*(6), 1391–1398. https://doi.org/10.1111/j.1462-2920.2009.02022.x

García-Rivero, M., & Peralta-Pérez, M. R. (2008). Cometabolism the biodegradation of hydrocarbons. *Revista Mexicana de Ingeniería Química*, *7*(1), 1–12.

Girish, K., & Kunhi, A. A. M. (2013). Microbial degradation of gamma-hexachlorocyclohexane (lindane). *African Journal of Microbiology Research*, *7*(17), 1635–1643. https://doi.org/10.5897/AJMRx12.001

Glass, N. L., Rasmussen, C., Roca, M. G., & Read, N. D. (2004). Hyphal homing, fusion and mycelial interconnectedness. *Trends in Microbiology*, *12*(3), 135–141. https://doi.org/10.1016/j.tim.2004.01.007

Golfinopoulos, S. K., Nikolaou, A. D., Kostopoulou, M. N., Xilourgidis, N. K., Vagi, M. C., & Lekkas, D. T. (2003). Organochlorine pesticides in the surface waters of Northern Greece. *Chemosphere*, *50*(4), 507–516. https://doi.org/10.1016/S0045-6535(02)00480-0

Goris, J., Konstantinidis, K. T., Klappenbach, J. A., Coenye, T., Vandamme, P., & Tiedje, J. M. (2007). DNA-DNA hybridization values and their relationship to whole-genome sequence similarities. *International Journal of Systematic and Evolutionary Microbiology*, *57*(Pt 1), 81–91. https://doi.org/10.1099/ijs.0.64483-0

Guillén-Jiménez, F. de M., Cristiani-Urbina, E., Cancino-Díaz, J. C., Flores-Moreno, J. L., & Barragán-Huerta, B. E. (2012). Lindane biodegradation by the *Fusarium verticillioides* AT-100 strain, isolated from Agave tequilana leaves: Kinetic study and identification of metabolites. *International Biodeterioration and Biodegradation*, 36–47. https://doi.org/10.1016/j.ibiod.2012.04.020

Gupta, A., Kaushik, C. P., & Kaushik, A. (2000). Degradation of hexachlorocyclohexane (HCH; α, β, γ and δ) by *Bacillus circulans* and *Bacillus brevis* isolated from soil contaminated with HCH. *Soil Biology and Biochemistry*, *32*(11–12), 1803–1805. https://doi.org/10.1016/S0038-0717(00)00072-9

Gurevich, A., Saveliev, V., Vyahhi, N., & Tesler, G. (2013). QUAST: Quality assessment tool for genome assemblies. *Bioinformatics*, *29*(8), 1072–1075. https://doi.org/10.1093/bioinformatics/btt086

Haider, K. (1979). Degradation and metabolization of lindane and other hexachlorocyclohexane isomers by anaerobic and aerobic soil microorganisms. *Zeitschrift Für Naturforschung C*, *34*(11), 1066–1069. https://doi.org/10.1515/znc-1979-1138

Haq, I. U., Zhang, M., Yang, P., & van Elsas, J. D. (2014). The interactions of bacteria with fungi in soil. In *Advances in Applied Microbiology* (Vol. 89, pp. 185–215). Elsevier. https://doi.org/10.1016/B978-0-12-800259-9.00005-6

Harms, H., Schlosser, D., & Wick, L. Y. (2011). Untapped potential: Exploiting fungi in bioremediation of hazardous chemicals. *Nature Reviews Microbiology*, *9*(3), 177–192. https://doi.org/10.1038/nrmicro2519

Hatakka, A. (1994). Lignin-modifying enzymes from selected white-rot fungi: Production and role from in lignin degradation. *FEMS Microbiology Reviews*, *13*(2), 125–135.

Hazen, T. C. (2010). Cometabolic bioremediation. In K. N. Timmis (Ed.), *Handbook of Hydrocarbon and Lipid Microbiology* (pp. 2505–2514). Springer. https://doi.org/10.1007/978-3-540-77587-4_185

Heaton, L. L. M., López, E., Maini, P. K., Fricker, M. D., & Jones, N. S. (2010). Growth-induced mass flows in fungal networks. *Proceedings of the Royal Society B: Biological Sciences*, *277*(1698), 3265–3274. https://doi.org/10.1098/rspb.2010.0735

Heaton, L., Obara, B., Grau, V., Jones, N., Nakagaki, T., Boddy, L., & Fricker, M. D. (2012). Analysis of fungal networks. *Fungal Biology Reviews*, *26*(1), 12–29. https://doi.org/10.1016/j.fbr.2012.02.001

Heritage, A. D., & MacRae, I. C. (1977). Degradation of lindane by cell-free preparations of *Clostridium sphenoides*. *Applied and Environmental Microbiology*, *34*(2), 222–224.

Heritage, A. D., & Rae, I. C. (1977). Identification of intermediates formed during the degradation of hexachlorocyclohexanes by *Clostridium sphenoides*. *Applied and Environmental Microbiology*, *33*(6), 1295–1297.

Huber, A., Bach, M., & Frede, H. G. (2000). Pollution of surface waters with pesticides in Germany: Modeling non-point source inputs. *Agriculture, Ecosystems & Environment*, *80*(3), 191–204. https://doi.org/10.1016/S0167-8809(00)00145-6

Huelsenbeck, J. P., & Ronquist, F. (2001). MRBAYES: Bayesian inference of phylogenetic trees. *Bioinformatics*, *17*(8), 754–755. https://doi.org/10.1093/bioinformatics/17.8.754

Humphreys, E. H., Janssen, S., Heil, A., Hiatt, P., Solomon, G., & Miller, M. D. (2008). Outcomes of the California ban on pharmaceutical lindane: Clinical and Ecologic Impacts. *Environmental Health Perspectives*, *116*(3), 297–302. https://doi.org/10.1289/ehp.10668

Ito, M., Prokop, Z., Klvaňa, M., Otsubo, Y., Tsuda, M., Damborský, J., & Nagata, Y. (2007). Degradation of β-hexachlorocyclohexane by haloalkane dehalogenase LinB from γ-hexachlorocyclohexane-utilizing bacterium Sphingobium sp. MI1205. *Archives of Microbiology*, *188*(4), 313–325. https://doi.org/10.1007/s00203-007-0251-8

Jagnow, G., Haider, K., & Ellwardt, P. C. (1977). Anaerobic dechlorination and degradation of hexachlorocyclohexane isomers by anaerobic and facultative anaerobic bacteria. *Archives of Microbiology*, *115*(3), 285–292. https://doi.org/10.1007/BF00446454

Janevska, S., Arndt, B., Niehaus, E.-M., Burkhardt, I., Rösler, S. M., Brock, N. L., Humpf, H.-U., Dickschat, J. S., & Tudzynski, B. (2016). Gibepyrone biosynthesis in the rice pathogen *Fusarium fujikuroi* is facilitated by a small polyketide synthase gene cluster. *Journal of Biological Chemistry*, *291*(53), 27403–27420. https://doi.org/10.1074/jbc.M116.753053

Jayaraj, R., Megha, P., & Sreedev, P. (2016). Organochlorine pesticides, their toxic effects on living organisms and their fate in the environment. *Interdisciplinary Toxicology*, *9*(3–4), 90–100. https://doi.org/10.1515/intox-2016-0012

Jehmlich, N., Schmidt, F., Taubert, M., Seifert, J., Bastida, F., von Bergen, M., Richnow, H.-H., & Vogt, C. (2010). Protein-based stable isotope probing. *Nature Protocols*, *5*(12), 1957–1966. https://doi.org/10.1038/nprot.2010.166

Jehmlich, N., Schmidt, F., von Bergen, M., Richnow, H.-H., & Vogt, C. (2008). Protein-based stable isotope probing (Protein-SIP) reveals active species within anoxic mixed cultures. *The ISME Journal*, *2*(11), Article 11. https://doi.org/10.1038/ismej.2008.64

Jehmlich, N., Vogt, C., Lünsmann, V., Richnow, H. H., & von Bergen, M. (2016). Protein-SIP in environmental studies. *Current Opinion in Biotechnology*, *41*, 26–33. https://doi.org/10.1016/j.copbio.2016.04.010

Jennings, D. H. (1987). Translocation of solutes in fungi. *Biological Reviews*, *62*(3), 215–243. https://doi.org/10.1111/j.1469-185X.1987.tb00664.x

Joshi, N., & Fass, J. N. (2011). Sickle-A windowed adaptive trimming tool for FASTQ files using quality. *Version 1.33*.

Jürgens, H.-J., & Roth, R. (1989). Case study and proposed decontamination steps of the soil and groundwater beneath a closed herbicide plant in Germany. *Chemosphere*, *18*(1–6), 1163–1169. https://doi.org/10.1016/0045-6535(89)90250-6

Kaur, H., Kapoor, S., & Kaur, G. (2016). Application of ligninolytic potentials of a white-rot fungus *Ganoderma lucidum* for degradation of lindane. *Environmental Monitoring and Assessment*, *188*(10), 588. https://doi.org/10.1007/s10661-016-5606-7

Kaur, J., Verma, H., Tripathi, C., Khurana, J. P., & Lal, R. (2013). Draft genome sequence of a hexachlorocyclohexane-degrading bacterium, *Sphingobium baderi* Strain LL03T. *Genome Announcements*, *1*(5), e00751-13. https://doi.org/10.1128/genomeA.00751-13

Kawahara, K., Kuraishi, H., & Zähringer, U. (1999). Chemical structure and function of glycosphingolipids of *Sphingomonas* spp and their distribution among members of the alpha-4 subclass of Proteobacteria. *Journal of Industrial Microbiology & Biotechnology*, *23*(4–5), 408–413. https://doi.org/10.1038/sj.jim.2900708

Khan, N., Brizola Toscan, R., Lunayo, A., Wamalwa, B., Muge, E., Mulaa, F. J., Kallies, R., Harms, H., Wick, L. Y., & Nunes da Rocha, U. (2022). Draft genome sequences of two *Sphingobium* species associated with hexachlorocyclohexane (HCH) degradation isolated from an HCH-contaminated soil. *Microbiology Resource Announcements*, *11*(3), e00886-21. https://doi.org/10.1128/mra.00886-21

Khan, N., Toscan, R. B., Lunayo, A., Wamalwa, B., Muge, E., Mulaa, F. J., Kallies, R., Harms, H., Wick, L. Y., & Nunes da Rocha, U. (2021). Draft genome sequence of *Fusarium*

*equiseti* K3, a fungal species isolated from hexachlorocyclohexane-contaminated soil. *Microbiology Resource Announcements*, *10*(47), e00885-21. https://doi.org/10.1128/MRA.00885-21

Kim, H. J., Boedicker, J. Q., Choi, J. W., & Ismagilov, R. F. (2008). Defined spatial structure stabilizes a synthetic multispecies bacterial community. *Proceedings of the National Academy of Sciences*, *105*(47), 18188–18193. https://doi.org/10.1073/pnas.0807935105

Knudsen, B. E., Ellegaard-Jensen, L., Albers, C. N., Rosendahl, S., & Aamand, J. (2013). Fungal hyphae stimulate bacterial degradation of 2,6-dichlorobenzamide (BAM). *Environmental Pollution*, *181*, 122–127. https://doi.org/10.1016/j.envpol.2013.06.013

Kohlmeier, S., Smits, T. H. M., Ford, R. M., Keel, C., Harms, H., & Wick, L. Y. (2005). Taking the fungal highway: Mobilization of pollutant-degrading bacteria by fungi. *Environmental Science & Technology*, *39*(12), 4640–4646. https://doi.org/10.1021/es047979z

Korf, I. (2004). Gene finding in novel genomes. *BMC Bioinformatics*, *5*(1), 59. https://doi.org/10.1186/1471-2105-5-59

Kumar, D., & Pannu, R. (2018). Perspectives of lindane (γ-hexachlorocyclohexane) biodegradation from the environment: A review. *Bioresources and Bioprocessing*, *5*(1), 29. https://doi.org/10.1186/s40643-018-0213-9

Kumari, R., Subudhi, S., Suar, M., Dhingra, G., Raina, V., Dogra, C., Lal, S., van der Meer, J. R., Holliger, C., & Lal, R. (2002). Cloning and characterization of lin genes responsible for the degradation of hexachlorocyclohexane isomers by *Sphingomonas paucimobilis* strain B90. *Applied and Environmental Microbiology*, *68*(12), 6021–6028. https://doi.org/10.1128/AEM.68.12.6021-6028.2002

Lal, R., Dogra, C., Malhotra, S., Sharma, P., & Pal, R. (2006). Diversity, distribution and divergence of lin genes in hexachlorocyclohexane-degrading sphingomonads. *Trends in Biotechnology*, *24*(3), 121–130. https://doi.org/10.1016/j.tibtech.2006.01.005

Lal, R., Pandey, G., Sharma, P., Kumari, K., Malhotra, S., Pandey, R., Raina, V., Kohler, H.-P. E., Holliger, C., Jackson, C., & Oakeshott, J. G. (2010). Biochemistry of microbial degradation

of hexachlorocyclohexane and prospects for bioremediation. *Microbiology and Molecular Biology Reviews*, *74*(1), 58–80. https://doi.org/10.1128/MMBR.00029-09

Lal, R., & Saxena, D. M. (1982). Accumulation, metabolism, and effects of organochlorine insecticides on microorganisms. *Microbiol. Rev.*, *46*, 33.

Laslett, D. (2004). ARAGORN, a program to detect tRNA genes and tmRNA genes in nucleotide sequences. *Nucleic Acids Research*, *32*(1), 11–16. https://doi.org/10.1093/nar/gkh152

Leveau, J. H. J., & Preston, G. M. (2008). Bacterial mycophagy: Definition and diagnosis of a unique bacterial-fungal interaction. *The New Phytologist*, *177*(4), 859–876. https://doi.org/10.1111/j.1469-8137.2007.02325.x

Little, A. E. F., Robinson, C. J., Peterson, S. B., Raffa, K. F., & Handelsman, J. (2008). Rules of Engagement: Interspecies interactions that regulate microbial communities. *Annual Review of Microbiology*, *62*(1), 375–401. https://doi.org/10.1146/annurev.micro.030608.101423

Lünsmann, V., Kappelmeyer, U., Benndorf, R., Martinez-Lavanchy, P. M., Taubert, A., Adrian, L., Duarte, M., Pieper, D. H., von Bergen, M., Müller, J. A., Heipieper, H. J., & Jehmlich, N. (2016). In situ protein-SIP highlights *Burkholderiaceae* as key players degrading toluene by para ring hydroxylation in a constructed wetland model: Protein-SIP in a toluene-degrading wetland. *Environmental Microbiology*, *18*(4), 1176–1186. https://doi.org/10.1111/1462-2920.13133

Ma, A., Wu, J., Zhang, G., Wang, T., & Li, S. (2005). Isolation and characterization of a HCH degradation *Sphingomanas* sp. Stain BHC-A. *Wei Sheng Wu Xue Bao = Acta Microbiologica Sinica*, *45*(5), 728–732.

Maeda, A. H., Kunihiro, M., Ozeki, Y., Nogi, Y., & Kanaly, R. A. Y. 2015. (2015). *Sphingobium barthaii* sp. Nov., a high molecular weight polycyclic aromatic hydrocarbon-degrading bacterium isolated from cattle pasture soil. *International Journal of Systematic and Evolutionary Microbiology*, *65*(Pt_9), 2919–2924. https://doi.org/10.1099/ijs.0.000356

Manickam, N., Reddy, M. K., Saini, H. S., & Shanker, R. (2008). Isolation of hexachlorocyclohexane-degrading *Sphingomonas* sp. By dehalogenase assay and

characterization of genes involved in γ-HCH degradation. *Journal of Applied Microbiology*, *104*(4), 952–960. https://doi.org/10.1111/j.1365-2672.2007.03610.x

Mansour, S. A. (2009). Persistent organic pollutants (POPs) in Africa: Egyptian scenario. *Human & Experimental Toxicology*, *28*(9), 531–566. https://doi.org/10.1177/0960327109347048

Marete, M. G., Lalah, .J.O, Mputhia, J., & Wekesa, V. W. (2019). Contamination from organochlorine pesticides (OCPs) and other pesticides in agricultural soils of Buuri, Imenti South and Imenti North sub counties, Meru County Agroecosystem in Kenya. *Journal of Agriculture*, *3*(1), Article 1.

Martinez-Toledo, M. V., Salmeron, V., Rodelas, B., Pozo, C., & Gonzalez-Lopez, J. (1993). Studies on the effects of a chlorinated hydrocarbon insecticide, lindane, on soil microorganisms. *Chemosphere*, *27*(11), 2261–2270. https://doi.org/10.1016/0045-6535(93)90137-T

Mertens, B., Boon, N., & Verstraete, W. (2006). Slow-release inoculation allows sustained biodegradation of γ-hexachlorocyclohexane. *Applied and Environmental Microbiology*, *72*(1), 622–627. https://doi.org/10.1128/AEM.72.1.622-627.2006

Middeldorp, P. J. M., Jaspers, M., Zehnder, A. J. B., & Schraa, G. (1996). Biotransformation of α-, β-, γ-, and δ-Hexachlorocyclohexane under methanogenic conditions. *Environmental Science & Technology*, *30*(7), 2345–2349. https://doi.org/10.1021/es950782+

Miyamoto, Y., Masunaka, A., Tsuge, T., Yamamoto, M., Ohtani, K., Fukumoto, T., Gomi, K., Peever, T. L., Tada, Y., Ichimura, K., & Akimitsu, K. (2010). ACTTS3 encoding a polyketide synthase is essential for the biosynthesis of ACT-toxin and pathogenicity in the tangerine pathotype of *Alternaria alternata*. *Molecular Plant-Microbe Interactions: MPMI*, *23*(4), 406–414. https://doi.org/10.1094/MPMI-23-4-0406

Miyauchi, K., Adachi, Y., Nagata, Y., & Takagi, M. (1999). Cloning and sequencing of a novel meta-cleavage dioxygenase gene whose product is involved in degradation of gamma-hexachlorocyclohexane in *Sphingomonas paucimobilis*. *Journal of Bacteriology*, *181*(21), 6712–6719. https://doi.org/10.1128/JB.181.21.6712-6719.1999

Miyauchi, K., Lee, H.-S., Fukuda, M., Takagi, M., & Nagata, Y. (2002). Cloning and characterization of linR, involved in regulation of the downstream pathway for gamma-hexachlorocyclohexane degradation in Sphingomonas paucimobilis UT26. *Applied and Environmental Microbiology*, *68*(4), 1803–1807. https://doi.org/10.1128/AEM.68.4.1803-1807.2002

Miyauchi, K., Suh, S.-K., Nagata, Y., & Takagi, M. (1998). Cloning and sequencing of a 2,5-dichlorohydroquinone reductive dehalogenase gene whose product is involved in degradation of γ-hexachlorocyclohexane by *Sphingomonas paucimobilis*. *Journal of Bacteriology*, *180*(6), 1354–1359.

Mohn, W. W., Mertens, B., Neufeld, J. D., Verstraete, W., & de Lorenzo, V. (2006). Distribution and phylogeny of hexachlorocyclohexane-degrading bacteria in soils from Spain. *Environmental Microbiology*, *8*(1), 60–68. https://doi.org/10.1111/j.1462-2920.2005.00865.x

Morris, B. E. L., Henneberger, R., Huber, H., & Moissl-Eichinger, C. (2013). Microbial syntrophy: Interaction for the common good. *FEMS Microbiology Reviews*, *37*(3), 384–406. https://doi.org/10.1111/1574-6976.12019

Mortazavi, N., Asadikaram, G., Ebadzadeh, M., Kamalati, A., Pakmanesh, H., Dadgar, R., Moazed, V., Paydar, P., Fallah, H., & Abolhassani, M. (2019). Organochlorine and organophosphorus pesticides and bladder cancer: A case-control study. *Journal of Cellular Biochemistry*, *120*(9), 14847–14859. https://doi.org/10.1002/jcb.28746

Mougin, C., Pericaud, C., Malosse, C., Laugero, C., & Asther, M. (1996). Biotransformation of the insecticide lindane by the white rot basidiomycete *Phanerochaete chrysosporium*. *Pesticide Science*, *47*(1), 51–59. https://doi.org/10.1002/(SICI)1096-9063(199605)47:1<51::AID-PS391>3.0.CO;2-V

Muchiri, M., Gitahi, S. M., Harper, D. M., Tole, M. P., & Ng'ang'a, R. N. (2002). Organochlorine and organophosphorus pesticide concentrations in water, sediment, and selected organisms in Lake Naivasha (Kenya). https://karuspace.karu.ac.ke/handle/20.500.12092/2055

Murthy, H. M. R., & Manonmani, H. K. (2007). Aerobic degradation of technical hexachlorocyclohexane by a defined microbial consortium. *Journal of Hazardous Materials*, *149*(1), 18–25. https://doi.org/10.1016/j.jhazmat.2007.03.053

Nagata, Y., Endo, R., Ito, M., Ohtsubo, Y., & Tsuda, M. (2007). Aerobic degradation of lindane (γ-hexachlorocyclohexane) in bacteria and its biochemical and molecular basis. *Applied Microbiology and Biotechnology*, *76*(4), 741–752. https://doi.org/10.1007/s00253-007-1066-x

Nagata, Y., Miyauchi, K., & Takagi, M. (1999). Complete analysis of genes and enzymes for gamma-hexachlorocyclohexane degradation in *Sphingomonas paucimobilis* UT26. *Journal of Industrial Microbiology & Biotechnology*, *23*(4–5), 380–390. https://doi.org/10.1038/sj.jim.2900736

Nagata, Y., Ohtsubo, Y., Endo, R., Ichikawa, N., Ankai, A., Oguchi, A., Fukui, S., Fujita, N., & Tsuda, M. (2010). Complete genome sequence of the representative γ-hexachlorocyclohexane-degrading bacterium *Sphingobium japonicum* UT26. *Journal of Bacteriology*, *192*(21), 5852–5853. https://doi.org/10.1128/JB.00961-10

Nagpal, V., Srinivasan, M. C., & Paknikar, K. M. (2008). Biodegradation of γ-hexachlorocyclohexane (Lindane) by a non-white rot fungus *Conidiobolus* 03-1-56 isolated from litter. *Indian Journal of Microbiology*, *48*(1), 134–141. https://doi.org/10.1007/s12088-008-0013-6

Nayyar, N., & Lal, R. (2016). Hexachlorocyclohexane contamination and solutions: Brief history and beyond. Emerging model to study evolution of catabolic genes and pathways. *Journal of Bioremediation & Biodegradation*, *07*(02). https://doi.org/10.4172/2155-6199.1000338

Nayyar, N., Sangwan, N., Kohli, P., Verma, H., Kumar, R., Negi, V., Oldach, P., Mahato, N. K., Gupta, V., & Lal, R. (2014). Hexachlorocyclohexane: Persistence, toxicity and decontamination. *Reviews on Environmental Health*, *29*(1–2), 49–52. https://doi.org/10.1515/reveh-2014-0015

Nazir, R., Warmink, J. A., Boersma, H., & van Elsas, J. D. (2010). Mechanisms that promote bacterial fitness in fungal-affected soil microhabitats. *FEMS Microbiology Ecology*, *71*(2), 169–185. https://doi.org/10.1111/j.1574-6941.2009.00807.x

Nelson, K., Muge, E., & Wamalwa, B. (2021). Cellulolytic Bacillus species isolated from the gut of the desert locust *Schistocerca gregaria*. *Scientific African*, *11*, e00665. https://doi.org/10.1016/j.sciaf.2020.e00665

Neufeld, J. D., Dumont, M. G., Vohra, J., & Murrell, J. C. (2007a). Methodological considerations for the use of stable isotope probing in microbial ecology. *Microbial Ecology*, *53*(3), 435–442. https://doi.org/10.1007/s00248-006-9125-x

Neufeld, J. D., Vohra, J., Dumont, M. G., Lueders, T., Manefield, M., Friedrich, M. W., & Murrell, J. C. (2007b). DNA stable-isotope probing. *Nature Protocols*, *2*(4), Article 4. https://doi.org/10.1038/nprot.2007.109

Niharika, N., Moskalikova, H., Kaur, J., Khan, F., Sedlackova, M., Hampl, A., Damborsky, J., Prokop, Z., & Lal, R. (2013). *Sphingobium czechense* sp. Nov., isolated from a hexachlorocyclohexane dump site. *International Journal of Systematic and Evolutionary Microbiology*, *63*(Pt 2), 723–728. https://doi.org/10.1099/ijs.0.039396-0

Nolan, K., Kamrath, J., & Levitt, J. (2012). Lindane Toxicity: A comprehensive review of the medical literature: Lindane toxicity. *Pediatric Dermatology*, *29*(2), 141–146. https://doi.org/10.1111/j.1525-1470.2011.01519.x

Nzila, A. (2013). Update on the cometabolism of organic pollutants by bacteria. *Environmental Pollution*, *178*, 474–482. https://doi.org/10.1016/j.envpol.2013.03.042

Ohisa, N., Yamaguchi, M., & Kurihara, N. (1980). Lindane degradation by cell-free extracts of *Clostridium rectum*. *Archives of Microbiology*, *125*(3), 221–225. https://doi.org/10.1007/BF00446880

Okai, M., Kubota, K., Fukuda, M., Nagata, Y., Nagata, K., & Tanokura, M. (2010). Crystal Structure of γ-Hexachlorocyclohexane Dehydrochlorinase LinA from *Sphingobium*

*japonicum* UT26. *Journal of Molecular Biology*, *403*(2), 260–269. https://doi.org/10.1016/j.jmb.2010.08.043

Okeke, B. C., Siddique, T., Arbestain, M. C., & Frankenberger, W. T. (2002). Biodegradation of gamma-hexachlorocyclohexane (lindane) and alpha-hexachlorocyclohexane in water and a soil slurry by a *Pandoraea* species. *Journal of Agricultural and Food Chemistry*, *50*(9), 2548–2555. https://doi.org/10.1021/jf011422a

Osoro, E. (2016). Organochlorine pesticides residues in water and sediment from Rusinga island, Lake Victoria, Kenya. *IOSR Journal of Applied Chemistry*.

Österreicher-Cunha, P., Langenbach, T., Torres, J. P. M., Lima, A. L. C., de Campos, T. M. P., Vargas, E. do A., & Wagener, A. R. (2003). HCH distribution and microbial parameters after liming of a heavily contaminated soil in Rio de Janeiro. *Environmental Research*, *93*(3), 316–327. https://doi.org/10.1016/S0013-9351(03)00091-4

Otieno, P. O., Owuor, P. O., Lalah, J. O., Pfister, G., & Schramm, K.-W. (2013). Impacts of climate-induced changes on the distribution of pesticides residues in water and sediment of Lake Naivasha, Kenya. *Environmental Monitoring and Assessment*, *185*(3), 2723–2733. https://doi.org/10.1007/s10661-012-2743-5

Pal, R., Bala, S., Dadhwal, M., Kumar, M, Dhingra, G., Prakash, O., Prabagaran, S.R., Shivaji, S., Cullum, J, Holliger, C., & Lal, R. (2005). Hexachlorocyclohexane-degrading bacterial strains *Sphingomonas paucimobilis* B90A, UT26 and Sp+, having similar lin genes, represent three distinct species, *Sphingobium indicum* sp. Nov., *Sphingobium japonicum* sp. Nov. And *Sphingobium francense* sp. Nov., and reclassification of *Sphingomonas chungbukensis* as *Sphingobium chungbukense* comb. Nov. *International Journal of Systematic and Evolutionary Microbiology*, *55*(5), 1965–1972. https://doi.org/10.1099/ijs.0.63201-0

Pant, G., Mistry, S. K., & Sibi, G. (2013). Isolation, identification and characterization of p, p-DDT degrading bacteria from soil. https://doi.org/10.3923/jest.2013.130.137

Parks, D. H., Imelfort, M., Skennerton, C. T., Hugenholtz, P., & Tyson, G. W. (2015). CheckM: Assessing the quality of microbial genomes recovered from isolates, single cells, and metagenomes. *Genome Research*, *25*(7), 1043–1055. https://doi.org/10.1101/gr.186072.114

Pérez-Lucas, G., Vela, N., El Aatik, A., & Navarro, S. (2019). Environmental risk of groundwater pollution by pesticide leaching through the soil profile. In M. Larramendy & S. Soloneski (Eds.), *Pesticides—Use and Misuse and Their Impact in the Environment*. IntechOpen. https://doi.org/10.5772/intechopen.82418

Phillips, T. A., Summerfelt, R. C., Wu, J., & Laird, D. A. (2003). Toxicity of Chlorpyrifos adsorbed on humic colloids to larval walleye (*Stizostedion vitreum*). *Archives of Environmental Contamination and Toxicology*, *45*(2), 258–263. https://doi.org/10.1007/s00244-002-0066-1

Phillips, T. M., Lee, H., Trevors, J. T., & Seech, A. G. (2006). Full-scale in situ bioremediation of hexachlorocyclohexane-contaminated soil. *Journal of Chemical Technology & Biotechnology*, *81*(3), 289–298. https://doi.org/10.1002/jctb.1390

Phillips, T. M., Seech, A. G., Lee, H., & Trevors, J. T. (2001). Colorimetric assay for lindane dechlorination by bacteria. *Journal of Microbiological Methods*, *47*(2), 181–188. https://doi.org/10.1016/S0167-7012(01)00299-8

Phillips, T. M., Seech, A. G., Lee, H., & Trevors, J. T. (2005). Biodegradation of hexachlorocyclohexane (HCH) by microorganisms. *Biodegradation*, *16*(4), 363–392. https://doi.org/10.1007/s10532-004-2413-6

Pino, N. J., Dominguez, M. C., & Penuela, G. A. (2011). Isolation of a selected microbial consortium capable of degrading methyl parathion and p-nitrophenol from a contaminated soil site. *Journal of Environmental Science and Health. Part. B, Pesticides, Food Contaminants, and Agricultural Wastes*, *46*(2), 173–180. https://doi.org/10.1080/03601234.2011.539142

Pomés, A., Rodríguez-Farré, E., & Suñol, C. (1994). Disruption of GABA-dependent chloride flux by cyclodienes and hexachlorocyclohexanes in primary cultures of cortical neurons. *The Journal of Pharmacology and Experimental Therapeutics*, *271*(3), 1616–1623.

Popp, P., Brüggemann, L., Keil, P., Thuß, U., & Weiß, H. (2000). Chlorobenzenes and hexachlorocyclohexanes (HCHs) in the atmosphere of Bitterfeld and Leipzig (Germany). *Chemosphere*, *41*(6), 849–855. https://doi.org/10.1016/S0045-6535(99)00531-7

Porto, A. L. M., Melgar, G. Z., Kasemodel, M. C., & Nitschke, M. (2011). Biodegradation of pesticides. In *Pesticides in the Modern World—Pesticides Use and Management*. IntechOpen. https://doi.org/10.5772/17686

Prakash, O., & Lal, R. (2006). Description of *Sphingobium fuliginis* sp. Nov., a phenanthrene-degrading bacterium from a fly ash dumping site, and reclassification of *Sphingomonas cloacae* as *Sphingobium cloacae* comb. Nov. *International Journal of Systematic and Evolutionary Microbiology*, *56*(Pt 9), 2147–2152. https://doi.org/10.1099/ijs.0.64080-0

Prakash, O., Suar, M., Raina, V., Rawat, C., Pal, R., & Lal, R. (2004). Residues of hexachlorocyclohexane (HCH) isomers in soil and water samples from Delhi and adjoining areas. *Current Science*, *87*.

Quintero, J. C., Lú-Chau, T. A., Moreira, M. T., Feijoo, G., & Lema, J. M. (2007). Bioremediation of HCH present in soil by the white-rot fungus Bjerkandera adusta in a slurry batch bioreactor. *International Biodeterioration & Biodegradation*, *60*(4), 319–326. https://doi.org/10.1016/j.ibiod.2007.05.005

Quintero, J., Mt, M., G, F., & Jm, L. (2005). Anaerobic degradation of hexachlorocyclohexane isomers in liquid and soil slurry systems. *Chemosphere*, *61*(4). https://doi.org/10.1016/j.chemosphere.2005.02.010

Raina, V., Suar, M., Singh, A., Prakash, O., Dadhwal, M., Gupta, S. K., Dogra, C., Lawlor, K., Lal, S., van der Meer, J. R., Holliger, C., & Lal, R. (2008). Enhanced biodegradation of hexachlorocyclohexane (HCH) in contaminated soils via inoculation with *Sphingobium indicum* B90A. *Biodegradation*, *19*(1), 27–40. https://doi.org/10.1007/s10532-007-9112-z

Regnery, J., & Püttmann, W. (2010). Seasonal fluctuations of organophosphate concentrations in precipitation and storm water runoff. *Chemosphere*, *78*(8), 958–964. https://doi.org/10.1016/j.chemosphere.2009.12.027

Reinhart, D. R., Pohland, F. G., Gould, J. P., & Cross, W. H. (1991). The Fate of Selected Organic Pollutants Codisposed with Municipal Refuse. 10.

Richnow, H. H., Vieth, A., Kastner, M., Gehre, M., & Meckenstock, R. U. (2002). Isotope fractionation of toluene: A perspective to characterise microbial in situ degradation. *The Scientific World Journal*, *2*, 1227–1234. https://doi.org/10.1100/tsw.2002.210

Rigas, F., Papadopoulou, K., Philippoussis, A., Papadopoulou, M., & Chatzipavlidis, J. (2009). Bioremediation of lindane contaminated soil by *Pleurotus ostreatus* in non-sterile conditions using multilevel factorial design. *Water, Air, and Soil Pollution*, *197*(1), 121–129. https://doi.org/10.1007/s11270-008-9795-8

Rijnaarts, H. H. M., Bachmann, A., Jumelet, J. C., & Zehnder, A. J. B. (1990). Effect of desorption and intraparticle mass transfer on the aerobic biomineralization of. alpha. -hexachlorocyclohexane in a contaminated calcareous soil. *Environmental Science & Technology*, *24*(9), 1349–1354. https://doi.org/10.1021/es00079a008

Ritz, K., & Young, I. M. (2004). Interactions between soil structure and fungi. *Mycologist*, *18*(2), 52–59. https://doi.org/10.1017/S0269-915X(04)00201-0

Roy, C., Gaillardon, P., & Montfort, F. (2000). The effect of soil moisture content on the sorption of five sterol biosynthesis inhibiting fungicides as a function of their physicochemical properties. *Pest Management Science*, *56*(9), 795–803. https://doi.org/10.1002/1526-4998(200009)56:9<795::AID-PS193>3.0.CO;2-Y

Rubinos, D. A., Villasuso, R., Muniategui, S., Barral, M. T., & Díaz-Fierros, F. (2007). Using the landfarming technique to remediate soils contaminated with hexachlorocyclohexane isomers. *Water, Air, and Soil Pollution*, *181*(1), 385–399. https://doi.org/10.1007/s11270-006-9309-5

Russell, R. J., Harcourt, R. L., & Oakeshott, J. G. (1998). Bioremediation of pesticides using enzymes. *Seeking Agricultural Produce Free of Pesticide Residues*, 341–348.

Sachsenberg, T., Herbst, F.-A., Taubert, M., Kermer, R., Jehmlich, N., von Bergen, M., Seifert, J., & Kohlbacher, O. (2015). MetaProSIP: Automated inference of stable isotope incorporation rates in proteins for functional metaproteomics. *Journal of Proteome Research*, *14*(2), 619–627. https://doi.org/10.1021/pr500245w

Sáez, F., Pozo, C., Gómez, M. A., Martínez-Toledo, M. V., Rodelas, B., & Gónzalez-López, J. (2006). Growth and denitrifying activity of *Xanthobacter autotrophicus* CECT 7064 in the presence of selected pesticides. *Applied Microbiology and Biotechnology*, *71*(4), 563–567. https://doi.org/10.1007/s00253-005-0182-8

Saez, J. M., Álvarez, A., Benimeli, C. S., & Amoroso, M. J. (2014). Enhanced lindane removal from soil slurry by immobilized *Streptomyces* consortium. *International Biodeterioration & Biodegradation*, *93*, 63–69. https://doi.org/10.1016/j.ibiod.2014.05.013

Saez, J. M., Alvarez, A., Fuentes, M. S., Amoroso, M. J., & Benimeli, C. S. (2017). An overview on microbial degradation of lindane. In S. N. Singh (Ed.), *Microbe-Induced Degradation of Pesticides* (pp. 191–212). Springer International Publishing. https://doi.org/10.1007/978-3-319-45156-5_9

Sagar, V., & Singh, D. P. (2011). Biodegradation of lindane pesticide by non-white-rots soil fungus *Fusarium* sp. *World Journal of Microbiology and Biotechnology*, *27*(8), 1747–1754. https://doi.org/10.1007/s11274-010-0628-8

Sahu, S. K., Patnaik, K. K., Sharmila, M., & Sethunathan, N. (1990). Degradation of alpha-, beta-, and gamma-hexachlorocyclohexane by a soil bacterium under aerobic conditions. *Applied and Environmental Microbiology*, *56*(11), 3620–3622.

Sang, S., & Petrovic, S. (1999). Lindane – A review of toxicity and environmental fate. 65.

Sauviat, M.-P., & Pages, N. (2002). Cardiotoxicity of lindane, a gamma isomer of hexachlorocyclohexane. *Journal De La Societe De Biologie*, *196*(4), 339–348.

Schamfuß, S., Neu, T. R., Harms, H., & Wick, L. Y. (2014). A Whole cell bioreporter approach to assess transport and bioavailability of organic contaminants in water unsaturated systems. *Journal of Visualized Experiments*, *94*. https://doi.org/10.3791/52334

Schamfuß, S., Neu, T. R., van der Meer, J. R., Tecon, R., Harms, H., & Wick, L. Y. (2013). Impact of mycelia on the accessibility of Fluorene to PAH-degrading bacteria. *Environmental Science & Technology*, *47*(13), 6908–6915. https://doi.org/10.1021/es304378d

Seemann, T. (2014). Prokka: Rapid prokaryotic genome annotation. *Bioinformatics*, *30*(14), 2068–2069. https://doi.org/10.1093/bioinformatics/btu153

Semple, K. T., Doick, K. J., Jones, K. C., Burauel, P., Craven, A., & Harms, H. (2004). Defining bioavailability and bioaccessibility of contaminated soil and sediment is complicated. *Environmental Science & Technology*, *38*(12), 228A-231A. https://doi.org/10.1021/es040548w

Semple, K. T., Morriss, A. W. J., & Paton, G. I. (2003). Bioavailability of hydrophobic organic contaminants in soils: Fundamental concepts and techniques for analysis: Organic contaminants in soil. *European Journal of Soil Science*, *54*(4), 809–818. https://doi.org/10.1046/j.1351-0754.2003.0564.x

Senoo, K., & Wada, H. (1989). Isolation and identification of an aerobic γ-HCH-decomposing bacterium from soil. *Soil Science and Plant Nutrition*, *35*(1), 79–87. https://doi.org/10.1080/00380768.1989.10434739

Shah, M. M., Barr, D. P., Chung, N., & Aust, S. D. (1992). Use of white rot fungi in the degradation of environmental chemicals. *Toxicology Letters*, *64–65*, 493–501. https://doi.org/10.1016/0378-4274(92)90224-8

Sharma, P., Raina, V., Kumari, R., Malhotra, S., Dogra, C., Kumari, H., Kohler, H.-P. E., Buser, H.-R., Holliger, C., & Lal, R. (2006). Haloalkane dehalogenase LinB is responsible for beta- and delta-hexachlorocyclohexane transformation in *Sphingobium indicum* B90A. *Applied and Environmental Microbiology*, *72*(9), 5720–5727. https://doi.org/10.1128/AEM.00192-06

Shen, L., Wania, F., Lei, Y. D., Teixeira, C., Muir, D. C. G., & Bidleman, T. F. (2004). Hexachlorocyclohexanes in the North American atmosphere. *Environmental Science & Technology*, *38*(4), 965–975. https://doi.org/10.1021/es034998k

Shoeib, M., & Harner, T. (2002). Using measured octanol-air partition coefficients to explain environmental partitioning of organochlorine pesticides. *Environmental Toxicology and Chemistry*, *21*(5), 984–990. https://doi.org/10.1002/etc.5620210513

Sievers, S., & Friesel, P. (1989). Soil contamination patterns of chlorinated organic compounds: Looking for the source. *Chemosphere*, *19*(1–6), 691–698. https://doi.org/10.1016/0045-6535(89)90392-5

Simão, F. A., Waterhouse, R. M., Ioannidis, P., Kriventseva, E. V., & Zdobnov, E. M. (2015). BUSCO: Assessing genome assembly and annotation completeness with single-copy orthologs. *Bioinformatics*, *31*(19), 3210–3212. https://doi.org/10.1093/bioinformatics/btv351

Sims, J. W., Fillmore, J. P., Warner, D. D., & Schmidt, E. W. (2005). Equisetin biosynthesis in *Fusarium heterosporum*. *Chemical Communications*, *2*, 186. https://doi.org/10.1039/b413523g

Singh, A. K., Chaudhary, P., Macwan, A. S., Diwedi, U. N., & Kumar, A. (2007). Selective loss of lin genes from hexachlorocyclohexane-degrading *Pseudomonas aeruginosa* ITRC-5 under different growth conditions. *Applied Microbiology and Biotechnology*, *76*(4), 895–901. https://doi.org/10.1007/s00253-007-1056-z

Singh, A., & Lal, R. (2009). *Sphingobium ummariense* sp. Nov., a hexachlorocyclohexane (HCH)-degrading bacterium, isolated from HCH-contaminated soil. *International Journal of Systematic and Evolutionary Microbiology*, *59*(1), 162–166. https://doi.org/10.1099/ijs.0.65712-0

Singh, B. K., & Kuhad, R. C. (1999). Biodegradation of lindane (γ-hexachlorocyclohexane) by the white-rot fungus *Trametes hirsutus*. *Letters in Applied Microbiology*, *28*(3), 238–241. https://doi.org/10.1046/j.1365-2672.1999.00508.x

Singh, B. K., & Kuhad, R. C. (2000). Degradation of insecticide lindane (γ-HCH) by white-rot fungi Cyathus bulleri and Phanerochaete sordida. *Pest Management Science*, *56*(2), 142–146. https://doi.org/10.1002/1526-4998(200002)56:2<142::AID-PS104>3.0.CO;2-I

Singh, K. P., Malik, A., & Sinha, S. (2007). Persistent organochlorine pesticide residues in soil and surface water of Northern Indo-Gangetic Alluvial plains. *Environmental Monitoring and Assessment*, *125*(1), 147–155. https://doi.org/10.1007/s10661-006-9247-0

Slade, R. (1945). The gamma isomer of hexachlorocyclohexane ('Gammexane')*:* An Insecticide with Outstanding Properties. *Imperial Chemical Industries*.

Stanke, M., Keller, O., Gunduz, I., Hayes, A., Waack, S., & Morgenstern, B. (2006). AUGUSTUS: Ab initio prediction of alternative transcripts. *Nucleic Acids Research*, *34* (Web Server), W435–W439. https://doi.org/10.1093/nar/gkl200

Stein, S. E., Mikaia, A., Linstrom, P., Mirokhin, Y., Tchekhovskoi, D., Mallard, W. G., Sparkman, O. D., & Sparkman, J. A. (2008). For Use with Microsoft® Windows User's Guide. 49.

Steinberg, G. (2007). Hyphal Growth: A tale of motors, lipids, and the spitzenkörper. *Eukaryotic Cell*, *6*(3), 351–360. https://doi.org/10.1128/EC.00381-06

Studt, L., Wiemann, P., Kleigrewe, K., Humpf, H.-U., & Tudzynski, B. (2012). Biosynthesis of Fusarubins accounts for pigmentation of *Fusarium fujikuroi* perithecia. *Applied and Environmental Microbiology*, *78*(12), 4468–4480. https://doi.org/10.1128/AEM.00823-12

Sun, Y.-P., Unestam, T., Lucas, S. D., Johanson, K. J., Kenne, L., & Finlay, R. (1999). Exudation-reabsorption in a mycorrhizal fungus, the dynamic interface for interaction with soil and soil microorganisms. *Mycorrhiza*, *9*(3), 137–144. https://doi.org/10.1007/s005720050298

Sutherland, T. D., Horne, I., Weir, K. M., Coppin, C. W., Williams, M. R., Selleck, M., Russell, R. J., & Oakeshott, J. G. (2004). Enzymatic bioremediation: From enzyme discovery to applications. *Clinical and Experimental Pharmacology & Physiology*, *31*(11), 817–821. https://doi.org/10.1111/j.1440-1681.2004.04088.x

Tabata, M., Ohhata, S., Kawasumi, T., Nikawadori, Y., Kishida, K., Sato, T., Ohtsubo, Y., Tsuda, M., & Nagata, Y. (2016). Complete genome sequence of a γ-hexachlorocyclohexane degrader, *Sphingobium* sp. strain TKS, isolated from a γ-hexachlorocyclohexane-degrading microbial community. *Genome Announcements*, *4*(2), e00247-16. https://doi.org/10.1128/genomeA.00247-16

Taubert, M., Jehmlich, N., Vogt, C., Richnow, H. H., Schmidt, F., von Bergen, M., & Seifert, J. (2011). Time resolved protein-based stable isotope probing (Protein-SIP) analysis allows quantification of induced proteins in substrate shift experiments. *Proteomics*, *11*(11), 2265–2274. https://doi.org/10.1002/pmic.201000788

Taubert, M., Vogt, C., Wubet, T., Kleinsteuber, S., Tarkka, M. T., Harms, H., Buscot, F., Richnow, H.-H., von Bergen, M., & Seifert, J. (2012). Protein-SIP enables time-resolved analysis of the carbon flux in a sulfate-reducing, benzene-degrading microbial consortium. *The ISME Journal*, *6*(12), 2291–2301. https://doi.org/10.1038/ismej.2012.68

Thomas, J. C., Berger, F., Jacquier, M., Bernillon, D., Baud-Grasset, F., Truffaut, N., Normand, P., Vogel, T. M., & Simonet, P. (1996). Isolation and characterization of a novel gamma-hexachlorocyclohexane-degrading bacterium. *Journal of Bacteriology*, *178*(20), 6049–6055. https://doi.org/10.1128/jb.178.20.6049-6055.1996

Tsygankov, V. Yu., Lukyanova, O. N., Boyarova, M. D., Gumovskiy, A. N., Donets, M. M., Lyakh, V. A., Korchagin, V. P., & Prikhodko, Yu. V. (2019). Organochlorine pesticides in commercial pacific salmon in the Russian far Eastern seas: Food safety and human health risk assessment. *Marine Pollution Bulletin*, *140*, 503–508. https://doi.org/10.1016/j.marpolbul.2019.02.008

Van Hees, P. A. W., Rosling, A., Essén, S., Godbold, D. L., Jones, D. L., & Finlay, R. D. (2006). Oxalate and ferricrocin exudation by the extramatrical mycelium of an ectomycorrhizal fungus in symbiosis with *Pinus sylvestris*. *New Phytologist*, *169*(2), 367–378. https://doi.org/10.1111/j.1469-8137.2005.01600.x

Verdin, A., Lounès-Hadj Sahraoui, A., Newsam, R., Robinson, G., & Durand, R. (2005). Polycyclic aromatic hydrocarbons storage by *Fusarium solani* in intracellular lipid

vesicles. *Environmental Pollution (Barking, Essex: 1987)*, *133*(2), 283–291. https://doi.org/10.1016/j.envpol.2004.05.040

Vijgen, J., Abhilash, P. C., Li, Y. F., Lal, R., Forter, M., Torres, J., Singh, N., Yunus, M., Tian, C., Schäffer, A., & Weber, R. (2011). Hexachlorocyclohexane (HCH) as new Stockholm convention POPs—A global perspective on the management of lindane and its waste isomers. *Environmental Science and Pollution Research*, *18*(2), 152–162. https://doi.org/10.1007/s11356-010-0417-9

Vijgen, J., de Borst, B., Weber, R., Stobiecki, T., & Forter, M. (2019). HCH and lindane contaminated sites: European and global need for a permanent solution for a long-time neglected issue. *Environmental Pollution*, *248*, 696–705. https://doi.org/10.1016/j.envpol.2019.02.029

Vijgen, J., International HCH &. Pesticides Association. (2006). The legacy of Lindane HCH isomer production. a global overview of residue management, formulation and disposal*:* Main report. *International HCH & Pesticides Association*.

Vijgen, J., Weber, R., Lichtensteiger, W., & Schlumpf, M. (2018). The legacy of pesticides and POPs stockpiles—A threat to health and the environment. *Environmental Science and Pollution Research*, *25*(32), 31793–31798. https://doi.org/10.1007/s11356-018-3188-3

Vlčková, K., & Hofman, J. (2012). A comparison of POPs bioaccumulation in *Eisenia fetida* in natural and artificial soils and the effects of aging. *Environmental Pollution (Barking, Essex: 1987)*, *160*(1), 49–56. https://doi.org/10.1016/j.envpol.2011.08.049

Wacławek, S., Silvestri, D., Hrabák, P., Padil, V. V. T., Torres-Mendieta, R., Wacławek, M., Černík, M., & Dionysiou, D. D. (2019). Chemical oxidation and reduction of hexachlorocyclohexanes: A review. *Water Research*, *162*, 302–319. https://doi.org/10.1016/j.watres.2019.06.072

Wadaskar, J. V., Ekhe, J. D., & Kale, S. P. (2006). Adsorption-desorption of HCH and Endosulfan on a soil. *Environmental Technology*, *27*(9), 1011–1017. https://doi.org/10.1080/09593332708618709

Wahid, P. A., & Sethunathan, N. (1979). Sorption-desorption of alpha-, beta-, and gamma- isomers of hexachlorocyclohexane in soils. *Journal of Agricultural and Food Chemistry*, *27*(5), 1050–1053. https://doi.org/10.1021/jf60225a020

Walker, K., Vallero, D. A., & Lewis, R. G. (1999). Factors influencing the distribution of lindane and other hexachlorocyclohexanes in the environment. *Environmental Science & Technology*, *33*(24), 4373–4378. https://doi.org/10.1021/es990647n

Wandiga, S. (2001). Use and distribution of organochlorine pesticides. The future in Africa. *Pure and Applied Chemistry - PURE APPL CHEM*, *73*, 1147–1155. https://doi.org/10.1351/pac200173071147

Wessels, J. G. H. (1996). Hydrophobins: Proteins that change the nature of the fungal surface. In R. K. Poole (Ed.), *Advances in Microbial Physiology* (Vol. 38, pp. 1–45). Academic Press. https://doi.org/10.1016/S0065-2911(08)60154-X

White, D. C., Sutton, S. D., & Ringelberg, D. B. (1996). The genus Sphingomonas: Physiology and ecology. *Current Opinion in Biotechnology*, *7*(3), 301–306. https://doi.org/10.1016/s0958-1669(96)80034-6

Whitfield, J. (2007). Underground networking. *Nature*, *449*(7159), Article 7159. https://doi.org/10.1038/449136a

Wick, L. Y. (2020). Bioavailability as a microbial system property: Lessons learned from biodegradation in the mycosphere. In J. J. Ortega-Calvo & J. R. Parsons (Eds.), *Bioavailability of Organic Chemicals in Soil and Sediment* (pp. 267–289). Springer International Publishing. https://doi.org/10.1007/698_2020_568

Wick, L. Y., Furuno, S., & Harms, H. (2010). Fungi as transport vectors for contaminants and contaminant-degrading bacteria. In K. N. Timmis (Ed.), *Handbook of Hydrocarbon and Lipid Microbiology* (pp. 1555–1561). Springer Berlin Heidelberg. https://doi.org/10.1007/978-3-540-77587-4_107

Wick, L. Y., Remer, R., Würz, B., Reichenbach, J., Braun, S., Schäfer, F., & Harms, H. (2007). Effect of fungal hyphae on the access of bacteria to Phenanthrene in soil. *Environmental Science & Technology*, *41*(2), 500–505. https://doi.org/10.1021/es061407s

Willett, K. L., Ulrich, E. M., & Hites, R. A. (1998). Differential toxicity and environmental fates of hexachlorocyclohexane isomers. *Environmental Science & Technology*, *32*(15), 2197–2207. https://doi.org/10.1021/es9708530

Wollenberg, R. D., Saei, W., Westphal, K. R., Klitgaard, C. S., Nielsen, K. L., Lysøe, E., Gardiner, D. M., Wimmer, R., Sondergaard, T. E., & Sørensen, J. L. (2017). Chrysogine biosynthesis is mediated by a two-module nonribosomal peptide synthetase. *Journal of Natural Products*, *80*(7), 2131–2135. https://doi.org/10.1021/acs.jnatprod.6b00822

Worrich, A., Stryhanyuk, H., Musat, N., König, S., Banitz, T., Centler, F., Frank, K., Thullner, M., Harms, H., Richnow, H.-H., Miltner, A., Kästner, M., & Wick, L. Y. (2017). Mycelium-mediated transfer of water and nutrients stimulates bacterial activity in dry and oligotrophic environments. *Nature Communications*, *8*, 15472. https://doi.org/10.1038/ncomms15472

Worrich, A., Wick, L. Y., & Banitz, T. (2018). Ecology of contaminant biotransformation in the mycosphere: Role of transport processes. In *Advances in Applied Microbiology* (Vol. 104, pp. 93–133). Elsevier. https://doi.org/10.1016/bs.aambs.2018.05.005

Wösten, H. A. B., van Wetter, M.-A., Lugones, L. G., van der Mei, H. C., Busscher, H. J., & Wessels, J. G. H. (1999). How a fungus escapes the water to grow into the air. *Current Biology*, *9*(2), 85–88. https://doi.org/10.1016/S0960-9822(99)80019-0

Wu, J., Hong, Q., Han, P., He, J., & Li, S. (2007). A gene LinB2 responsible for the conversion of β-HCH and 2,3,4,5,6-pentachlorocyclohexanol in *Sphingomonas* sp. BHC-A. *Applied Microbiology and Biotechnology*, *73*(5), 1097–1105. https://doi.org/10.1007/s00253-006-0579-z

Xu, G., Li, Y., Zheng, W., Peng, X., Li, W., & Yan, Y. (2007). Mineralization of chlorpyrifos by co-culture of *Serratia* and *Trichosporon* spp. *Biotechnology Letters*, *29*(10), 1469–1473. https://doi.org/10.1007/s10529-007-9444-0

Yang, C.-H., Menge, J. A., & Cooksey, D. A. (1994). Mutations Affecting hyphal colonization and pyoverdine production in *Pseudomonads* antagonistic toward *Phytophthora parasitica*. *Appl. Environ. Microbiol.*, 9.

Yeo, H.-G., Choi, M., Chun, M.-Y., & Sunwoo, Y. (2003). Concentration distribution of polychlorinated biphenyls and organochlorine pesticides and their relationship with temperature in rural air of Korea. *Atmospheric Environment*, *37*(27), 3831–3839. https://doi.org/10.1016/S1352-2310(03)00456-4

You, X., Kallies, R., Kühn, I., Schmidt, M., Harms, H., Chatzinotas, A., & Wick, L. Y. (2022). Phage co-transport with hyphal-riding bacteria fuels bacterial invasion in a water-unsaturated microbial model system. *The ISME Journal*, *16*(5), Article 5. https://doi.org/10.1038/s41396-021-01155-x

Young, I. M., & Crawford, J. W. (2004). Interactions and self-organization in the soil-microbe complex. *Science (New York, N.Y.)*, *304*(5677), 1634–1637. https://doi.org/10.1126/science.1097394

Yuan, Y., Hays, M. P., Hardwidge, P. R., & Kim, J. (2017). Surface characteristics influencing bacterial adhesion to polymeric substrates. *RSC Advances*, *7*(23), 14254–14261. https://doi.org/10.1039/C7RA01571B

Zhang, L., Xu, M., Liu, Y., Zhang, F., Hodge, A., & Feng, G. (2016). Carbon and phosphorus exchange may enable cooperation between an arbuscular mycorrhizal fungus and a phosphate-solubilizing bacterium. *New Phytologist*, *210*(3), 1022–1032. https://doi.org/10.1111/nph.13838

Zhang, W., Lin, Z., Pang, S., Bhatt, P., & Chen, S. (2020). Insights into the biodegradation of lindane (γ-hexachlorocyclohexane) using a microbial system. *Frontiers in Microbiology*, *11*, 522. https://doi.org/10.3389/fmicb.2020.00522

Zhu, Y., Liu, H., Xi, Z., Cheng, H., & Xu, X. (2005). Organochlorine pesticides (DDTs and HCHs) in soils from the outskirts of Beijing, China. *Chemosphere*, *60*(6), 770–778. https://doi.org/10.1016/j.chemosphere.2005.04.018

# APPENDICES

## Appendix 1: Supplementary material for Chapter 3

### S1Materials and Methods

**Table S1: Polymerase chain reaction (PCR) primers used in the study.**
The PCR primers were previously described by Kumari et al. (2002) and were designed based on published *lin* gene sequences from *Sphingobium japonicum* UT26 and *Sphingobium indicum* B90A.

| Name | Sequences (5'− 3') |
|---|---|
| *linA*-F | GCGGATCCGCATGAGTGATCTAGACAGACTT |
| *linA*-R | GCCTCGAGTTATGCGCCGGACGGTGCGAAATG |
| *linB*-F | GCGGATCCGCATGAGCCTCGGCGCAAAGCCA |
| *linB*-R | GCCTCGAGTTATGCTGGGCGCAATCGCCGGAC |
| *linC*-F | GCGGATCCGCATGTCTGATTTGAGCGGC |
| *linC*-R | GCCTCGAGTCAGATCGCGGTAAAGCCGCCGTC |
| *linD*-F | GCGAATTCAATGAGCGCTGATACAGAA |
| *linD*-R | GCCTCGAGTTAGGCGTTGCTCAGGAGATGGAT |
| *linE*-F | AGGAATTCCATGATGCAACTGCCCGAA |
| *linE*-R | AGCTCGAGCTCAAATGACGATCGGATC |
| *linR*-F | TGGGATCCCCGTGAATATAGATGACCTGG |
| *linR*-R | GGGTCGACTCACACTCGCGCGGACAG |
| *linX*-F | GCGGATCCGCATGGCTAACAGACTCGCAGGCA |
| *linX*-R | GCCTCGAGTCAAACACCCACGGACCAGCCTCC |
| *IS6100*-F | CAATGCCAAAAGCTCTCTCC |
| IS*6100*-R | GGCTCTGTTGCAAAAATCG |

## S2Results

### S2.1 HCH degradation in liquid culture

**Table S2.1:** Tables showing percentage residual HCH following bacterial degradation.

| HCH isomers | *Sphingobium* sp. S6 | *Sphingobium* sp. S8 | Control |
|---|---|---|---|
| α-HCH | 98.1 ±8.7 | 99.5 ±6.5 | 1.7 ±5.7 |
| β-HCH | 52.3 ±1.1 | 59.0 ±4.7 | -1.5 ±3.7 |
| γ-HCH | 99.1 ±4.0 | 99.9 ±6.1 | -2.0 ±2.3 |
| δ-HCH | 94.1 ±1.6 | 93.7 ±5.1 | 4.9 ±1.6 |

### S2.2 Multiple sequence alignment of *lin* genes

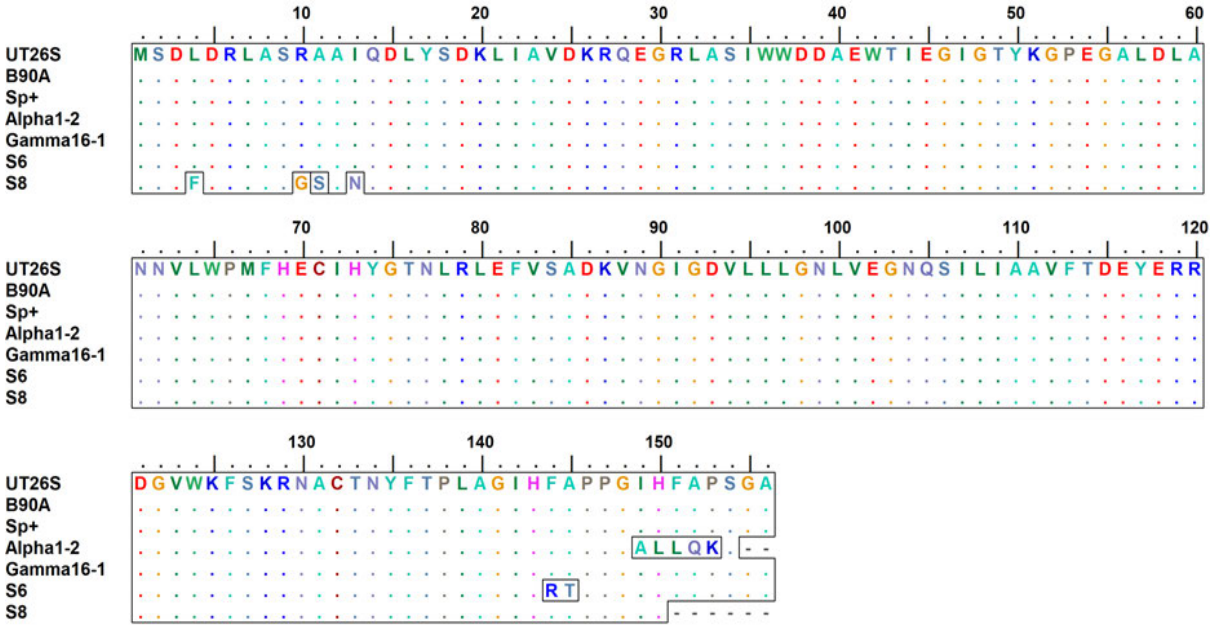


**Figure S2.2.1:** Multiple sequence alignment of LinA from *Sphingobium* sp. strains (S6 and S8) and their homologues from known HCH-degrading bacteria. The LinA sequences and accession numbers are as follows: **UT26S**; *S. japonicum* UT26 (BAI9660.1), **B90A**; *S. indicum* B90A (APL95055.1), **Sp+**; *S. francense* Sp+ (AAU11089.2), **Alpha1-2**; *Sphingobium* sp. α1-2 (CAI43920.1), **Gamma16-1**; *Sphingobium* sp. γ16-1 (CAI43919.1), **S6**; *Sphingobium* sp. Strain S6 (QGJ16213.1) and **S8**; *Sphingobium* sp. Strain S8 (QGJ16206.1).

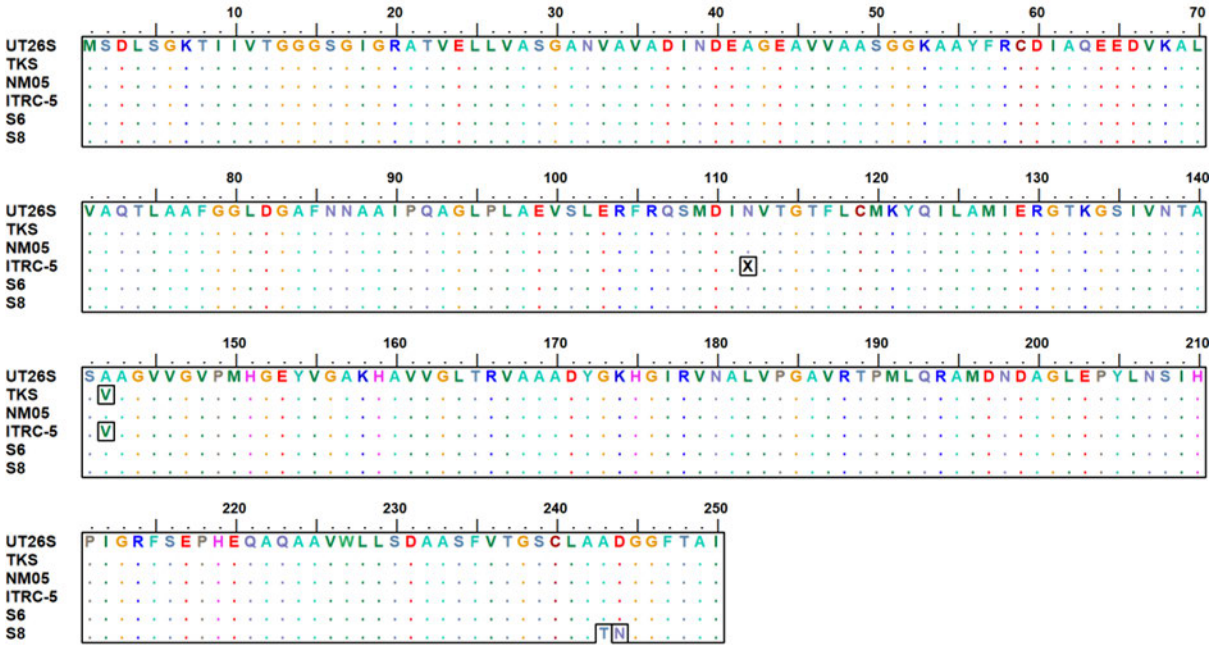


**Figure 2.2.2:** Multiple sequence alignment of LinC from *Sphingobium* sp. strains (S6 and S8) and their homologues from known HCH-degrading bacteria. The LinC sequences and accession numbers are as follows: **UT26S**; *S. japonicum* UT26 (BAI95393.1), TKS; *Sphingobium* sp. TKS (AMK21445.1), **NM05**; *Sphingomonas* sp. NM05 (ABG77568.1), **ITRC-5**; *P. aeruginosa* ITRC-5 (ABP93367.1), **S6**; *Sphingobium* sp. Strain S6 (QGJ16215.1) and **S8**; *Sphingobium* sp. Strain S8 (QGJ16208.1).

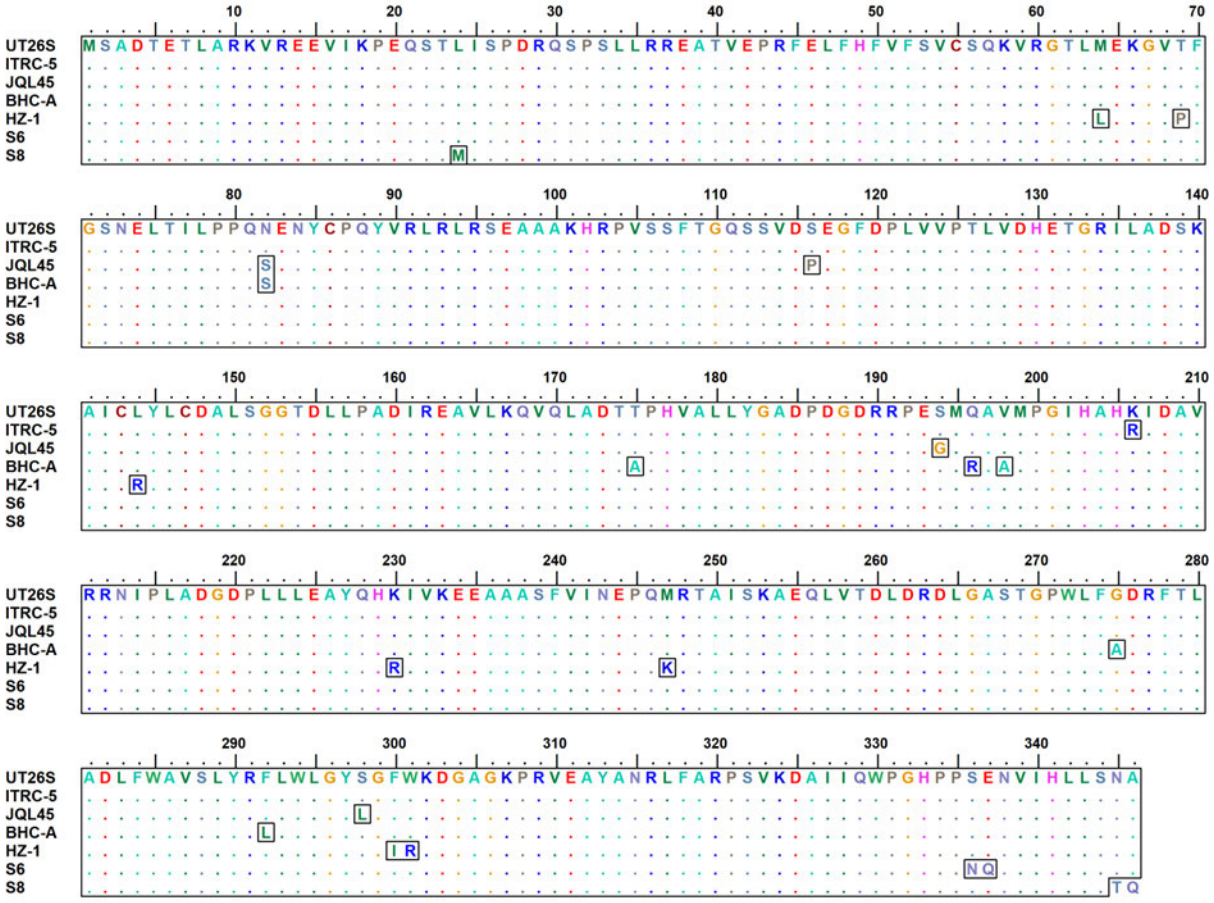


**Figure 2.2.3:** Multiple sequence alignment of LinD from *Sphingobium* sp. strains (S6 and S8) and their homologues from known HCH-degrading bacteria. The LinD sequences and accession numbers are as follows: **UT26S**; *S. japonicum* UT26 (sp|D4Z909.1), **ITRC-5**; *P. aeruginosa* ITRC-5 (ABP93365.1), **JQL45**; *Sphingobium* sp. JQL45 (ABE03743.1), **BHC-A**; *Sphingobium* sp. BHC-A (ABE98170.1), **HZ-1**; *Sphingobium* sp. HZ-1 (ACV91874.1), **S6**; *Sphingobium* sp. Strain S6 (QGJ16216.1) and **S8**; *Sphingobium* sp. Strain S8 (QGJ16209.1).

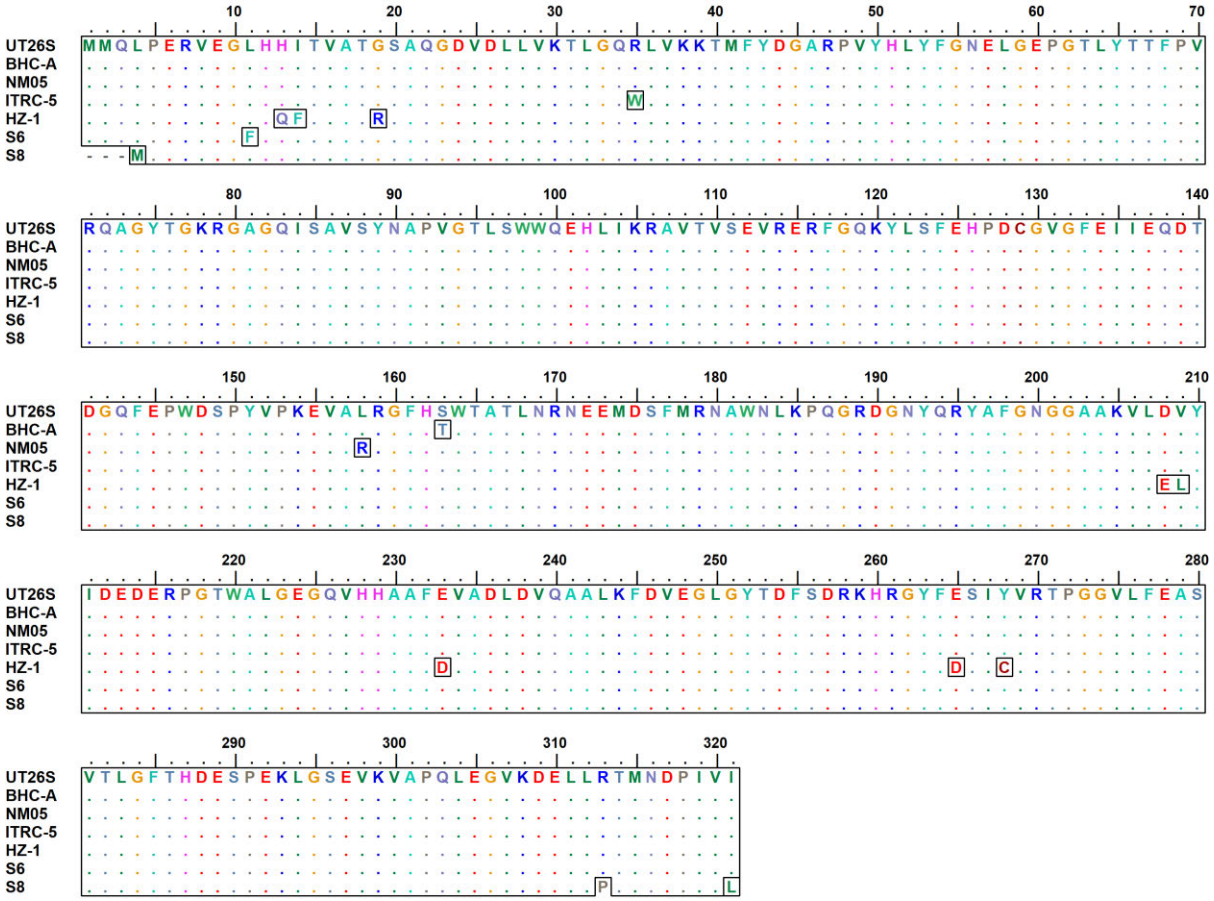


**Figure 2.2.4:** Multiple sequence alignment of LinE from *Sphingobium* sp. strains (S6 and S8) and their homologues from known HCH-degrading bacteria. The LinE sequences and accession numbers are as follows: **UT26S**; *S. japonicum* UT26 (Q9WXE6.1), **BHC-A**; *Sphingobium* sp. BHC-A (ABD66585.1), **NM05**; *Sphingomonas* sp. NM05 (ABG77570.1), **ITRC-5**; *P. aeruginosa* ITRC-5 (ABP93364.1), **HZ-1**; *Sphingobium* sp. HZ-1 (ACV91875.1), **S6**; *Sphingobium* sp. Strain S6 (QGJ16217.1) and **S8**; *Sphingobium* sp. Strain S8 (QGJ16210.1).

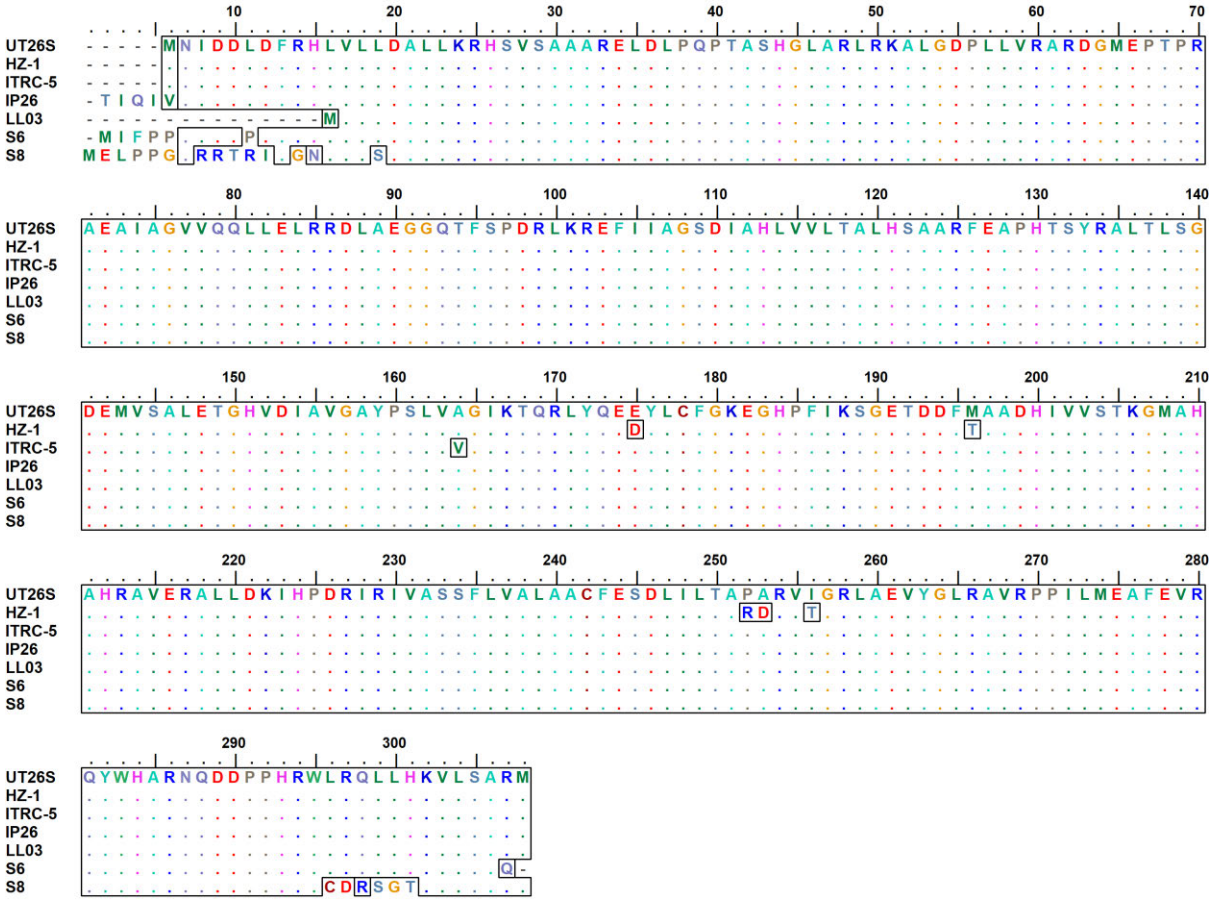


**Figure 2.2.5:** Multiple sequence alignment of LinR from *Sphingobium* sp. strains (S6 and S8) and their homologues from known HCH-degrading bacteria. The LinR sequences and accession numbers are as follows: **UT26S**; *S. japonicum* UT26 (Q9ZN79.3), **HZ-1**; *Sphingobium* sp. HZ-1 (ACV91876.1), **ITRC-5**; P. aeruginosa ITRC-5 (ABP93363.1), **IP26**; *S. chinhatense* IP26 (EPR17852.1), **LL03**; S. baderi LL03 (EQA99717.1), **S6**; *Sphingobium* sp. Strain S6 (QGJ16218.1) and **S8**; *Sphingobium* sp. Strain S8 (QGJ16211.1).

## Appendix 2: Supplementary material for Chapter 5

### S1. Materials and Methods

#### S1.2.2 Protein-SIP analysis using LC-MS/MS

Peptides were analyzed by LC-MS/MS as described before (Sachsenberg et al., 2015). After tryptic digestion of the samples, the resulting peptides were subjected to a shotgun proteomics workflow (nanoLC-MS/MS). Briefly, peptide lysate was injected into a nanoLC system (UltiMate 3000, Dionex, Thermo Fisher Scientific). Peptides were first trapped for 3 min on a C18-reverse phase trapping column (Acclaim PepMap® 100, 75 µm x 2 cm, particle size 3 µM, nanoViper, Thermo Fisher Scientific), followed by separation on a C18-reverse phase analytical column (Acclaim PepMap® 100, 75 µm x 25 cm, particle size 3 µM, nanoViper, Thermo Fisher Scientific) using a two-step gradient (90 min from 4 % to 30% B, then 30 min from 30% to 55% B; A: 0.1% formic acid in MS-grade water; B: 80% acetonitrile, 0.1% formic acid in MS-grade water) with a solvent flow-rate of 300 nL/min and a column temperature of 35°C. Eluting peptides were ionized by a nano ion source (Advion, TriVersa Nanomate, Ithaca, NY, USA) and analyzed at the Q Exactive HF mass spectrometer (Thermo Fisher Scientific) with the following settings: MS resolution 120,000, MS automatic gain control (AGC) target 3,000,000 ions, maximum injection time for MS 80 ms, intensity threshold for MS/MS of 17,000 ions, dynamic exclusion 30 sec, TopN=20, isolation window 1.6 *m/z*, MS/MS resolution 15,000, MS/MS AGC target 50,000 ions, maximum injection time for MS/MS 120 ms.

### S1.1 Microcosm set-ups

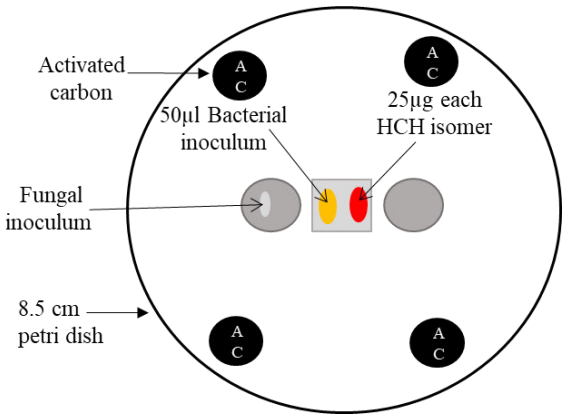


**Figure S1.1:** Top view of the HCH degradation microcosm set-ups showing the position of the activated carbon included in the experiment.

## S2. Results

### Table S2.1 Total crude protein extracts (in mg) estimated by Bradford assay

| Experimental setup | Total crude protein extract (mg) |
|---|---|
| **Mycelia** (bacteria grown in presence of $^{13}C$ labeled mycelia) | 0.45 ± 0.06 |
| **Glass fiber** (bacteria grown in presence of glass fiber) | 0.37 ± 0.02 |
| **Control** (bacteria grown directly on $^{13}C$ glucose) | 0.66 ± 0.006 |
| **Negative control** (bacteria grown in MSM without any carbon source) | 0.29 ± 0.01 |
| ANOVA statistically significant difference [$F(3,8) = 76.56$; $n = 12$, $p < 3.12 \times 10^{-6}$] | |

### Table S2.2 Computed average RIA and LR of the total bacterial proteome and selected proteins from different experimental setups

| | RIA (%) | | | LR | | |
|---|---|---|---|---|---|---|
| **Proteins** | **Mycelia** | **Glass fiber** | **Control** | **Mycelia** | **Glass fiber** | **Control** |
| Chaperone DnaK | 9.4 ± 2.6 | 88.8 ± 27.6 | 89.2 ± 6.9 | 0.13 ±0.04 | 0.15 ±0.05 | 0.82 ±0.05 |
| ATP synthase subunit-β | 10.4 ± 2.1 | 96.9 ± 2.5 | 94.2 ± 4.1 | 0.24 ±0.05 | 0.11 ±0.16 | 0.38 ±0.05 |
| Peptidoglycan associated lipoprotein | 14.2 ± 1.7 | 90.7 ± 12.2 | 96.2 ± 0.1 | 0.14 ±0.02 | 0.12 ±0.06 | 0.67 ±0.03 |
| Haloalkane dehalogenase (LinB) | 9.5 ± 3.0 | 86.6 ± 28.8 | 92.7 ±6 .0 | 0.35 ±0.31 | 0.34 ±0.26 | 0.67 ±0.16 |
| dichloro-2,5-cyclohexadiene-1,4-diol dehydrogenase (Lin C) | 7.06 ± 0.27 | 94.3 ± 16.0 | 87.8 ± 14.9 | 0.34 ±0.02 | 0.15 ±0.01 | 0.39 ±0.13 |
| Total selected proteins | 10.1 ± 2.6 | 91.4 ± 4.2 | 92.0 ± 3.5 | 0.24 ±0.10 | 0.17 ±0.09 | 0.59 ±0.19 |
| Total proteome | 10.9 ± 0.27 | 93.9 ± 17.0 | 92.9 ± 11.4 | 0.22 ±0.17 | 0.15 ±0.12 | 0.57 ±0.19 |

## S2.3 Estimation of HCH degradation efficiency

To account for possible variations of the amounts of the four HCH isomer added (e.g., due to volatilization of the isomers), the amounts of the individual isomers recovered immediately after application onto patch 2 were taken as the initial amounts of HCH ($A_{t0}$). Subsequently, HCH amounts ($A_{deg,\ t10}$), and the residual ($F_{res,\ t10}$) and degraded fractions ($F_{deg,\ t10}$) of added HCH after 10 d were derived from equations eqs. S1– 4. $A_{t10}$ is the residual amounts of HCH, $A_{abiotic,\ t10}$ the residual HCH amounts in the abiotic control, $A_{P1,\ t10\ or\ P2,\ t10\ or\ P3,\ t10}$ the residual HCH amounts on patches 1, 2 or 3, and $A_{AC,\ t10}$ the residual HCH amount on activated charcoal. $A_{air,\ t10}$ is the HCH amount lost by volatilization after 10 days and $F_{air,\ t10}$ (%) the corresponding fraction of HCH lost by volatilization (cf. **Tables S2.3.1- S2.3.4 & Table S2.4)-**.

$$A_{t10} = A_{P1,t10} + A_{P2,t10} + A_{P3,t10} + A_{AC,t10} \quad \text{eq. S1}$$

$$A_{deg,\ t10} = A_{abiotic,\ t10} - A_{t10} \quad \text{eq. S2}$$

$$F_{deg,t10}\ (\%) = (A_{deg,t10}/A_{abiotic,t10}) * 100 \quad \text{eq. S3}$$

$$F_{res,\ t10}\ (\%) = (A_{t10} / A_{abiotic,\ t10}) * 100 \quad \text{eq. S4}$$

$$A_{air,\ t10} = A_{abiotic,\ t10} - A_{t0} \quad \text{eq. S5}$$

$$F_{air,\ t10}\ (\%) = (A_{air,\ t10}/A_{t0}) * 100 \quad \text{eq. S6}$$

**Table S2.3.1 Estimated HCH degradation efficiency for *α*-HCH (cf. S2.3 eqs. S1 – 4)** based on residual HCH amounts after 10 days in quadruplicate laboratory microcosms (Fig. 1A) in presence of *Sphingobium* sp. strain S8 (bacterial mono-culture), *Fusarium equiseti* strain K3 (fungal mono-culture) and fungal bacterial co-cultures.

| ***α*-HCH** | | | | | | | | | |
|---|---|---|---|---|---|---|---|---|---|
| **Experimental setups** | $A_{t0}$ | $A_{P1,\,t10}$ | $A_{P2,\,t10}$ | $A_{P3,\,t10}$ | $A_{AC,\,t10}$ | $A_{t10}$ | $A_{deg,\,t10}$ | $F_{deg,\,t10}$ | $F_{air,\,t10}$ |
| Abiotic control 1 | 23.558 | 0.012 | 3.274 | 0.010 | 13.882 | 17.178 | | | 27.1 |
| Abiotic control 2 | 21.107 | 0.008 | 3.697 | 0.012 | 14.647 | 18.365 | | | 13.0 |
| Abiotic control 3 | 21.352 | 0.006 | 3.637 | 0.006 | 13.570 | 17.219 | | | 19.4 |
| Abiotic control 4 | 26.819 | 0.007 | 4.073 | 0.007 | 15.892 | 19.979 | | | 25.5 |
| Fungal mono-culture 1 | 23.558 | 1.006 | 0.814 | 0.214 | 12.829 | 14.864 | 3.321 | 18.3 | |
| Fungal mono-culture 2 | 21.107 | 0.776 | 0.470 | 0.230 | 14.970 | 16.446 | 1.739 | 9.6 | |
| Fungal mono-culture 3 | 21.352 | 0.942 | 0.763 | 0.182 | 14.639 | 16.527 | 1.659 | 9.1 | |
| Fungal mono-culture 4 | 26.819 | 0.484 | 0.501 | 0.041 | 13.382 | 14.407 | 3.778 | 20.8 | |
| bacterial mono-culture 1 | 23.558 | 0.056 | 1.027 | 0.121 | 10.640 | 11.845 | 6.340 | 34.9 | |
| bacterial mono-culture 2 | 21.107 | 0.010 | 1.213 | 0.025 | 8.249 | 9.497 | 8.688 | 47.8 | |
| bacterial mono-culture 3 | 21.352 | 0.009 | 1.286 | 0.032 | 10.300 | 11.627 | 6.558 | 36.1 | |
| bacterial mono-culture 4 | 26.819 | 0.025 | 1.064 | 0.016 | 12.011 | 13.115 | 5.070 | 27.9 | |
| Fungal-bacterial co-culture 1 | 23.558 | 0.160 | 0.119 | 0.020 | 3.900 | 4.199 | 13.986 | 76.9 | |
| Fungal-bacterial co-culture 2 | 21.107 | 0.342 | 0.383 | 0.015 | 4.616 | 5.356 | 12.829 | 70.5 | |
| Fungal-bacterial co-culture 3 | 21.352 | 0.200 | 0.138 | 0.008 | 5.050 | 5.395 | 12.790 | 70.3 | |
| Fungal-bacterial co-culture 4 | 26.819 | 0.153 | 0.126 | 0.038 | 5.618 | 5.936 | 12.250 | 67.4 | |

**Table S2.3.2 Estimated HCH degradation efficiency for *β*-HCH (cf. S2.3 eqs. S1 – 4)** based on residual HCH amounts after 10 days in quadruplicate laboratory microcosms (Fig. 1A) in presence of *Sphingobium* sp. strain S8 (bacterial mono-culture), *Fusarium equiseti* strain K3 (fungal mono-culture) and fungal bacterial co-cultures.

| ***β*-HCH** | | | | | | | | | |
|---|---|---|---|---|---|---|---|---|---|
| **Experimental setups** | $A_{t0}$ | $A_{P1,\,t10}$ | $A_{P2,\,t10}$ | $A_{P3,\,t10}$ | $A_{AC,\,t10}$ | $A_{t10}$ | $A_{deg,\,t10}$ | $F_{deg,\,t10}$ | $F_{air,\,t10}$ |
| Abiotic control 1 | 28.935 | 0.212 | 26.003 | 0.217 | 0.198 | 26.630 | | | 8.0 |
| Abiotic control 2 | 28.365 | 0.194 | 25.453 | 0.171 | 0.193 | 26.011 | | | 8.3 |
| Abiotic control 3 | 34.924 | 0.157 | 30.255 | 0.185 | 0.214 | 30.811 | | | 11.8 |
| Abiotic control 4 | 31.447 | 0.239 | 27.249 | 0.219 | 0.250 | 27.957 | | | 11.1 |
| Fungal mono-culture 1 | 28.935 | 0.565 | 24.906 | 0.250 | 0.046 | 25.767 | 2.086 | 7.5 | |
| Fungal mono-culture 2 | 28.365 | 0.521 | 24.704 | 0.270 | 0.032 | 25.526 | 2.326 | 8.4 | |
| Fungal mono-culture 3 | 34.924 | 0.870 | 22.541 | 0.309 | 0.071 | 23.791 | 4.061 | 14.6 | |
| Fungal mono-culture 4 | 31.447 | 0.641 | 22.505 | 0.127 | 0.057 | 23.330 | 4.523 | 16.2 | |
| bacterial mono-culture 1 | 28.935 | 0.595 | 11.971 | 0.184 | 0.010 | 12.760 | 15.092 | 54.2 | |
| bacterial mono-culture 2 | 28.365 | 0.108 | 14.280 | 0.182 | 0.017 | 14.587 | 13.266 | 47.6 | |
| bacterial mono-culture 3 | 34.924 | 0.075 | 14.989 | 0.168 | 0.014 | 15.245 | 12.607 | 45.3 | |
| bacterial mono-culture 4 | 31.447 | 0.216 | 11.844 | 0.147 | 0.014 | 12.221 | 15.631 | 56.1 | |
| Fungal-bacterial co-culture 1 | 28.935 | 0.130 | 9.930 | 0.101 | 0.014 | 10.175 | 17.677 | 63.5 | |
| Fungal-bacterial co-culture 2 | 28.365 | 0.133 | 12.775 | 0.068 | 0.028 | 13.005 | 14.848 | 53.3 | |
| Fungal-bacterial co-culture 3 | 34.924 | 0.071 | 12.864 | 0.114 | 0.033 | 13.082 | 14.770 | 53.0 | |
| Fungal-bacterial co-culture 4 | 31.447 | 0.108 | 11.296 | 0.133 | 0.030 | 11.566 | 16.286 | 58.5 | |

**Table S2.3.3 Estimated HCH degradation efficiency for $\gamma$-HCH (cf. S2.3 eqs. S1 – 4)** based on residual HCH amounts after 10 days in quadruplicate laboratory microcosms (Fig. 1A) in presence of *Sphingobium* sp. strain S8 (bacterial mono-culture), *Fusarium equiseti* strain K3 (fungal mono-culture) and fungal bacterial co-cultures.

| $\gamma$-HCH | | | | | | | | | |
|---|---|---|---|---|---|---|---|---|---|
| **Experimental setups** | $A_{t0}$ | $A_{P1,\,t10}$ | $A_{P2,\,t10}$ | $A_{P3,\,t10}$ | $A_{AC,\,t10}$ | $A_{t10}$ | $A_{deg,\,t10}$ | $F_{deg,\,t10}$ | $F_{air,\,t10}$ |
| Abiotic control 1 | 23.951 | 0.017 | 1.573 | 0.017 | 5.915 | 7.522 | | | 68.6 |
| Abiotic control 2 | 27.115 | 0.011 | 1.676 | 0.017 | 5.660 | 7.365 | | | 72.8 |
| Abiotic control 3 | 21.594 | 0.009 | 1.505 | 0.012 | 6.083 | 7.609 | | | 64.8 |
| Abiotic control 4 | 21.123 | 0.013 | 1.923 | 0.013 | 8.401 | 10.351 | | | 51.0 |
| Fungal mono-culture 1 | 23.951 | 1.818 | 0.391 | 0.212 | 5.589 | 8.010 | 0.201 | 2.4 | |
| Fungal mono-culture 2 | 27.115 | 1.664 | 0.229 | 0.228 | 6.186 | 8.306 | -0.095 | -1.2 | |
| Fungal mono-culture 3 | 21.594 | 1.787 | 0.362 | 0.143 | 6.735 | 9.028 | -0.817 | -9.9 | |
| Fungal mono-culture 4 | 21.123 | 1.056 | 0.242 | 0.056 | 5.955 | 7.308 | 0.903 | 11.0 | |
| bacterial mono-culture 1 | 23.951 | 0.043 | 0.440 | 0.119 | 3.606 | 4.208 | 4.004 | 48.8 | |
| bacterial mono-culture 2 | 27.115 | 0.009 | 0.509 | 0.029 | 3.046 | 3.593 | 4.618 | 56.2 | |
| bacterial mono-culture 3 | 21.594 | 0.011 | 0.590 | 0.044 | 3.767 | 4.412 | 3.799 | 46.3 | |
| bacterial mono-culture 4 | 21.123 | 0.020 | 0.487 | 0.019 | 4.650 | 5.175 | 3.036 | 37.0 | |
| Fungal-bacterial co-culture 1 | 23.951 | 0.321 | 0.038 | 0.029 | 1.232 | 1.620 | 6.591 | 80.3 | |
| Fungal-bacterial co-culture 2 | 27.115 | 0.583 | 0.130 | 0.019 | 1.628 | 2.360 | 5.851 | 71.3 | |
| Fungal-bacterial co-culture 3 | 21.594 | 0.290 | 0.047 | 0.012 | 1.682 | 2.030 | 6.182 | 75.3 | |
| Fungal-bacterial co-culture 4 | 21.123 | 0.279 | 0.061 | 0.047 | 1.929 | 2.315 | 5.896 | 71.8 | |

**Table S2.3.4 Estimated HCH degradation efficiency for *δ*-HCH (cf. S2.3 eqs. S1 – 4)** based on residual HCH amounts after 10 days in quadruplicate laboratory microcosms (Fig. 1A) in presence of *Sphingobium* sp. strain S8 (bacterial mono-culture), *Fusarium equiseti* strain K3 (fungal mono-culture) and fungal bacterial co-cultures.

| ***δ*-HCH** | | | | | | | | | |
|---|---|---|---|---|---|---|---|---|---|
| Experimental setups | $A_{t0}$ | $A_{P1,\,t10}$ | $A_{P2,\,t10}$ | $A_{P3,\,t10}$ | $A_{AC,\,t10}$ | $A_{t10}$ | $A_{deg,\,t10}$ | $F_{deg,\,t10}$ | $F_{air,\,t10}$ |
| Abiotic control 1 | 25.738 | 0.364 | 8.261 | 0.341 | 0.123 | 9.090 | | | 64.7 |
| Abiotic control 2 | 27.885 | 0.288 | 9.078 | 0.224 | 0.115 | 9.704 | | | 65.2 |
| Abiotic control 3 | 23.107 | 0.264 | 9.317 | 0.290 | 0.122 | 9.993 | | | 56.8 |
| Abiotic control 4 | 23.136 | 0.457 | 10.033 | 0.378 | 0.100 | 10.968 | | | 52.6 |
| Fungal mono-culture 1 | 25.738 | 3.616 | 3.787 | 1.648 | 0.057 | 9.108 | 0.831 | 8.4 | |
| Fungal mono-culture 2 | 27.885 | 4.309 | 4.419 | 1.771 | 0.039 | 10.537 | -0.599 | -6.0 | |
| Fungal mono-culture 3 | 23.107 | 5.068 | 3.322 | 1.162 | 0.084 | 9.636 | 0.303 | 3.0 | |
| Fungal mono-culture 4 | 23.136 | 3.571 | 3.732 | 0.440 | 0.064 | 7.807 | 2.132 | 21.5 | |
| bacterial mono-culture 1 | 25.738 | 0.190 | 4.504 | 0.075 | 0.010 | 4.779 | 5.160 | 51.9 | |
| bacterial mono-culture 2 | 27.885 | 0.068 | 4.678 | 0.172 | 0.017 | 4.936 | 5.003 | 50.3 | |
| bacterial mono-culture 3 | 23.107 | 0.085 | 5.028 | 0.199 | 0.015 | 5.327 | 4.612 | 46.4 | |
| bacterial mono-culture 4 | 23.136 | 0.105 | 4.603 | 0.157 | 0.019 | 4.884 | 5.055 | 50.9 | |
| Fungal-bacterial co-culture 1 | 25.738 | 0.322 | 1.143 | 0.097 | 0.005 | 1.567 | 8.372 | 84.2 | |
| Fungal-bacterial co-culture 2 | 27.885 | 0.377 | 1.456 | 0.061 | 0.006 | 1.900 | 8.039 | 80.9 | |
| Fungal-bacterial co-culture 3 | 23.107 | 0.216 | 1.210 | 0.122 | 0.008 | 1.556 | 8.383 | 84.3 | |
| Fungal-bacterial co-culture 4 | 23.136 | 0.326 | 2.110 | 0.178 | 0.008 | 2.622 | 7.317 | 73.6 | |

**Table S2.4: Average residual fractions of HCH isomers** based on residual HCH amounts after 10 days in quadruplicate laboratory microcosms (Fig. 1A) in presence of *Sphingobium* sp. strain S8 (bacterial mono-culture), *Fusarium equiseti* strain K3 (fungal mono-culture) and fungal bacterial co-cultures.

| | $F_{res, t10}$ (%) | | | |
|---|---|---|---|---|
| **Setups** | ***α*-HCH** | ***β*-HCH** | ***γ*-HCH** | ***δ*-HCH** |
| **Fungal mono-culture** | 97.7 ±6.8 | 91.6 ±4.6 | 99.4 ±8.7 | 93.3 ±11.5 |
| **Bacterial mono-culture** | 72.3 ±9.4 | 51.0 ±5.4 | 52.9% ±7.9% | 50.1 ±2.4 |
| **Fungal-bacterial co-culture** | 32.8 ±4.6, | 44.5 ±5.1 | 25.3 ±4.2 | 19.2 ±5.0 |

**Table S2.5: Average degraded fractions of HCH isomers** based on residual HCH amounts after 10 days in quadruplicate laboratory microcosms (Fig. 1A) in presence of *Sphingobium* sp. strain S8 (bacterial mono-culture), *Fusarium equiseti* strain K3 (fungal mono-culture) and fungal bacterial co-cultures.

| $F_{deg, t10}$ (%) | | | | |
|---|---|---|---|---|
| **Setups** | **α-HCH** | **β-HCH** | **γ-HCH** | **δ-HCH** |
| **Fungal mono-culture** | 14.43 ± 5.97 | 11.66 ±4.39 | 6.14 ± 5.06 | 9.72 ± 8.11 |
| **Bacterial mono-culture** | 36.64 ± 8.25 | 50.80 ± 5.17 | 47.06 ± 7.94 | 49.88 ± 2.40 |
| **Fungal-bacterial co-culture** | 71.29 ± 4.02 | 57.07 ± 4.94 | 74.65 ± 4.15 | 80.77 ± 5.08 |

**Table S2.6: Average degradation benefits of HCH isomers in presence of fungal-bacterial co-culture as compared to fungal or bacterial mono-culture.**

| **Degradation benefit** | | | | |
|---|---|---|---|---|
| **Setups** | **α-HCH** | **β-HCH** | **γ-HCH** | **δ-HCH** |
| **Fungal-bacterial co-culture/Bacterial mono-culture** | 1.9 ± 0.1 | 1.1 ± 0.1 | 1.6 ± 0.1 | 1.6 ± 0.1 |
| **Fungal-bacterial co-culture/Fungal mono-culture** | 4.9 ± 0.3 | 4.9 ± 0.4 | 12.2 ± 0.7 | 8.3 ± 0.5 |